Available online at www.sciencedirect.com
SCIENCE DIRECT®
Progress in Energy and Combustion Science 30 (2004) 119–174
PROGRESS IN ENERGY AND COMBUSTION SCIENCE
www.elsevier.com/locate/pecs

Fundamental process and system design issues in CO_2 vapor compression systems

Man-Hoe Kim[a,*], Jostein Pettersen[b], Clark W. Bullard[c]

[a]*Department of Mechanical Engineering, Korea Advanced Institute of Science and Technology, Science Town, Daejeon 305-701, South Korea*
[b]*Department of Energy and Process Engineering, Norwegian University of Science and Technology, NO-7491 Trondheim, Norway*
[c]*Department of Mechanical and Industrial Engineering, University of Illinois at Urbana-Champaign, 1206 West Green Street, Urbana, IL 61801, USA*

Received 25 February 2003; accepted 15 September 2003

Abstract

This paper presents recent developments and state of the art for transcritical CO_2 cycle technology in various refrigeration, air-conditioning and heat pump applications. The focus will be on fundamental process and system design issues, including discussions of properties and characteristics of CO_2, cycle fundamentals, methods of high-side pressure control, thermodynamic losses, cycle modifications, component/system design, safety factors, and promising application areas. The article provides a critical review of literature, and discusses important trends and characteristics in the development of CO_2 technology in refrigeration, air-conditioning and heat pump applications. Advanced cycle design options are also introduced suggesting possible performance improvements of the basic cycle.

Keywords: Natural refrigerant; CO_2 (R-744); Transcritical cycle; Vapor compression system; COP; Air-conditioning; Heat pump; Compressor; Heat exchanger

Contents

* Corresponding author. Tel.: +82-42-869-3089; fax: +82-42-869-3210.
E-mail address: kimmh@asme.org (M.-H. Kim).

0360-1285/$ - see front matter © 2003 Published by Elsevier Ltd.
doi:10.1016/j.pecs.2003.09.002

1. Introduction

1.1. Background

Over the last decades, the refrigeration, air conditioning and heat pump industry has been forced through major changes caused by restrictions on refrigerants The change-over to 'ozone-friendly' chlorine-free substances is not finished yet, as the HCFC fluids still need to be replaced, mostly involving R-22 in air-conditioning and heat pump applications. The HFC refrigerants that were once expected to be acceptable permanent replacement fluids are now on the list of regulated substances due to their impact on climate change [1], and there is growing concern about future use. The global warming potential (GWP) is an index that relates the potency of a greenhouse gas to the CO_2 emission over a 100-year period. As shown in Table 1, the GWPs of the HFCs (R-134a, R-407C, R-410A) are in the order of 1300–1900 related to CO_2 with GWP = 1, and the HFCs are included in the greenhouse gases covered by

Nomenclature

COP	coefficient of performance
c_p	specific heat, kJ/kg K
F_c	compressor torque, N m
G	mass flux, kg/m^2 s
GWP	global warming potential
h	enthalpy, kJ/kg
HPF	heating performance factor
HSPF	heating seasonal performance factor
HX	heat exchanger
IHX	internal heat exchanger (suction-line liquid-line heat exchanger)
L	internal heat exchanger length, m
LMTD	log mean temperature difference, °C or K
m	refrigerant charge, kg
m_r	refrigerant mass flow rate, g/s
NTU	number of transfer unit
ODP	ozone depletion potential
P	pressure, bar or MPa
p_m	mean effective pressure, bar
Pr	Prandtl number
Q	capacity, kW
q	heat flux, kW/m^2
q_0	specific refrigeration capacity, kW/kg
q_v	volumetric refrigeration capacity, kJ/m^3
RH	relative humidity, %
s	entropy, kJ/kg K
SPF	seasonal performance factor
T	temperature, °C or K
T_{eai}	evaporator air inlet temperature, °C
T_{ex}	refrigerant temperature at the exit of gas cooler, °C
T_0	evaporating temperature, °C
TEWI	total equivalent warming impact
V	volume, m^3
V_c	outdoor air flow rate, m^3/min
V_e	indoor air flow rate, m^3/min
v	specific volume, m^3/kg
w	specific compressor work, kJ/kg
x	quality
ε	effectiveness
η_{is}	isentropic efficiency
κ	thermal conductivity, W/m K
λ	volumetric efficiency
μ	viscosity, kg/m s
π	pressure ratio
ρ	density, kg/m^3
σ	surface tension, N/m

Subscripts

f	liquid
g	vapor
max	maximum
opt	optimum
pseudo	pseudocritical state
ref	reference point

Table 1
Characteristics of some refrigerants

	R-12	R-22	R-134a	R-407C[a]	R-410A[b]	R-717	R-290	R-744
ODP/GWP[c]	1/8500	0.05/1700	0/1300	0/1600	0/1900	0/0	0/3	0/1
Flammability/toxicity	N/N	N/N	N/N	N/N	N/N	Y/Y	Y/N	N/N
Molecular mass (kg/kmol)	120.9	86.5	102.0	86.2	72.6	17.0	44.1	44.0
Normal boiling point[d] (°C)	−29.8	−40.8	−26.2	−43.8	−52.6	−33.3	−42.1	−78.4
Critical pressure (MPa)	4.11	4.97	4.07	4.64	4.79	11.42	4.25	7.38
Critical temperature (°C)	112.0	96.0	101.1	86.1	70.2	133.0	96.7	31.1
Reduced pressure[e]	0.07	0.10	0.07	0.11	0.16	0.04	0.11	0.47
Reduced temperature[f]	0.71	0.74	0.73	0.76	0.79	0.67	0.74	0.90
Refrigeration capacity[g] (kJ/m^3)	2734	4356	2868	4029	6763	4382	3907	22545
First commercial use as a refrigerant [14]	1931	1936	1990	1998	1998	1859	?	1869

[a] Ternary mixture of R-32/125/134a (23/25/52, %).
[b] Binary mixture of R-32/125 (50/50, %).
[c] Global warming potential in relation to 100 years integration time, from the Intergovernmental Panel on Climate Change (IPCC).
[d] ASRAE handbook 2001 fundamentals.
[e] Ratio of saturation pressure at 0 °C to critical pressure.
[f] Ratio of 273.15 K (0 °C) to critical temperature in Kelvin.
[g] Volumetric refrigeration capacity at 0 °C.

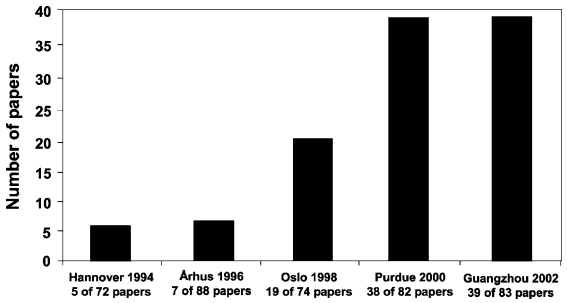

Fig. 1. Number of papers on CO_2 as a primary refrigerant presented at the IIR-Gustav Lorentzen Conference on Natural Working Fluids.

the Kyoto Protocol. The Kyoto protocol is not yet in force since the number of countries that have ratified it is not sufficient, but the spirit of Kyoto is certainly gaining impetus and something will be achieved at a reasonable level whether it is ratified or not [2]. The focus on greenhouse effect of fluorinated compounds has led to a proposed gradual phase-out of refrigerant R-134a in mobile air conditioning in EU, starting from 2008.

In this situation it is hardly surprising that the industry is looking for completely different long-term solutions. Instead of continuing the search for new chemicals, there is an increasing interest in technology based on ecologically safe 'natural' refrigerants, i.e. fluids like water, air, noble gases, hydrocarbons, ammonia and carbon dioxide. Among these, carbon dioxide (CO_2, R-744) is the only non-flammable and non-toxic[1] fluid that can also operate in a vapor compression cycle below 0 °C. Thus, CO_2 has the potential to offer environmental and personal safety in a system based on the well-proven and cost-efficient Evans–Perkins cycle.

During the 10 years since the refrigerant CO_2 was 'rediscovered' [3], there has been a considerable increase in the interest and development activity internationally. The number of papers on CO_2 as a primary refrigerant presented at the biennial IIR Conference on Natural Working Fluids has increased markedly since 1994 as shown in Fig. 1.

1.2. The history and reinvention of CO_2

CO_2 is an 'old' refrigerant, and it is therefore natural to start the paper by briefly looking back on the history of 'carbonic' systems This section outlines the early history, including some views on why the use declined after World War II. The recent revival of CO_2 is also discussed.

During the first decades of the 20th century, CO_2 was widely used as a refrigerant, mainly in marine systems but also in air conditioning and stationary refrigeration applications. Alexander Twining appears to be the first to propose CO_2 as a refrigerant in his 1850 British Patent [4], but the first CO_2 system was not built until the late 1860s by the American Thaddeus S.C. Lowe [5]. Lowe, who received a British Patent in 1867, did not develop his ideas further [6]. In Europe, Carl Linde built the first CO_2 machine in 1881 [7]. Franz Windhausen of Germany advanced the technology considerably, and was awarded a British Patent in 1886. The company J. & E. Hall in Britain purchased the patent rights in 1887, and after having further improved the technology, Hall commenced manufacture in about 1890 [6]. Hall made the first two-stage CO_2 machine in 1889 [5]. The primary application was in marine refrigeration, a field where CO_2 dominated as a refrigerant until 1950–1960 as shown in Fig. 2 [8].

In Europe, CO_2 machines were often the only choice due to legal restrictions on the use of toxic or flammable refrigerants like NH_3 and SO_2 [9]. In the United States, CO_2 was used in refrigerating systems from about 1890 and in comfort cooling from about 1900 [6]. The refrigeration applications included small cold storage systems, display counters, food markets, kitchen and restaurant systems, while comfort-cooling systems were installed for instance in passenger ships, hospitals, theatres and restaurants. Most of these systems used calcium chloride solutions as a secondary refrigerant. Compressors were slow-running double- or single-acting crosshead machines with atmospheric crankcase pressure, and expansion valves were usually of the manual-control type. Condensers were often water-cooled double-pipe units [4].

The safety compared to refrigerants like NH_3 and SO_2 gave CO_2 a preference on board of ships and in public buildings. The commonly reported disadvantages of CO_2 were loss of capacity and low COP at high heat rejection temperature, compared to other common refrigerants. Especially in warm climates, this gave CO_2 a disadvantage. Refrigerant containment at high pressure was difficult with the sealing technology available at that time. By operation at supercritical high-side pressure or by various two-stage arrangements, the capacity and efficiency loss could be reduced. The so-called multiple-effect compression,

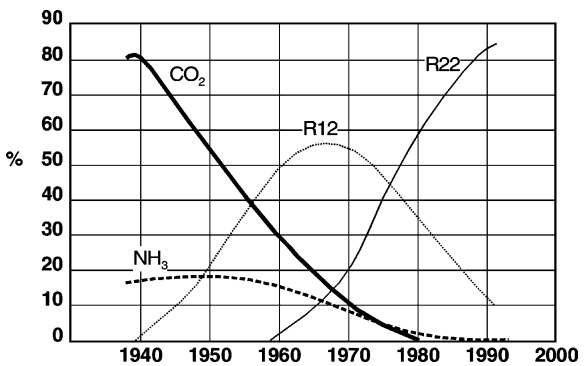

Fig. 2. Percentage use of main primary refrigerants in existing marine cargo installations classed by Lloyd's Register [8].

[1] There are physiological effects from breathing air with high concentrations of CO_2. A maximum acceptable concentration of about 4–5% by volume seems to be a reasonable limit.

as devised by Voorhees in 1905 [10], is one example of the improvements that were made. When supercritical high-side operation was needed, this was obtained by charging more refrigerant into the system.

As the CFC fluids were introduced in the 1930s and 1940s, these 'safety refrigerants' eventually replaced the old working fluids in most applications. Although the major argument in their favor was improved safety compared to fluids like ammonia and sulfur dioxide, CO_2 was also displaced by this transition to CFC. There is no single reason why the use of CO_2 declined, but a number of factors probably contributed. These factors included high-pressure containment problems, capacity and efficiency loss at high temperature (aggravated by the need to use air cooling instead of water), aggressive marketing of CFC products, low-cost tube assembly in competing systems, and a failure of CO_2 system manufacturers to improve and modernize the design of systems and machinery.

With the CFC problem becoming a pressing issue in the late 1980s, the whole industry was searching for viable refrigerant alternatives. In Norway, Professor Gustav Lorentzen believed that the old refrigerant CO_2 could have a renaissance. In a 1989 international patent application [11], he devised a 'transcritical' CO_2 cycle system, where the high-side pressure was controlled by the throttling valve. One of the intended applications for this system was automobile air-conditioning, a sector that dominated the global CFC refrigerant emissions, and also an application where a non-toxic and non-flammable refrigerant was needed. The potential for more compact components due to high pressure was also an interesting feature.

In 1992, Lorentzen and Pettersen [3] published the first experimental results on a prototype CO_2 system for automobile air conditioning. A comparison was made between a state-of-the-art R-12 system and a laboratory prototype CO_2 system with equal heat exchanger dimensions and design-point capacity. Although simple cycle calculations indicated that the CO_2 system efficiency would be inferior, a number of practical factors made the actual efficiencies of the two systems equal.

Based on these and other results, the interest in CO_2 as a refrigerant increased considerably throughout the nineties, in spite of resistance from the fluorocarbon industry [12] and conservative parts of the automotive industry [13]. A number of development and co-operation projects were initiated by the industry and the research sector, including the European industry consortium project 'RACE' on car air conditioning, the European 'COHEPS' project on CO_2 heat pumps, and the CO_2 activities within the international IEA (International Energy Agency) Annexes on Natural Working Fluids and Selected Issues in CO_2 systems.

1.3. Structure of paper

This article provides a critical review of transcritical CO_2 cycle technology in various refrigeration, air-conditioning and heat pump applications. Recent research results in the world are introduced suggesting the possible applications for the particular purpose and the barriers that should be overcome before commercialization.

The history and reinvention of CO_2 have been introduced in Section 1 since it is not a new refrigerant. The thermodynamic and transport properties of CO_2 are quite different from all the conventional refrigerants and are important for the system design, especially for cycle simulation, heat transfer and pressure drop calculations. Section 2 presents the properties of CO_2 and its comparison with other refrigerants. Section 3 discusses some peculiarities of transcritical cycles and systems. A large number of cycle modifications are possible, including staging of compression and expansion, splitting of flows, use of internal heat exchange, and work-generating expansion instead of throttling. Some of these options are discussed in Section 4. Section 5 presents the heat transfer and pressure drop issues in CO_2 systems, which focus on supercritical flow and flow vaporization. Section 6 deals with issues and design characteristics related to high operating pressure. Operating pressures in CO_2 systems are typically 5–10 times higher than with conventional refrigerants, and this gives several effects that influence the design of components and their performance. In addition, high pressure may create perceived safety problems unless the underlying issues are addressed properly. Section 7 presents component design issues for CO_2 system and those barriers that should be overcome before commercialization. Section 8 introduces some possible applications for the particular purpose such as mobile and residential air conditioning and heat pump applications, environmental control unit, heat pump water heaters which are available in the market, dehumidifier, commercial refrigeration, and heat recovery system. Future research challenges and concluding remarks are summarized in Section 9.

2. Properties of CO_2

The refrigerant properties are important for the design of the heat pump system and its components. The properties of CO_2 are well known and they are quite different from all the conventional refrigerants. Table 1 compares the characteristics and properties of CO_2 with other refrigerants [14,15]. CO_2 is a non-flammable natural refrigerant with no Ozone Depletion Potential and a negligible GWP. Its vapor pressure is much higher and its volumetric refrigeration capacity (22,545 kJ/m^3 at 0 °C) is 3–10 times larger than CFC, HCFC, HFC and HC refrigerants. The critical pressure and temperature of CO_2 are 7.38 MPa (73.8 bar) and 31.1 °C, respectively, and it is not possible to transfer heat to the ambient above this critical temperature by condensation as in the conventional vapor compression cycle. This heat transfer process (gas cooling) above the

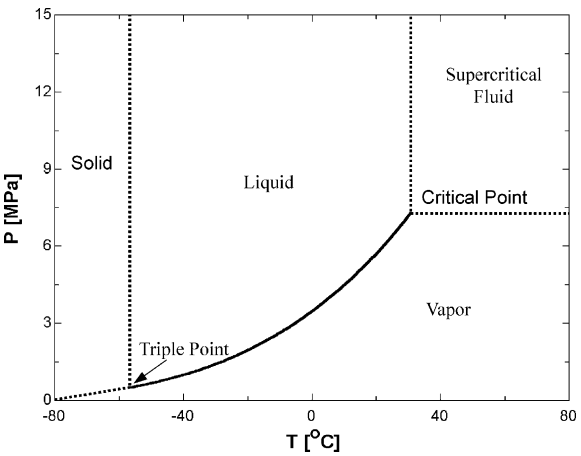

Fig. 3. Phase diagram of CO_2.

critical point results in the transcritical cycle, i.e. with subcritical low-side and supercritical high-side pressure (for a single-stage cycle). The high-side pressure and temperature in the supercritical region are not coupled and can be regulated independently to get the optimum operating condition. As may be observed from the phase diagram of CO_2 (Fig. 3), the temperature and pressure for the triple point are $-56.6\,^{\circ}C$ and 0.52 MPa, respectively, and the saturation pressure at $0\,^{\circ}C$ is 3.5 MPa. The reduced pressure at $0\,^{\circ}C$ for CO_2 is 0.47 (Table 1), which is much higher than those for the conventional fluids. Owing to the low critical temperature and high-reduced pressure of CO_2, the low-side conditions will be much closer to the critical point than with conventional refrigerants.

Regarding transport properties (viscosity and thermal conductivity), the work by Vesovic et al. [16] is a key reference. However, improved viscosity data were published by Fenghour et al. [17]. While the earlier viscosity data were based on partly inconsistent experimental liquid viscosity data and used separate gas-phase and liquid-phase equations, the 1998 publication used new experimental data and represented the viscosity for the whole thermodynamic surface with one equation.

Rieberer [14] developed the property database CO2REF for CO_2, which covers both the sub- and super-critical regions. The thermodynamic and transport properties based on CO2REF were in good agreement with those from VDI [18] in spite of using different equations of state. ASHRAE [19] also presented tabular data for the thermophysical properties of CO_2, which covered from the triple point to the critical point (Appendix A). Pettersen [20] presented some properties of CO_2 using the program library CO2lib developed at NTNU/SINTEF, and he focused on the effect of properties on evaporating characteristics. Liley and Desai [21] also presented thermophysical properties (specific heat, thermal conductivity, viscosity, speed of sound, and surface tension) of CO_2 in tabular form. The following sections will discuss the thermodynamic and transport properties of CO_2, compared to other refrigerants. Unless stated otherwise, all thermophysical properties were calculated using EES (Engineering Equation Solver), which uses the high-accuracy equation of state [22].

2.1. Thermodynamic properties

Span and Wagner [23] reviewed the available data on thermodynamic properties of CO_2 and presented a new equation of state in the form of a fundamental equation explicit in the Helmholtz free energy. In the technically most important region up to pressures of 30 MPa and up to temperatures of 523 K, the estimated uncertainty of the equation ranges from ± 0.03 to $\pm 0.05\%$ in the density, ± 0.03 to $\pm 1\%$ in the speed of sound, and $+0.15$ to $\pm 1.5\%$ in the isobaric specific heat. Special interest was focused on the description of the critical region and the extrapolation behavior of the formulation. Note that thermodynamic properties of CO_2 in EES [22] are provided using

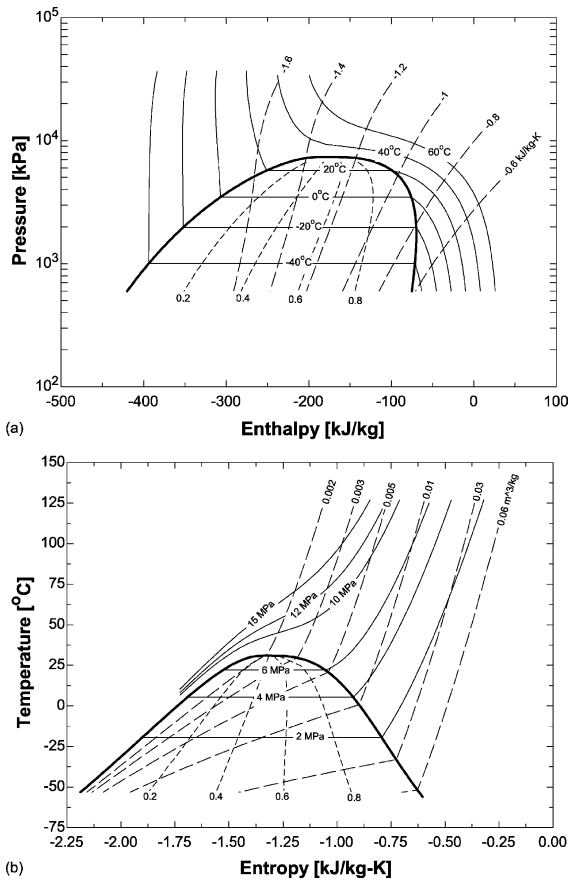

Fig. 4. Pressure–enthalpy and temperature–entropy diagrams of CO_2. (a) Pressure–enthalpy diagram, (b) Temperature–entropy diagram.

the fundamental equation of state developed by Span and Wagner [23].

Fig. 4 presents pressure–enthalpy and temperature–entropy diagrams of CO_2 and more detailed charts can be found elsewhere [14,19] (Appendix A). Fig. 5 shows enthalpy and entropy changes in gas cooling process at constant pressures. In the supercritical region, the enthalpy and entropy decrease with temperature with more abrupt changes near the critical point. The pressure influences the enthalpy and entropy above the critical temperature, while the effect of pressure is small below the critical temperature as the pressure drops may be allowed to be higher.

Figs. 6 and 7 present vapor pressure and slope of the saturation temperature curve of CO_2 compared to other fluids. The vapor pressure of CO_2 is much higher than other refrigerants, and its higher steepness near the critical point gives a smaller temperature change for a given pressure change. Thus, the temperature change associated with pressure drop in the evaporator will become smaller. For example, at 0 °C, the temperature change of

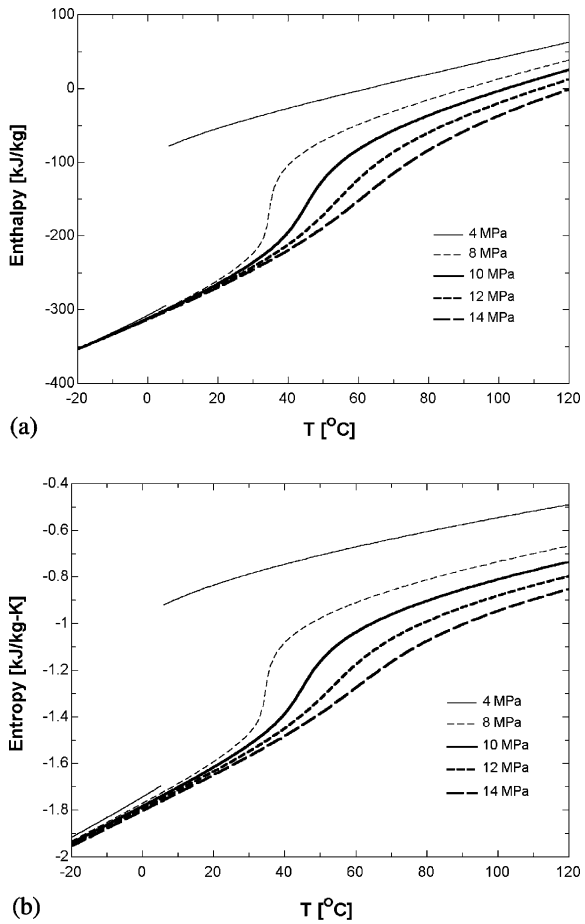

Fig. 5. Enthalpy and entropy changes of CO_2 in gas cooling process. (a) Enthalpy change, (b) entropy change.

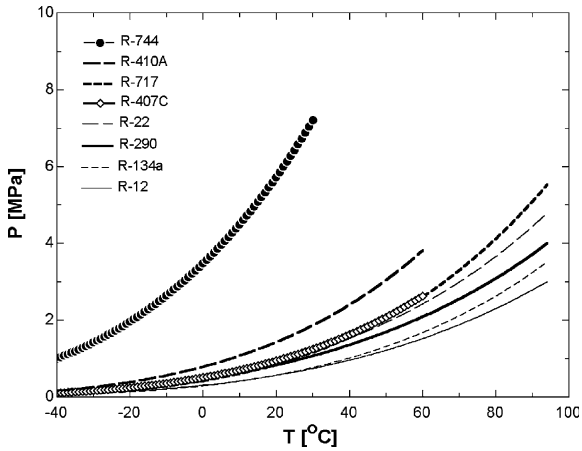

Fig. 6. Vapor pressure for refrigerants.

CO_2 for 1 kPa pressure drop is about 0.01 K. On the other hand, the same pressure drop with R-410A and R-134a give the temperature changes of 0.04 and 0.10 K, respectively, i.e. about 4–10 times higher, as shown in Fig. 7.

The high vapor pressure and closeness to the critical point result in quite different characteristics of liquid and vapor density of CO_2 compared to other refrigerants. The high vapor density may have significant effects on two-phase flow patterns where differences in phase density determine phase separation characteristics, and vapor density influences the flow momentum of the vapor phase and shear force between vapor and liquid phase [20]. Figs. 8 and 9 show density of CO_2 at varying temperature and the ratio of liquid to vapor density for several refrigerants. The density of CO_2 changes rapidly with temperature near the critical point, and the density ratio of CO_2 is much smaller than other refrigerants. At 0 °C, for instance, the ratio of liquid (927 kg/m^3) to vapor density (98 kg/m^3) of CO_2 is around 10, whereas R-410A and R-134a have the density ratios of 65 and 89, respectively. The vapor densities of R-410A and R-134a are 31 and 14 kg/m^3, which are 32

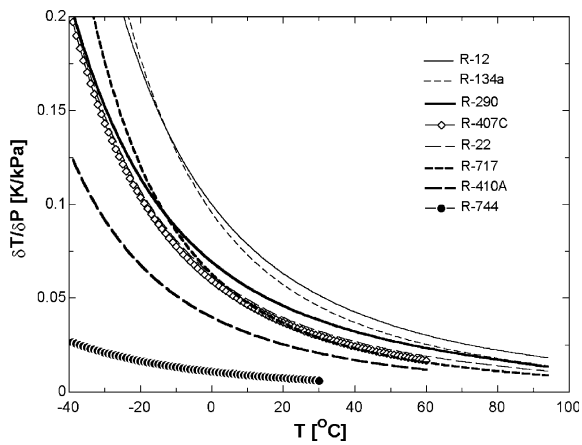

Fig. 7. Slope of saturation pressure curve dT/dP for refrigerants.

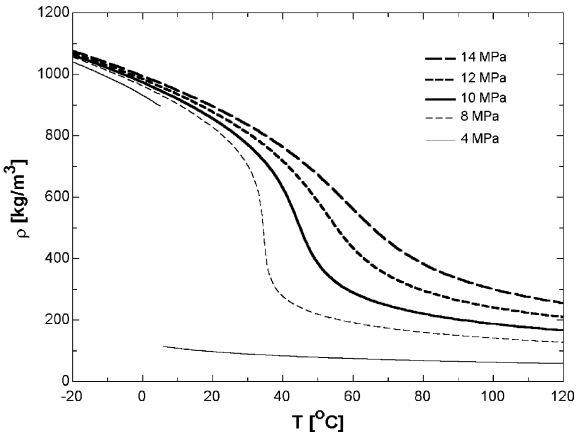

Fig. 8. Density of CO_2.

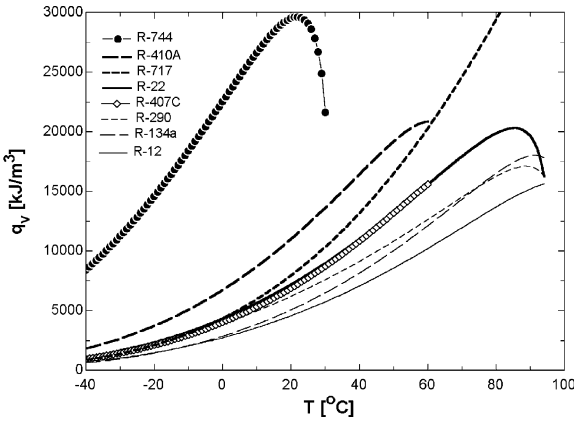

Fig. 10. Volumetric refrigeration capacity for refrigerants.

and 14% of the CO_2 vapor density, respectively. The low-density ratio of CO_2 may give more homogenous two-phase flow than with other refrigerants [24]. The liquid to vapor density ratio plays an important role in an evaporator since it determines the flow pattern and thus the heat transfer coefficient [20].

The higher vapor density gives the high volumetric refrigeration capacity of CO_2, which is defined as product of vapor density and latent heat of evaporation. The volumetric refrigeration capacity of CO_2 increases with temperature, has a maximum at 22 °C, and then decreases again. By definition it is zero at the critical point as shown in Fig. 10.

Surface tension of the refrigerants influences nucleate boiling and two-phase flow characteristics. A small surface tension reduces the superheat required for nucleation and growth of vapor bubbles, which may positively affect heat transfer. Wetting characteristics of the liquid is affected by surface tension, thus influencing evaporation heat transfer. Reduced liquid surface stability with small surface tension may affect heat transfer negatively due to increased droplet formation and entrainment [20]. Fig. 11 presents surface tension of saturated CO_2 liquid at varying temperatures, compared to other fluids. The surface tension of the refrigerants decreases with temperature and becomes zero at the critical point. As shown in Fig. 11, the surface tension of CO_2 is smaller than those of other fluids. For instance at 0 °C it is 0.0044 N/m, which is 2.5 times smaller than that of R-134a at the same temperature. Surface tension data for CO_2 can be estimated based on the publication of Rathjen and Straub [25], and speed-of-sound data were derived by Estrada-Alexanders and Trusler [26].

One of the most important characteristics of supercritical fluids near the critical point is that their properties change rapidly with temperature in an isobaric process, especially near the pseudocritical points (the temperature at which the specific heat becomes a maximum for a given pressure). This may be clearly seen from Figs. 12 and 13, where the isobaric specific heat and pseudocritical temperature are depicted. It should be noted that the ε-NTU or LMTD method requires that the specific heat be constant over the test section. Thus when the data are analyzed using

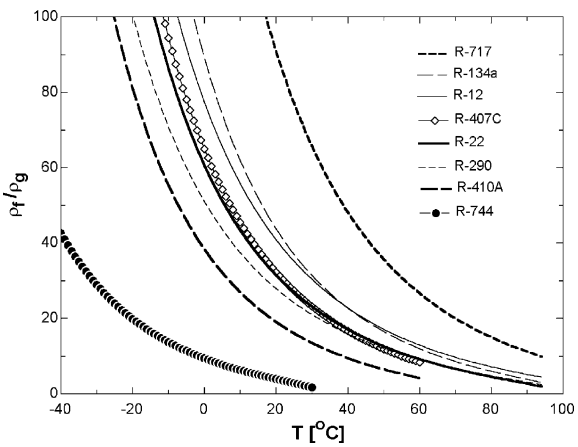

Fig. 9. Ratio of liquid to vapor density at saturation for refrigerants.

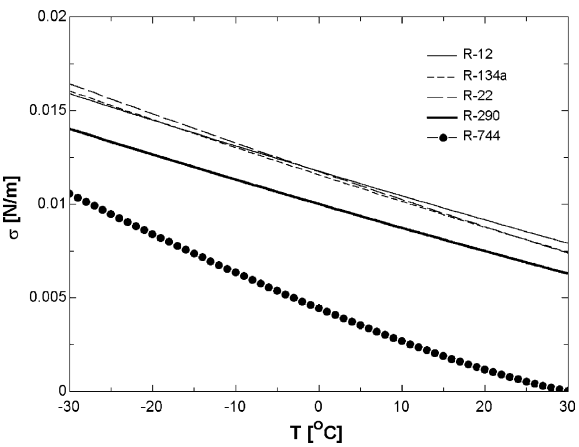

Fig. 11. Surface tension for refrigerants.

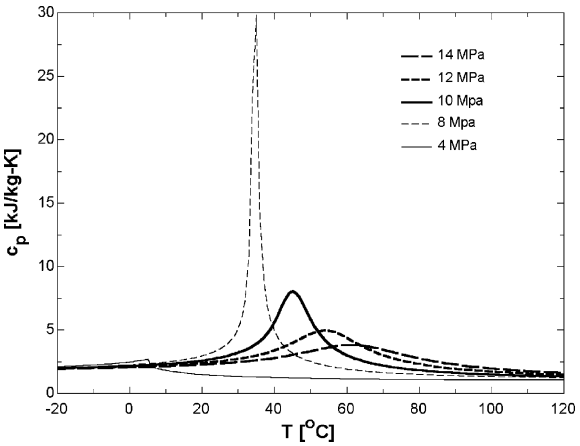

Fig. 12. Isobaric specific heat of CO_2.

the ε-NTU or LMTD method, it should be carefully investigated whether the specific heat is constant. The pseudocritical temperature of CO_2 was calculated using the following algebraic equation [27]

$$T_{\text{pseudo}} = -122.6 + 6.124P - 0.1657P^2 + 01773P^{2.5} - 0.0005608P^3, \qquad 75 \le P \le 140 \tag{1}$$

where the temperature (T_{pseudo}) and pressure (P) are in °C and bar, respectively.

2.2. Transport properties

The transport properties of refrigerants play an important role in heat transfer and pressure drop characteristics. Fig. 14 shows the transport properties, which are thermal conductivity and viscosity at subcritical and supercritical pressures at varying temperatures. A high thermal conductivity is essential for heat transfer coefficients both in single-phase and two-phase flow. Viscosity, particularly of the liquid

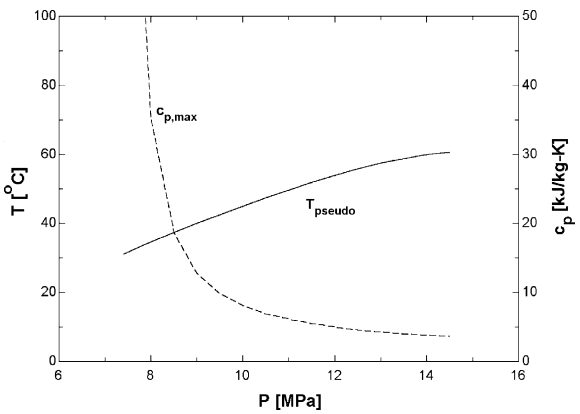

Fig. 13. Pseudocritical temperature and maximum isobaric specific heat of CO_2.

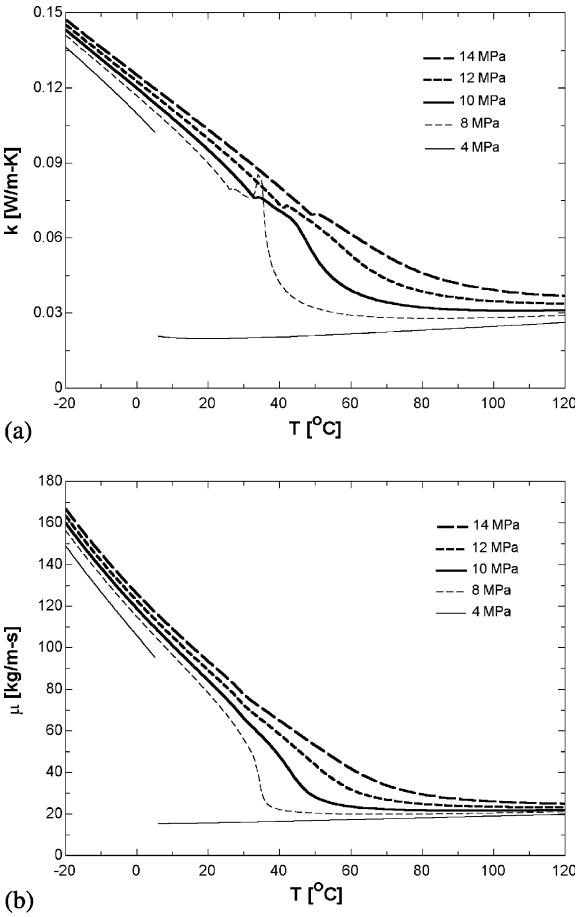

Fig. 14. Transport properties of CO_2. (a) Thermal conductivity, (b) viscosity.

phase, and the ratio of liquid to vapor viscosity, are important parameters for the fluid flow behaviors, convection characteristics and two-phase heat transfer and pressure drop. The thermal conductivities of saturated CO_2 liquid and vapor at 0 °C are 20 and 60% higher than of R-134a liquid and vapor, respectively, while the viscosity of CO_2 liquid is only 40% of R-134a liquid viscosity, and the vapor viscosities of the two fluids are comparable [20].

The Prandtl number is an important parameter for the heat transfer coefficient. Fig. 15 depicts the Prandtl number of supercritical and liquid/vapor CO_2 at varying temperatures. It has a maximum at the pseudocritical temperature associated with the corresponding specific heat, and the maximum value decreases with pressure. The effect of the temperature on the Prandtl number depends on pressure. The Prandtl number becomes higher with pressure for $T >$ about 60 °C in the supercritical region, whereas it decreases with pressure when temperature is smaller than about 20 °C. This results in a strongly varying local heat transfer coefficient depending on temperature and pressure [14]. In summary, the thermodynamic and transport properties of

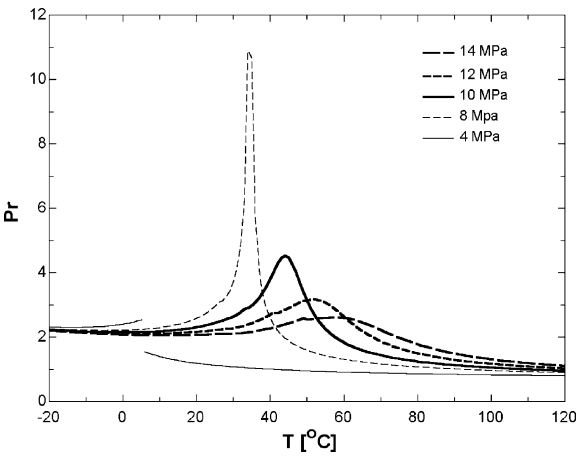

Fig. 15. Prandtl number of CO_2.

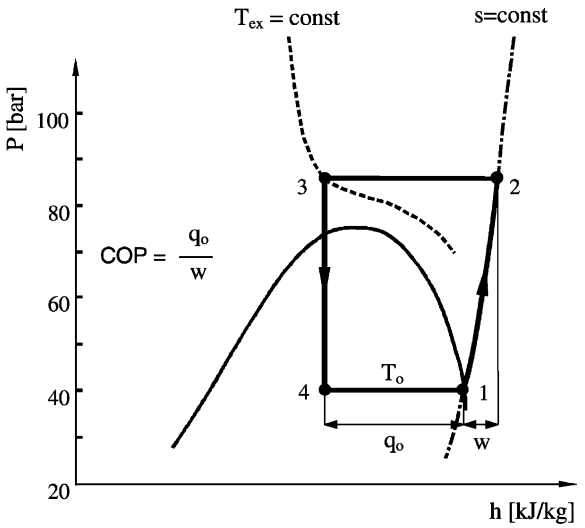

Fig. 16. Transcritical cycle in the CO_2 pressure–enthalpy diagram.

CO_2 seem to be favorable in terms of heat transfer and pressure drop, compared to other typical refrigerants.

3. Transcritical vapor compression cycle

Compared to conventional refrigerants, the most remarkable property of CO_2 is the low critical temperature of 31.1 °C Vapor compression systems with CO_2 operating at normal refrigeration, heat pump and air-conditioning temperatures will therefore work close to and even partly above the critical pressure of 7.38 MPa. Heat rejection will in most cases take place at supercritical pressure, causing the pressure levels in the system to be high, and the cycle to be 'transcritical', i.e. with subcritical low-side and supercritical high-side pressure (for a single-stage cycle). Some peculiarities of transcritical cycles and systems are discussed in the following text.

3.1. Fundamentals of transcritical cycle

During operation at high ambient air temperatures the CO_2 system will operate in a *transcritical* cycle most of the time Heat rejection then takes place by cooling the compressed fluid at supercritical high-side pressure. The low-side conditions remain subcritical, however, as shown in Fig. 16.

At supercritical pressure, no saturation condition exists and the pressure is independent of the temperature. In conventional subcritical cycles, the specific enthalpy in point 3 is mainly a function of temperature, but at supercritical high-side conditions the pressure also has a marked influence on enthalpy. This effect may be observed as non-vertical or S-shaped isotherms in the supercritical and near-critical region. An important consequence of this is that it is necessary to control the high-side pressure, since the pressure at the throttling valve inlet will determine specific refrigeration capacity. As in conventional systems, the compressor work and thereby also the COP will depend on the discharge pressure. However, while the COP tends to drop with increasing pressure in conventional cycles, the behavior is quite different in a transcritical cycle, as will be shown in the following [28].

Fig. 17 shows the theoretical influence from varying high-side pressure on specific refrigerating capacity (q_0), specific compressor work (w) and cooling COP. The refrigerant outlet temperature from the gas cooler (T_{ex}) is assumed to be constant. In practice, this temperature will be some degrees higher than the coolant inlet temperature. The curves are based on ideal cycle calculations, with evaporating temperature ($T_0 = 5$ °C) and a minimum heat rejection temperature (T_{ex}) of 35 °C (left), and 50 °C (right). Note that all curves are normalized (Fig. 17).

As the high-side pressure is increased, the COP reaches a maximum above which the added capacity no longer fully compensates for the additional work of compression. In Fig. 16, it may be observed that the T_{ex}-isotherm becomes steeper as the pressure increases, thereby reducing the capacity enhancement from a given pressure increment. In contrast, the isentropic (compression) line shows a nearly linear shape. Differentiation of cooling COP $= (h_1 - h_3)/(h_2 - h_1)$ with respect to the high-side pressure gives maximum COP for $\partial \mathrm{COP}/\partial p = 0$ at a pressure (p) defined by Inokuty [29]

$$\left(\frac{\partial h_3}{\partial p}\right)_T = -\mathrm{COP}\left(\frac{\partial h_2}{\partial p}\right)_s \tag{2}$$

That is, the 'optimum' pressure is reached when the marginal increase in capacity equals COP times the marginal increase in work. The enthalpy h_1 is constant. Curves in Fig. 17 are normalized by the values for COP, q_0 and w at the optimum high-side pressure. At $T_{ex} = 35$ °C

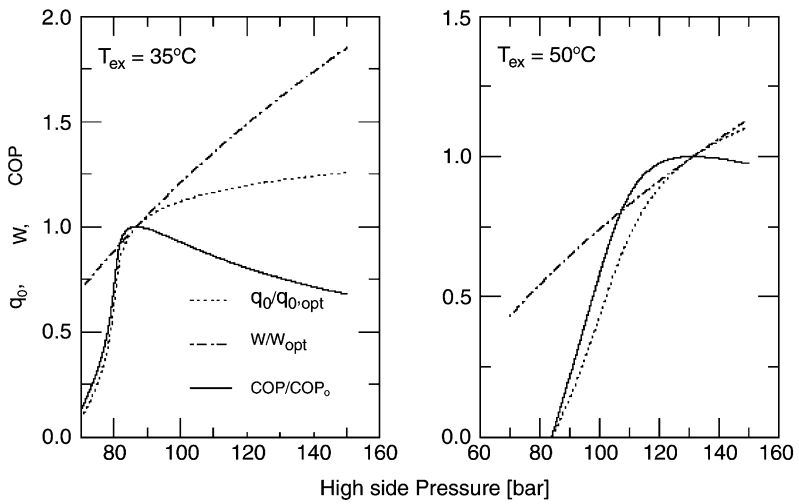

Fig. 17. Influence of varying high-side pressure on specific refrigerating capacity (q_0), specific compressor work (w) and COP in a transcritical CO_2 cycle. The results are based on isentropic compression, evaporating temperature ($T_0 = 5$ °C) and a refrigerant outlet temperature (T_{ex}) from the gas cooler of 35 °C (left) and 50 °C (right).

the theoretical maximum COP is reached at a pressure of 8.7 MPa (87 bar), while at 50 °C, the optimum is at 13.1 MPa (131 bar). In practice, the cooling capacity (q) curve will also go through a maximum, as compressor volumetric capacity drops off at higher discharge pressures. In most situations there will also be a capacity-maximum, usually at a somewhat higher pressure than the COP-maximum.

High-side pressure regulation can be applied to maintain the COP at its maximum and/or to regulate the cooling or heating capacity. The optimum pressure increases steadily and almost linearly as T_{ex} is raised, and the influence from varying evaporating temperature is quite small.

3.2. Methods of high-side pressure control

The high-side pressure in a CO_2 system may be either subcritical or supercritical. In case of subcritical operation, the system will behave as conventional systems, with high-side pressure determined by condensing temperature. In case of supercritical operation, however, the pressure in the high side is determined by the relationship between refrigerant charge (mass), inside volume and temperature. Refrigerant properties can be described by an equation of state in the following form:

$$p = p(v, T) = p\left(\frac{V}{m}, T\right) \tag{3}$$

As a result, there are three fundamentally different ways of controlling pressure [30]:

- Varying the refrigerant charge (m) in the high side of the circuit,
- Varying the inside volume (V) of the high-side, and
- Allowing the refrigerant temperature (T) to control the pressure.

While the first two options give possibilities for active pressure control, the last method is actually a passive scheme where the refrigerant charge/volume conditions are adapted to give the desired change in pressure when temperature varies. Thus, in case of leakage, the temperature/pressure relation will change when using a passive scheme and this may give loss of capacity and COP.

Even though high-side conditions are supercritical a large part of the time, the circuit and control system must also be designed for subcritical (condensing) high-side conditions as well, since this type of operation will be encountered when heat rejection temperatures are moderate or low.

3.2.1. Systems with high-side charge control

In systems where the high-side pressure is controlled by varying the high-side refrigerant charge, the circuit must include means for controlling the momentary mass of refrigerant located between the compressor outlet and the expansion valve inlet. Assuming that the total refrigerant charge in the circuit is constant, a refrigerant buffer must be provided so that the high-side charge can be varied without flooding or drying up the evaporator. Several buffer volume locations and control concepts are possible. The various solutions can be divided into low-pressure and intermediate-pressure buffer systems.

Low pressure buffer systems. Systems with low-pressure buffers include circuits with low-pressure receiver on the evaporator outlet, and systems with liquid separator using gravity, pump or possibly ejector circulation. A system with low-pressure receiver on the evaporator outlet is shown in Fig. 18 [11]. High-side pressure is controlled by

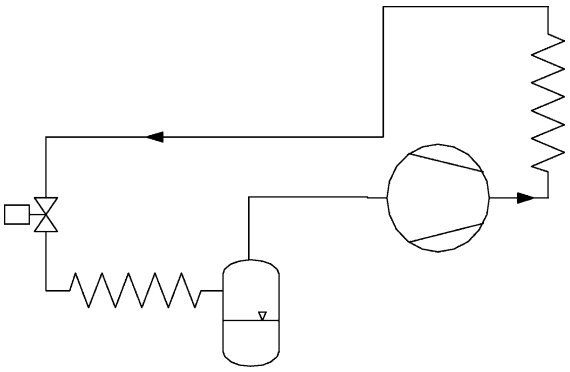

Fig. 18. System with low-pressure receiver.

adjusting the expansion valve, temporarily changing the balance between compressor mass flow rate and valve flow rate. By reducing the valve opening, a temporary reduction in the valve mass flow rate gives refrigerant accumulation in the high side, and the pressure rises until a new balance point between valve flow rate and compressor flow rate is found. The vapor fraction at the evaporator outlet may temporarily rise while pressure is rising, and the additional high-side charge is transferred from the low-side buffer. Conversely, increased valve opening will reduce the high-side charge and pressure, and the excess high-side charge is deposited as liquid in the buffer. In practice, such systems will in most cases need a liquid bleed from the receiver in order to return lubricant to the compressor and to maintain the evaporator outlet slightly wet. The liquid surplus may be an advantage when the high-side pressure is raised, to avoid drying up the evaporator. By installing an internal (suction line) heat exchanger, the liquid is evaporated before the compressor inlet, and the COP is improved at high heat rejection temperature. The use of internal heat exchange is discussed elsewhere in the paper.

Systems with medium-pressure buffer. Fig. 19 shows a system where the buffer is kept at an intermediate pressure [11]. An in-line receiver is located between a pressure-regulating valve (A), that controls the high-side pressure, and an electronic or thermostatic expansion valve (B), that regulates liquid flow to the evaporator. The receiver pressure may either be supercritical or subcritical.

In case of subcritical receiver pressure, the outlet from the pressure-regulating valve (A) will be on the saturation line during steady-state operation. The receiver pressure will adjust itself to this point, since vapor cannot escape. Adjustment of the valve opening temporarily moves the end-point of the throttling away from the saturation line, and the resulting imbalance between the mass flow rates through the two valves gives a transfer of mass to or from the receiver, thereby affecting high-side charge and pressure.

In case of supercritical receiver pressure, the refrigerant mass in the buffer is regulated by changing the buffer pressure, thereby modifying the density of the compressed fluid. The pressure can be controlled between the compressor discharge pressure and the critical pressure. A large receiver volume may be necessary in order to obtain the necessary range of high-side charge variation.

Another system with intermediate-pressure buffer is shown in Fig. 20 [11]. Here, the receiver is located in parallel to the flow circuit, connected to the high and low sides by valves. These two valves and the expansion valve are operated to control high-side charge and pressure.

3.2.2. Systems with high-side volume control

Instead of varying the mass, the pressure in the high side can be regulated by adjusting the internal volume of the high-side part of the circuit. For a given volume change, the largest pressure variation will be obtained at the lowest possible temperature (highest density). This makes the gas cooler refrigerant outlet the ideal location for a volume-control device. This device may be constructed in a number of ways, including bellows arrangement inside a pressure vessel or a cylinder where the displacement of a piston defines the refrigerant-side volume. The buffer design must consider factors like lubricant trapping and means for

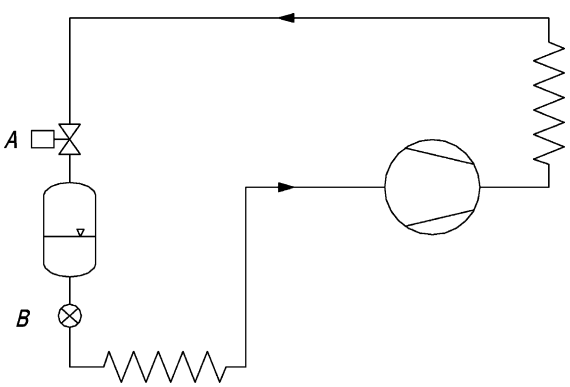

Fig. 19. System with in-line medium-pressure receiver.

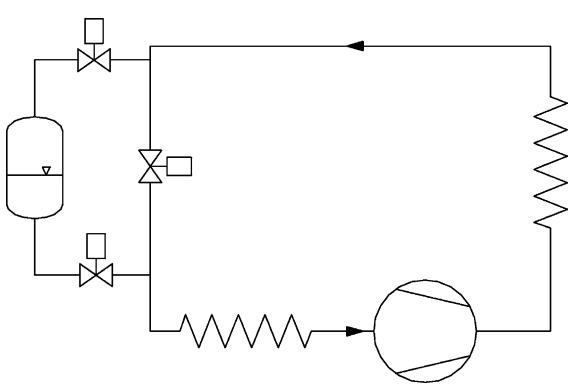

Fig. 20. System with medium-pressure receiver.

control of the volume through mechanical or hydraulic actuation.

3.3. Thermodynamic losses

Assuming given evaporating temperature and given minimum heat rejection temperature, the transcritical cycle suffers from larger thermodynamic losses than an 'ordinary' Evans–Perkins cycle with condensation, Fig. 21. Owing to the higher average temperature of heat rejection, and the larger throttling loss, the theoretical cycle work for CO_2 increases compared to a conventional refrigerant as R-134a as indicated. The throttling loss in a refrigerating cycle is given by temperatures before and after the throttling device, and by refrigerant properties. With temperatures given, the refrigerant properties become essential. Given the high liquid specific heat and low evaporation enthalpy of CO_2 near the critical point, the loss in refrigeration capacity (and the equal increase in compressor power) becomes large.

In reality though, as discussed in subsequent sections, the minimum heat rejection temperature will be lower in the CO_2 cycle when heat sink inlet temperature and heat exchanger size is given. In addition, the evaporating temperature tends to be higher for a given duty, heat source temperature, and heat exchanger size. Finally, the compressor losses, which are not shown in Fig. 21, tend to be lower in CO_2 machines.

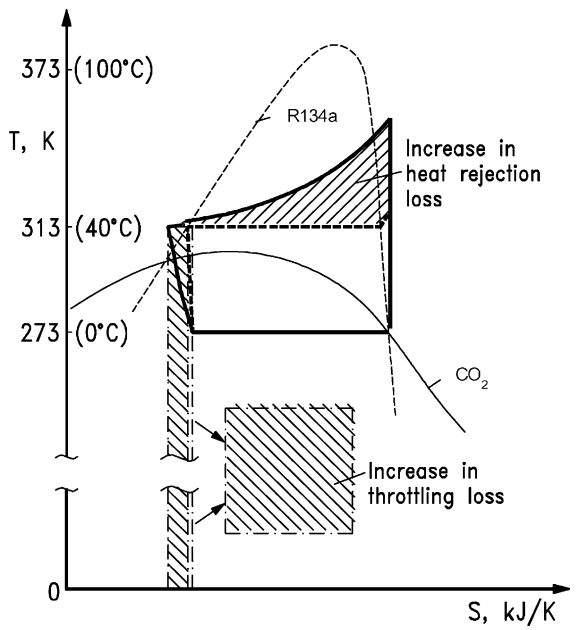

Fig. 21. Comparison of thermodynamic cycles for R-134a and CO_2 in temperature–entropy diagrams, showing additional thermodynamic losses for the CO_2 cycle when assuming equal evaporating temperature and equal minimum heat rejection temperature.

3.4. Transcritical cycles in heat pumps and systems with heat recovery

3.4.1. Temperature glide in heat rejection

As may be observed from Fig. 21, heat is rejected from the CO_2 cycle at gliding temperature, as the supercritical-pressure single-phase refrigerant is cooled. The temperature profile of the cooled refrigerant thus matches the heating-up curve of water or air to be heated, thus giving reduced thermodynamic losses in water- or air heating. This feature may be utilized in heat pumps for tap water heating and/or hydronic heating systems, and may also give advantages in heat recovery from refrigeration or air conditioning systems. In applications where the rejected heat is not of interest, the gliding temperature is not an advantage, since the average temperature of heat rejection becomes higher than necessary.

In water heating applications, the inlet temperature is often quite low, and the CO_2 temperature glide during heat rejection in a 'triangular' process with low inlet temperature is ideal for heating of service water from around 10 to 70–80 °C. By proper counterflow heat exchanger design and by adjustment of the high-side pressure, varying temperature requirements can be met. Application examples will be described in the following text.

3.4.2. Heating capacity and COP characteristics

In heat pump operation, the CO_2 system obtains a maximum COP at a certain high-side pressure, as explained above. By raising the pressure above this level, the heating capacity may be increased or maintained as the evaporating temperature is reduced. Despite the reduced COP, the overall efficiency of heating may then be increased in bivalent systems due to reduced supplementary heat. Another peculiarity of the CO_2 cycle is the smaller influence on heating capacity and COP by varying evaporating temperature, which enables the CO_2 system to maintain a high heating capacity at low ambient temperature. Both of these principles are illustrated for ideal cycles in Fig. 22, showing relative changes in heating capacity and heating COP with varying evaporating temperature and CO_2 high-side pressure [31]. Similar tendencies can also be observed for cooling capacity and cooling COP.

Even at the optimum pressure (opt), the CO_2 heat pump output is decreased less than with the other refrigerants as the evaporating temperature is reduced. At −15 °C, the capacity ratio CO_2/fluorocarbon is about 1.5, and the relative reduction in COP is smaller with CO_2 than with the other fluids. This diagram is intended to illustrate the effects of differences in thermodynamic properties on cycle behavior, and not to demonstrate the performance level of CO_2 compared to other refrigerants. By raising the high-side pressure, a further increase in heat pump capacity can be obtained. The actual operation with capacity-boosting will depend on factors like maximum allowable

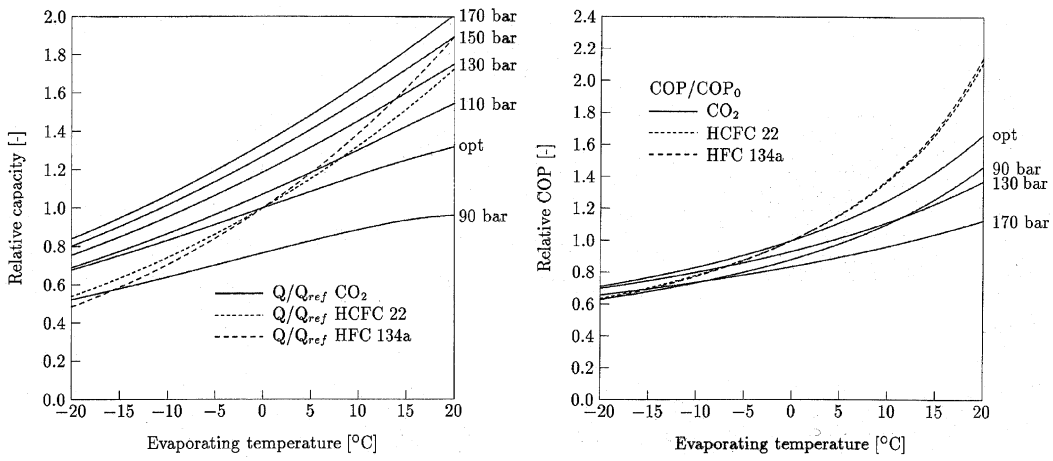

Fig. 22. Relative change in heating capacity (left) and heating COP (right) for R-22, R-134a and CO_2 at varying evaporating temperature, for a condenser/gas cooler exit temperature of 40 °C. Reference point: 0 °C evaporating temperature. Results for CO_2 are shown at COP-optimum high-side pressure, and with relative data for other high-side pressures. Based on ideal cycle calculations without subcooling or superheating.

pressure, maximum motor load, and compressor discharge temperature limitations.

3.5. Approach temperature and its importance

In applications where the rejected heat is not needed, the thermodynamic losses in heat transfer can be limited by allowing the CO_2 exit temperature from the gas cooler to approach the air- or cooling water inlet temperature as closely as possible. Heat exchanger design calculations and practical experience show that it is possible to obtain a temperature approach of a few degrees, even in air-cooled coils. Assuming that the mean temperature difference is approximately equal for a given heat exchanger size, the temperature approach must necessarily be lower when heat is rejected over a temperature glide than when it is rejected at constant temperature.

Owing to the relatively high throttling loss and the gliding heat rejection temperature, the cooling COP for a CO_2 system is very sensitive to the gas cooler refrigerant exit temperature. Fig. 23 shows the relative change in ideal cycle COP at varying condenser/gas cooler outlet temperature, normalized by the COP at 40 °C [31]. While the ideal COP for R-22 and R-134a is increased by about 40% through a 10 K condenser outlet temperature reduction, the effect on the CO_2 cycle COP is nearly twice as high (70%). The close temperature approach that is obtained in CO_2 gas coolers therefore contributes significantly to practical COP improvement.

3.6. Analysis of transcritical system energy efficiency

Comparisons of energy efficiency and/or TEWI (total equivalent warming impact) between baseline systems and CO_2 systems have to account for two important factors: The effect of climate, i.e. a seasonal data for comparisons of energy consumption, and a system approach, including the effects of supplementary heat and secondary power requirements for fans or pumps.

Most refrigeration, air-conditioning and heat pump systems are operated in a varying climate. Comparisons based on design point operation apply conditions that rarely occur—typically at an extreme ambient temperature. In order to obtain a realistic comparison of annual or seasonal energy consumption, realistic climatic data should

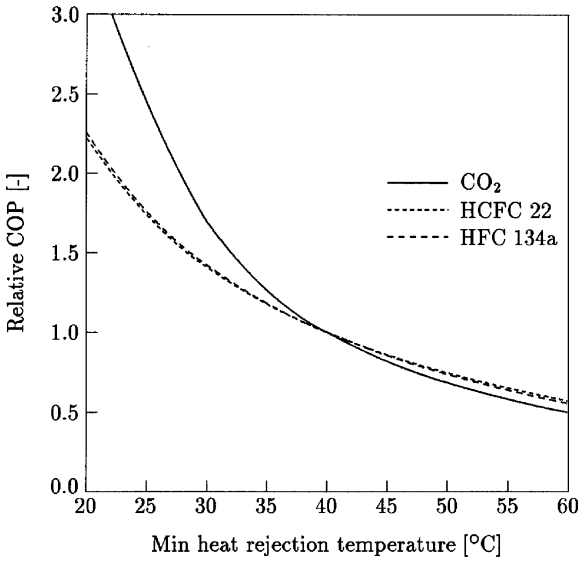

Fig. 23. Relative change in cooling COP for R-22, R-134a and CO_2 at varying refrigerant exit temperature from condenser/gas cooler (i.e. minimum heat rejection temperature). Evaporating temperature 0 °C. Reference point: 40 °C exit temperature. Based on ideal cycle calculations without subcooling or superheating.

be applied, e.g. temperature occurrence data. Even though the COP of the CO_2 system may be somewhat lower at an extreme ambient temperature, the seasonal energy consumption may be reduced compared to a baseline system using conventional refrigerants.

Differences in heating capacity characteristics between CO_2 and conventional refrigerants have to be taken into account in the comparison of CO_2 to baseline systems, since differences in supplementary heating requirements may significantly affect the system energy efficiency. In this respect, the system energy efficiency is calculated as *heating system* COP, i.e. the ratio of heat pump heat output plus supplementary heat, to heat pump energy use plus supplementary heat input. By reducing the need for supplementary heat the *system COP* of a CO_2 heat pump may often be higher than the baseline. The reason is that the baseline system does not maintain its heating capacity at lower heat source temperature, and more supplementary heat is needed.

In general, CO_2 systems may offer more possibilities for efficient and useful heat recovery, since higher temperatures can be provided. In comparisons between different systems, this factor should be taken into account through studies on overall energy requirements for cooling and heating.

Differences in fan and pump power requirements should also be considered, particularly since air-side pressure drops and air flow rates are likely to be different, thus giving differences in fan power. In a comparison with heat pumping systems using secondary fluid circuits, the pumping power should not be overlooked, particularly if a direct-evaporation CO_2 system may offer the same environmental and personal safety.

4. Modified cycles

There are several reasons for modifying the basic single-stage transcritical cycle, including improvement of energy efficiency, increase of capacity for given system and component size, and adaptation of the heat rejection temperature profile to given requirements, e.g. in a heating system. In principle, a large number of possible modifications are possible, including staging of compression and expansion, splitting of flows, use of internal heat exchange, and work-generating expansion instead of throttling. Lorentzen [32] outlined several advanced heat pump cycles and circuits for CO_2, including two-stage cycles, cycles with internal 'subcooling' and cycles with expander. In order to reduce the throttling loss and to adapt the heat rejection temperature profile, cycles with two or more compression/throttling stages, internal heat transfer, subcooling, and expansion work recovery can be applied.

The economic viability of the transcritical cycle is enhanced by making use of the high-temperature heat rejected, for example, for domestic hot water in stationary applications and for reheating/defogging in mobile applications. Theoretically the same options are available in subcritical systems, but the relatively small amount of recoverable high-temperature heat has meant that it is usually wasted. The potential payoff is generally greater in CO_2 systems. Therefore, in transcritical heat pumps many more options exist for reversing flow between heating and cooling modes and for meeting simultaneous loads. Placement of the reversing valves is further complicated by the existence of the internal heat exchanger, where decisions must be made about preferences for counter- vs. parallel flow in heating mode.

4.1. Internal heat exchange cycle

The impacts of liquid-line/suction-line heat exchange on cycle COP have been documented for a wide variety of refrigerants commonly used in subcritical cycles [33]. Two offsetting effects—capacity increase due to subcooling and power increase due to higher suction temperature—combine to produce net thermodynamic benefits for some refrigerants such as R-134a and penalties for others such as R-22. Kim [34] reported that application of the internal heat exchange cycle was beneficial to COPs of all fluids tested (R-22, R-134a, R-407C, R-32/134a), given that the low-pressure refrigerant was superheated in the internal heat exchanger. However, the influences of the internal heat exchange on the system overall efficiency depend on the working fluids and operating conditions. For R-22 and R-134a, the COP was not improved when the heat was transferred to low-pressure two-phase refrigerant (indicated by a low value of superheat leaving the suction-line heat exchanger). For the zeotropic mixtures (R-407C and R-32/134a), COPs were improved even at small values of superheat leaving the suction-line heat exchanger. The benefits of this heat exchange between subcooled high-pressure liquid and two-phase low-pressure refrigerant has been hypothesized in literature [35], but has not been quantified and warrants further investigation. In practical systems there may be some benefits due to improved heat transfer caused by absence of superheating, and higher compressor efficiency due to higher suction temperature.

For CO_2 the benefits are substantial, because the COP-optimizing discharge pressure is lower when an internal heat exchanger is present. Moreover, internal heat exchange brings the capacity- and efficiency-maximizing discharge pressures closer together, creating opportunities for using less precise or simpler control systems and strategies. Second-law analyses of the transcritical cycle demonstrate how the internal heat exchanger increases compressor discharge temperature and consequently the irreversibility of high-side heat rejection from the gas cooler, and introduces a finite temperature difference of its own due to the difference between specific heats of the suction gas and supercritical fluid. However, these inefficiencies are more than offset by the reduction in

throttling loss [36]. In some high-lift applications such as refrigeration or space heating where a highly effective internal heat exchanger may produce compressor discharge temperatures high enough to damage the lubricant, the internal heat exchanger may employ a parallel-flow configuration. In case of given capacity requirement, the reduced high-side pressure needed in a system with internal heat exchanger may give a compressor discharge temperature which is comparable to a system without internal heat exchanger [37].

4.2. Expansion with work recovery

Internal heat exchange is only one option for reducing expansion losses Another approach is to extract and make use of the work potentially available from the process. Owing to the high throttling loss of CO_2, there is a considerable potential for COP improvement by the introduction of an expander. Several authors have therefore studied this potential.

Regarding cycles and circuits with work-producing expansion, Negishi [38] devised a system based on the Plank cycle [39] where the supplementary pump/compressor is driven by an expander in a self-contained unit. Ikoma et al. [40] suggested another approach that expansion from supercritical state in a single-stage cycle is allowed to continue until near the saturation curve, and a throttling valve controls the remaining pressure reduction down to the evaporator pressure. Thus, the expander operates with a single-phase fluid only.

From a hardware standpoint, the practical challenges are substantial because cooling systems experience a wide range of mass flow rates, requiring a robust design as detailed in Maurer and Zinn [41]. Positive-displacement devices, specifically internal and external gear pumps are theoretically more desirable because of the edge losses inherent in small turbines and even pistons. Research has focused on finding an instantaneous use for the highly variable work output, because of the inevitable losses associated with electric generators and motors. As a result, recent investigations have aimed to explore direct mechanical linkages to the high stage of a two-stage compressor [42–45].

Aside from implementation issues, the recovery of expansion work involves interesting thermodynamic tradeoffs with alternative methods of reducing expansion losses, such as internal heat exchange. A detailed parametric analysis revealed that internal heat exchange could increase cycle COP if the expander efficiency was only 30%, but would substantially decrease COP if the expander isentropic efficiency was 60% [36]. These results were based on a rather large assumed gas cooler outlet approach temperature difference (5 °C), so the impacts would be smaller if the gas cooler were more effective in reducing potential expansion losses (ineffective gas coolers lead to high evaporator inlet quality, hence more potentially recoverable expansion work). Nevertheless, the results of this parametric analysis reflect a fundamental reality: the large difference in specific heats between the suction gas and supercritical hot stream limit the second-law effectiveness of an internal heat exchanger, even as the first-law effectiveness approaches unity. An expander is subject to no such theoretical limit, only practical ones which have to date made internal heat exchange the technology of choice in prototype and production systems.

Maurer and Zinn [41] conducted a theoretical and experimental study of expanders for CO_2, including axial piston machines and gear machines. Measured energy efficiency reached 40–50% for axial piston machines, and 55% for gear machines. The higher efficiency of gear machines was somewhat unexpected, since these did not have any volume expansion (constant-volume machines). Important reasons for these results were lower friction losses and smaller clearances and leakage losses in the gear machine.

Heyl and Quack [42,46] discussed various cycles with expanders, and showed the design and results of a free-piston expander/compressor concept. The machine had two-double-acting pistons, which were connected by a piston rod. Each piston divided the cylinder into a compression and expansion volumes. In order to achieve a balance of forces over the entire stroke, the expansion was conducted at full pressure, i.e. in a ‘square’ process in the pressure–volume diagram. Thus, only about 78% of the available expansion power could be recovered. The machine was intended as a second-stage compressor (from intermediate to high pressure), driven by the expansion work from high to low pressure.

Nickl et al. [47] proposed the design principle of a rather simple second generation expander–compressor that provided a further 10% increase in COP compared with the first generation machine [42,46] and a 50% improvement over the same system with a throttle valve. They speculated that the discharge pressure of the main compressor could be further reduced.

Hesse and Tiedemann [48] showed the possible use of a pressure wave machine for expansion work recovery in a CO_2 system. The pressure wave machine could compress a part of the vapor from the evaporator outlet by using the expansion energy. Adachi et al. [49] showed a combined axial-piston compressor/expander unit with expansion ratio control means that could keep the high-side pressure at the optimum.

Heidelck and Kruse [50] discussed a conceptual design for a CO_2 expander based on a modified reciprocating (axial piston) machine. The expander needs mechanically controlled valves, and the authors showed a concept using a rotating control disc and slots similar to what is used in hydraulic machines. A design concept for a combined compressor–expander machine in one axial-piston unit was also outlined. Experiments on a modified hydraulic machine gave moderate efficiencies due to internal leakage in

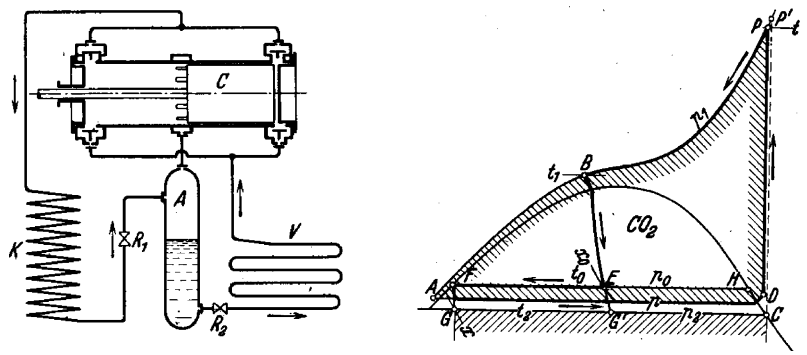

Fig. 24. Voorhees dual-effect compressor circuit (left) and thermodynamic cycle in temperature–entropy diagram (right) [10].

the control disc sealing surfaces. Hesse [51] proposed using a gear machine as expander in CO_2 vehicle air conditioning systems. By using helical gears, acceptable efficiency of the expansion process was predicted.

4.3. Two-stage cycle

The performance deterioration of the basic single-stage cycle can be largely mitigated by using multistage compressors and with intercooling of liquid and vapor refrigerant. In 1905, Voorhees [10] introduced a dual-effect compressor. The principle was that a supplementary suction orifice opened during compression, which allowed the refrigerant to be taken in at two different pressures. Figs. 24 and 25 show Voorhees dual-effect cycle [10], and Plank cycle [39] using an additional 'pump' stage near the expansion valve, respectively. The latter cycle uses two-stage compression, but instead of dividing the pressure rise into two stages, as commonly used, the cycle adds another, higher, pressure level before the compressed refrigerant is cooled. This reduces the enthalpy before throttling, and thus increases the cooling capacity. Due to the high refrigerant density in the second-stage compression, the power requirement is low—almost comparable to a liquid pump. In another publication, Plank [52] found that the intercooling of vapor by evaporation of liquid in a flash intercooler resulted in an increase of COP except for operating conditions near the critical point.

Thiessen [53] devised a two-stage system with single-stage compression, using the intermediate pressure accumulator as a buffer for pressure control. Advantages

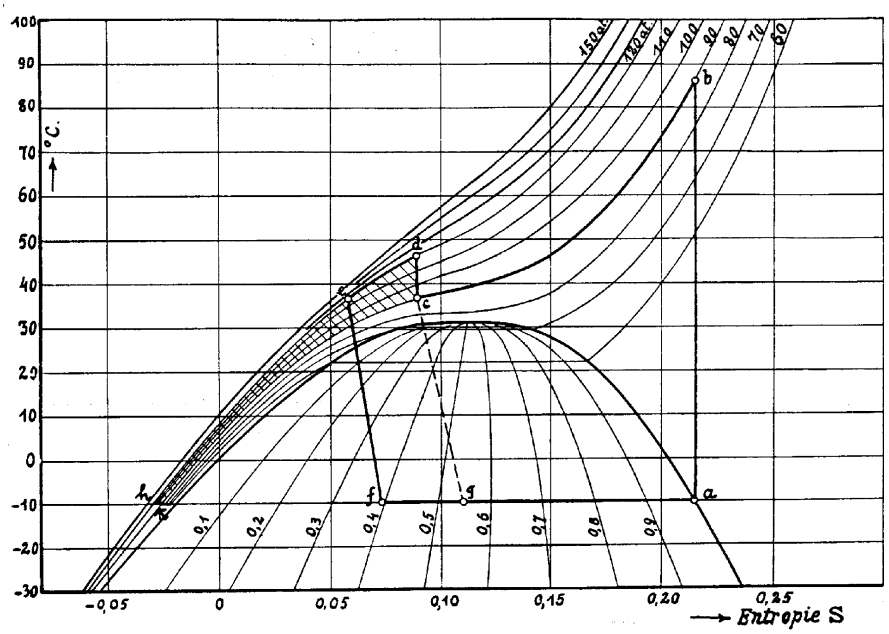

Fig. 25. Plank's two-stage cycle with high-pressure 'pump' [39].

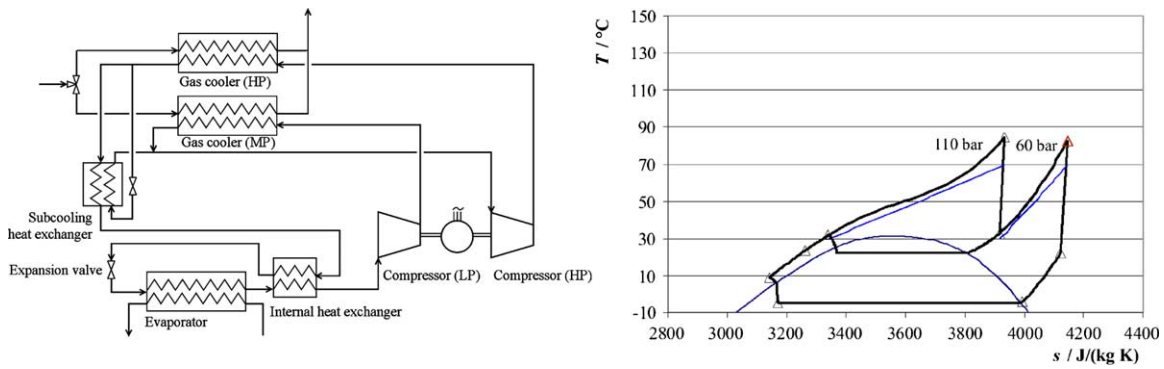

Fig. 26. Two-stage cycle with internal subcooling, internal heat exchange, and parallel heat transfer to heat sink [32,57].

of the concept are claimed to be better liquid distribution to the evaporator, and possibly a better behavior under non-stationary conditions. The need for three control valves is a disadvantage, however.

Ozaki et al. [54] described several circuit arrangements and control principles for cycles having two-stage throttling. By using a 'subcooling' heat exchanger as shown earlier by Lorentzen [32], the COP could be improved while capacity was increased and necessary high-side pressure was reduced. This circuit could have either a low-pressure accumulator or an intermediate-pressure accumulator.

Shunichi and Hiroshi [55] also described some two-stage cycle arrangements, primarily based on conventional circuits for industrial and commercial refrigeration systems. Many similar two-stage concepts are shown by Okaza et al. [56]. Another variant of this two-stage cycle is shown in Fig. 26, in this case with some high-pressure refrigerant being expanded into an internal subcooling heat exchanger operating at intermediate pressure [32,57].

Huff et al. [58] investigated three different variations for a two-stage transcritical CO_2 cycle by using simplified modeling assumptions. A flash cycle, a phase separation cycle, and a split cycle were considered and potential benefits for each cycle with an internal heat exchanger, a suction line heat exchanger, and intermediate cooling between the compressor stages were studied. They speculated that the split two-stage cycle showed the highest performance improvement (38–63%) over the basic single-stage cycle.

Inagaki et al. [59] also found that the capacity and COP of a CO_2 air-conditioning system were improved significantly by using a two-stage split cycle. The capacity and COP for moderate ambient temperature were improved 35 and 20%, respectively, while the increments of the capacity and COP were 10 and 5%, respectively, for higher ambient temperature conditions.

More advanced two-stage cycles may be of interest both to save compression power but also to adapt the heat rejection temperature glide to a heating system. An example of this concept is shown in Figs. 26 and 27, where compression to 6.0 and 11.0 MPa gives heat rejection temperature profiles that match heating of water from 30 to 70 °C in a hydronic heating network [57]. By using an internal heat exchanger the throttling loss is reduced as discussed above.

4.4. Flash gas bypass

Most prototypes of CO_2 systems have employed small-diameter or flat multiport tubes in evaporators to handle high

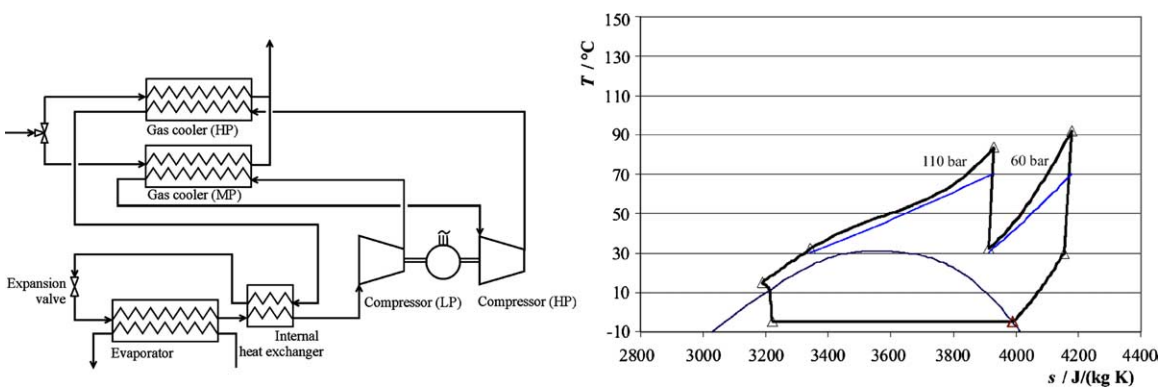

Fig. 27. Two-stage cycle with internal heat exchange and parallel heat transfer to heat sink [57].

pressures without adding weight or bulk. These evaporators face a challenging problem—how to distribute the developing two-phase flow from the header uniformly into so many circuits. Under normal conditions the void fraction at the evaporator inlet exceeds 0.8, and the liquid film and droplets are subject to a complex combination of inertial, gravitational and surface forces inside the header. While this problem is inherent to all microchannel evaporators and is not refrigerant-specific, it is being faced first with CO_2 because its high operating pressures favor the use of small-diameter channels. One approach to dealing with this problem is to install a separator downstream of the expansion device, bypass the vapor around the evaporator, feeding saturated liquid into the evaporator to eliminate altogether the problems of two-phase distribution. This splitting of the flow requires relocating the receiver, for example, from the evaporator outlet where it served to fix the evaporator outlet state to a location upstream of the evaporator where it serves a different purpose. Initial experiments with this approach have proved promising, and are summarized in Section 8.

While these cycle modifications may appear as small changes on a thermodynamic state diagrams, they are nevertheless significant in terms of their effects on improving component performance and increasing the value of services delivered by the system. Often their impacts on control strategies are greater than their impacts on system efficiency. Their benefits and costs tend to be system-specific, as illustrated by many of the prototype systems described in Section 8.

5. Heat transfer and fluid flow

Most studies on heat transfer and pressure drop in CO_2 system have focused on supercritical cooled flow, and flow vaporization, in microchannel tubes and in larger-diameter tubes. The term 'microchannel' is used for flowchannels with hydraulic diameter less than 1 mm. Data on condensation of CO_2 are very scarce, and this mode of heat transfer is not discussed here.

5.1. Supercritical-flow heat transfer and pressure drop

Olson [60] measured heat transfer for cooled supercritical CO_2 flow in a 10.9 mm ID (inner diameter) tube. Comparisons were made between the test data and correlations of Gnielinski [61] and a Krasnoshchekov and Protopopov [62] model developed for supercritical fluids. Olson [60] found that the Gnielinski model underpredicted the measured coefficients, and more so when using wall-based property data than bulk-based. The special supercritical model worked well as long as the temperature was above the pseudocritical temperature, but gave large scattering and overprediction at lower temperatures.

Pitla et al. [63] reviewed the available literature on supercritical CO_2 heat transfer, including:

- Physical factors influencing in-tube forced convection heat transfer
- Deterioration or improvement of heat transfer in the supercritical region
- Effects of buoyancy driven secondary flows on heat transfer in tube flow
- Heat transfer correlations for in-tube flow of a supercritical fluid
- Coefficient of friction of a supercritical fluid, and
- Influence of lubricant on heat transfer

For fully developed flow the supercritical-pressure heat transfer coefficient of CO_2 increases gradually as the flow is cooled, until a peak is reached at the pseudocritical state (maximum isobaric specific heat). Based on the experimental and numerical data of Pitla et al. [63], the use of the Gnielinski heat transfer correlation [61] was suggested, taking the average of calculated coefficient for wall and bulk conditions. Presence of lubricant reduced heat transfer (especially the peak value) and increased the pressure drop.

More extensive investigations of heat transfer in single tubes have been undertaken by several investigators, starting with a thorough literature review [64], to determine whether variations in transport and thermodynamic properties in the vicinity of the critical point have an effect on turbulence and therefore on heat transfer. A detailed model has been developed and verified experimentally for a 5 mm tube [65,66] but at this point there exists insufficient data or reasons to believe that the dependence of heat transfer and pressure drop on fluid properties are not captured adequately by conventional single-phase turbulent flow correlations that have been verified for the appropriate ranges of heat and mass flux and other non-dimensional variables. However, at high heat flux and at conditions close to the pseudocritical state, buoyancy effects and thermophysical property variation may be large, thus making ordinary single-phase correlations incorrect.

Pettersen et al. [67] measured and correlated heat transfer of cooled supercritical CO_2 flow in 0.8 mm microchannel tubes. The standard single-phase correlations such as the widely used Dittus–Boelter model and the Gnielinski correlation [61] gave good correspondence between measured and calculated heat transfer coefficient, and the Colebrook and White correlation reproduced the pressure drop data well.

Recently, Liao and Zhao [27] measured heat transfer coefficients from supercritical CO_2 flowing in horizontal micro/minitubes. Test tubes were stainless steel tubes having inside-diameters of 0.5, 0.7, 1.1, 1.4, 1.55 and 2.16 mm, respectively. A series of test were conducted for

the pressures and temperatures ranging from 7.4 to 12 MPa and 20–110 °C, respectively. The buoyancy force affected supercritical CO_2 flow significantly. The buoyancy effect became smaller as the tube diameter decreased, however. They reported that the existing correlations for larger tubes deviated notably from their test data for the micro/minitubes. Based on the test data, they developed a correlation for the axially averaged Nusselt number with the mean relative error of 9.8%.

5.2. Flow vaporization heat transfer and pressure drop

Bredesen et al. [24] measured heat transfer and pressure drop for flow vaporization of pure CO_2 in a horizontal 7 mm ID (inner diameter) aluminum test tube. The heat transfer test data indicated regimes of convective boiling at high mass flux and low evaporating temperature, and nucleate boiling regimes at lower mass flux and higher temperatures. At most conditions, the local heat transfer coefficient increased up to a vapor fraction of around 0.9, but at the highest evaporating temperature (5 °C), the behavior was quite different, with a decreasing heat transfer coefficient at increasing x. In the latter case ($G = 200$ kg/m^2 s, $T = 5$ °C, $q = 6$ kW/m^2), the heat transfer coefficient dropped from about 14,000 W/m^2 K at $x = 0.2$ to about 8000 W/m^2 K at $x = 0.9$. The authors explained this by the high pressure and low liquid/vapor density near the critical point. A comparison to a few common heat transfer correlations gave poor correspondence for all test data, the experimental coefficients being about twice as high as predicted.

Rieberer [14] found that common heat transfer correlations gave considerably higher predicted heat transfer coefficients than his experimental data from a rig where there was some compressor lubricant in the CO_2 flow. Models that gave best fit to the data of Bredesen et al. [24] overpredicted the experimental data of Rieberer [14] by a factor of 3–4. These large differences were probably caused by the presence of lubricant and the data gives some indication of a possible serious impact of lubricant on nucleate boiling heat transfer. Further test data by Rieberer [14] on a 10 mm tube (still including lubricant) shows that the heat transfer coefficient is almost unaffected by a doubling of the heat flux, and that the coefficient increases with mass flux. Both these observations indicate that nucleate boiling is not a dominant mechanism of heat transfer, or that this mechanism is suppressed by a lubricant concentration.

Sun and Groll [68] conducted flow vaporization experiments for pure CO_2 on a horizontal 4.6 mm ID (inner diameter) stainless steel tube. Test data were recorded at CO_2 mass flux between 500 and 1670 kg/m^2 s, heat flux 10–50 kW/m^2 and vapor fraction 0–0.95. Evaporating temperatures were maintained between −2 and +10 °C. In general, the heat transfer coefficient dropped at increasing x. A more or less abrupt drop in heat transfer above a vapor fraction of 0.4–0.6 was observed in most tests, and was explained by dryout of the liquid film. The heat transfer was not influenced much by varying mass flux at low vapor fractions, while heat flux variation had significant influence. This was taken as evidence of nucleate boiling as the dominant heat transfer mechanism at lower x. The heat transfer after dryout was influenced by mass flux, indicating a convection-dominated heat transfer.

Hihara and Tanaka [69] conducted measurements on a horizontal stainless steel microchannel test tube with 1 mm internal diameter. The authors measured very high heat transfer coefficients (around 10–20 kW/m^2 K) in the nucleate boiling regime at low vapor fractions. At the onset of dryout the coefficients dropped abruptly to only a small fraction of the nucleate boiling level. Onset of dryout occurred at a vapor fraction of around 0.8 at a mass flux of 360 kg/m^2 s, decreasing to 0.4 at a mass flux of 1440 kg/m^2 s.

Pettersen [20] conducted extensive studies on flow vaporization in microchannel tubes, using an aluminum test tube with 25 channels having 0.81 mm diameter. Vaporization heat transfer and pressure drop data were recorded over a wide range of conditions, including temperatures (0–25 °C), heat flux (5–20 kW/m^2), mass flux (190–570 kg/m^2 s), and vapor fraction (0.2–0.8). Test results showed that the nucleate boiling mechanism dominated at low/moderate vapor fractions. Dryout effects became very important at higher mass flux and temperature, where heat transfer coefficient (h) dropped rapidly at increasing vapor fraction (x). Heat transfer coefficients were correlated using a combination of models for nucleate boiling, convective evaporation, dryout inception, and post-dryout heat transfer.

Microchannel frictional pressure drop was correlated using the 'CESNEF-2' correlation by Lombardi and Carsana [70], with a mean/average deviation of 16.4/−1.1%. Special small-tube correlations from literature did not reproduce the test data well.

5.3. Two-phase flow patterns

Pettersen [20] conducted experiments for two-phase flow patterns at a temperature of 20 °C and for mass flux ranging from 100 to 580 kg/m^2 s, using a heated glass tube with 0.98 mm ID. The observations showed a dominance of intermittent (slug) flow at low x, and wavy annular flow with entrainment of droplets at higher x. At high mass flux, the annular/entrained droplet flow pattern could be described as dispersed. The aggravated dryout problem at higher mass flux could be explained by increased entrainment. Stratified flow was not observed in the tests with heat load. Bubble formation and growth could be observed in the liquid film, and the presence of bubbles gave differences in flow pattern compared to adiabatic flow.

The flow pattern observations on CO_2 did not fit any of the generalized maps or transition lines, including the map proposed by Kattan et al. [71]. Only the intermittent–annular

transition prediction of Weisman et al. [72] was close to the observed behavior. Compared to small-diameter observations with air/water at low pressure, the transition into annular flow occurred at much lower superficial vapor velocity (superficial velocity of approximately 0.5 m/s).

6. Issues related to high operating pressure

Pressures in CO_2 systems are typically 5–10 times higher than with conventional refrigerants, and this gives several effects that influence the design of components and their performance, in particular regarding compression and compressor design, and heat transfer and heat exchanger design In addition, high pressure may create perceived safety problems unless the underlying issues are addressed properly.

6.1. High pressure compression

Compressors in CO_2 systems will operate at high mean effective pressure and with large pressure differentials, but the pressure ratios will be quite low due to operation close to the critical point Fig. 28 indicates ideal (with 4% clearance volume) pressure/volume diagrams for compression of R-134a and CO_2 with equal cooling capacity at 0 °C [31]. As may be observed, the displacement of the R-134a machine is 6.7 times larger, and the pressure ratio (π) is 5.0 as compared to 3.1 with CO_2. Re-expansion losses are much smaller in CO_2 process. Owing to the higher pressure level and the different shape of the pV-diagram, the negative effect of valve pressure drops tends to be small in CO_2 compressors, thus giving higher efficiency. The compressor for the transcritical CO_2 cycle requires thicker walls to contain the high operating pressure, but since the volumetric capacity of the fluid is large, the compressor itself will

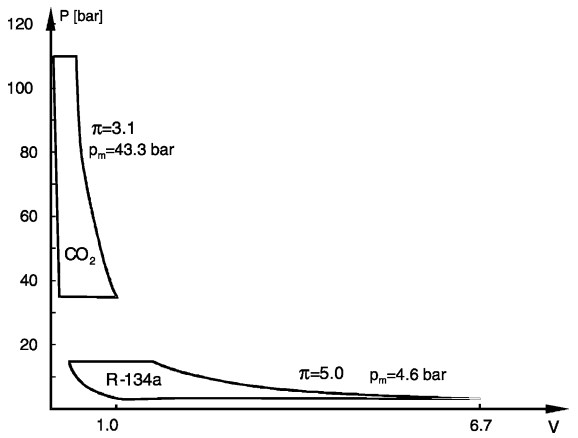

Fig. 28. Compressor pressure/volume diagrams for R-134a and CO_2, assuming equal cooling capacity (π : pressure ratio, p_m : mean effective pressure).

actually be smaller than refrigeration compressors for the same capacity using conventional refrigerants [73].

Internal leakage losses in valves and as piston blow-by were initially expected to be a problem with the large pressure differentials in CO_2 compressors. With appropriate design it has been shown that these losses account for less than 1% difference in cylinder charge compared to a zero leakage model [74], leading to the conclusion that the influence of leakage can be neglected in properly designed lubricated reciprocating compressors. This conclusion is supported by other investigations [75] measuring piston blow-by rates of 1.1–2.8% of the compressed mass flow at 9.0/3.5 MPa discharge/suction pressure.

6.2. High pressure heat transfer

Tolerable pressure drops in heat exchangers become higher as the pressure level increases, and this gives a possibility of improving heat transfer through higher flow velocities in high-pressure systems. This is of particular importance for single-phase heat transfer in the gas cooler of CO_2 systems. High pressure and proximity to the critical point gives increased specific heat, again leading to improved convective heat transfer.

Evaporator pressure drop leads to reduced temperature differences due to the corresponding drop in saturation temperature. Pettersen [31] showed how the relation between pressure drop and temperature loss in evaporators, i.e. the slope of the saturation pressure curve, was very different for CO_2 than for conventional refrigerants, since the pressure level of CO_2 was much higher. Nucleate boiling heat transfer is also affected to a large extent by pressure, since the wall superheat needed to initiate boiling becomes lower as the critical pressure is approached.

Owing to the higher pressures, optimum compact heat exchanger designs for CO_2 generally tend to use small-diameter flow channels, in many cases based on extruded ‘multiport’ tubing with parallel flow of refrigerant in several tubes and flow channels. In some cases it may be more economical to use conventional flat-fin/round-tube heat exchangers with small-diameter tubes. Also in this case, the internal diameter will most likely be smaller than for conventional refrigerants. Pettersen et al. [76] showed some compact heat exchanger concepts for CO_2 air conditioning systems having internal tube diameter of 2 mm.

6.3. Compactness of equipment

Low-side refrigerant line diameters (inner diameter) are typically reduced by 60–70% compared to HFC systems, due to the higher vapor density and flow velocity. High-side piping dimensions will also be reduced. Assuming a wall thickness that is more or less the same as in HFC piping of equal capacity, the pressure capability will be sufficient for CO_2 due to the reduced diameters

(inner diameter). For the same reasons as above, the compressor displacement is reduced by 80–85% for a given capacity. Compressor and heat exchanger size and weight reductions seem possible due to the reduced refrigerant-side volumes and cross-sections.

6.4. High-pressure safety issues

In general, the hazards of refrigerants and vapor compression systems are associated with the physical and chemical characteristics of the refrigerant as well as with the pressures and temperatures occurring in the system. Factors discussed by Pettersen et al. [77] in relation to CO_2 were

Flammability. CO_2 is non-flammable, and it is even used as a fire-fighting or fire-preventing gas. Thus, flammability is not an issue.

Inhalation safety. Although CO_2 is usually regarded as non-toxic there are physiological effects from breathing air with a CO_2-concentration above a few percent. At 2–3% concentration by volume, the breathing rate will increase, and headache may be experienced after some time. The IDLH (Immediate Danger to Life and Health) concentration is set to 4% [78], and the lowest reported lethal concentration is 10% [79]. In practice, a maximum allowable concentration of about 5% by volume seems to be a reasonable limit [79,80]. In the design and operation of CO_2 systems, this will be the maximum acceptable concentration as a result of sudden release or prolonged leakage of CO_2 into occupied space. The assessment of hazards resulting from accidental leakage of CO_2 into occupied space should consider factors like

- rate of CO_2 outflow at decreasing system pressure,
- formation of dry ice inside system at 0.52 MPa system pressure,
- amount of CO_2 dissolved in lubricant,
- room/cabin ventilation rate, and
- stratification (CO_2 is heavier than air).

Frost burn is probably not a problem with CO_2 since the triple point is at 0.52 MPa, i.e. there will be no boiling refrigerant at atmospheric pressure. Also, the toxic or irritating effects from decomposition products known to occur when fluorocarbon refrigerants contact flames or hot surfaces will not occur with CO_2.

Explosion or rupture of a pressurized component or vessel. The hazards may include blast effects and shocks, as well as flying fragments. Such incidents may be caused by a number of factors, such as malfunctioning safety device, overheating, over-charging, incorrect operation, construction weakness/corrosion, mechanical impact, etc. Low-side pressures in CO_2 systems are typically 3–4 MPa, and high-side pressures may be as high as 12–14 MPa. These pressures are 5–10 times higher than in traditional fluorocarbon systems. High pressure is not a safety issue in itself, since the equipment will be designed for this. In case of a component rupture, however, the explosion energy (stored energy) may characterize the extent of potential damage. The explosion energy can be estimated based on component (refrigerant-side) volumes, pressures and refrigerant property data. The possible occurrence of a BLEVE (Boiling Liquid Expanding Vapor Explosions) may create a more severe blast effect than by an ordinary refrigerant expansion. The following sections will address the two last issues—explosion energy and BLEVE—based on calculations and experimental data.

6.4.1. Explosion energy

The explosion energy can be estimated as the energy released by expansion of the refrigerant contained in a component or system The expansion process will be very rapid, with little or no time for heat transfer between the ambient air and the expanding gas, and the explosion energy can therefore be estimated as the reversible adiabatic (isentropic) work of expansion.

A detailed analysis of explosion energies should consider the refrigerant charge inside each component, as well as the local pressure, temperature and vapor fraction. In the current analysis, pressures are assumed to be equalized and temperatures uniform throughout the system. As a consequence, the charge and volume are assumed to reflect the refrigerant condition inside the entire system. When the temperature of the system is varied, the charge/volume ratio will remain constant (constant average specific volume), and pressure will vary either as saturation pressure, or as pressure along a constant-volume (isochoric) line in the gas region.

Pettersen [81] calculated and compared the explosion energies of equal-capacity (7 kW) ductless split residential air conditioning systems with R-22 and CO_2 as refrigerant. The R-22 system was based on flat-fin/round-tube heat exchangers, while the CO_2 prototype system had all-aluminum microchannel heat exchangers. Even though pressures were higher in the CO_2 system, reductions in internal volume and refrigerant charge gave comparable energy levels in the two systems. At room temperature, the CO_2 system energy was higher, while at elevated temperature that may occur in a fire the R-22 energy was highest. For the R-22 system, the total volume occupied by refrigerant was approximately 11.4 l, of which 0.7 l (6%) was in the indoor unit and 8.5 l (75%) in the outdoor unit. The remaining volume was in the 10 m of piping between the two units. The average refrigerant density in the system was then 300 kg/m^3 (3.5 kg charge/11.4 l refrigerant volume). Corresponding data for the CO_2 prototype system were: 4.2 l total volume, 0.27 l (6%) in the indoor unit and 3.3 l (78%) in the outdoor unit, and an average charge density of 260 kg/m^3 (1.1 kg/4.2 l). Fig. 29 shows the total explosion energies (in kJ) for the two systems at varying initial temperature. The energies are equal around 60 °C,

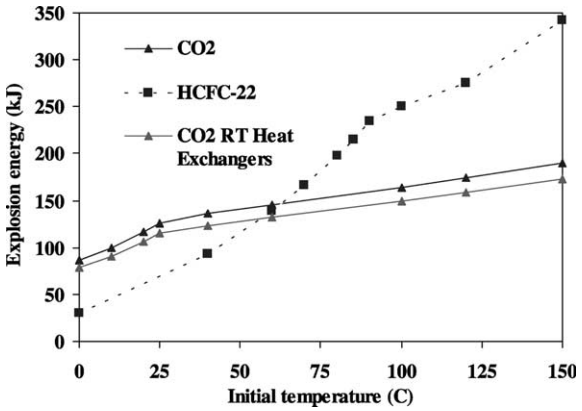

Fig. 29. Calculated total explosion energy for R-22 system and CO_2 system at varying initial temperature. Data for a CO_2 system with optimized round-tube (RT) heat exchangers is also shown [81].

but the R-22 system energy is more sensitive to temperature than the CO_2 system.

The above system data show that owing to the smaller volume and refrigerant charge in a CO_2 system, the actual explosion energies are in the same range. As may be observed from Fig. 29, the ratio of energies (CO_2/R-22) is about 2 at room temperature, and 0.7 at 100 °C. The difference in energy becomes significant at temperatures above 120–130 °C, and in an extreme situation such as a fire, the energy release from a R-22 system is likely to be much higher than from a CO_2 system. In both systems the refrigerant volume in the indoor unit is only about 6% of the total volume, so the largest potential energy release is clearly in the outdoor unit containing the accumulator, receiver (R-22 system) and compressor.

Calculations for R-134a and CO_2 mobile air-conditioning systems showed similar results [82]. The CO_2 system explosion energy typically ranged from 40 to 80 kJ, while the baseline R-134a system ranged from 20 to 80 kJ. Again, the baseline system energy was smaller at normal temperatures, but became higher at elevated temperature. Although, an explosion caused by the combustion of a flammable refrigerant is an entirely different scenario, it may be worthwhile to note that the energy released by combustion of one kilogram of propane (R-290) is 46,000 kJ (lower heating value).

6.4.2. Boiling liquid explosion

The duration of the energy release may be of equal importance as the amount of energy released. An important consequence of a possible explosive vaporization is shorter duration and thereby a more severe blast effect than from ordinary refrigerant expansion, even though the energy is the same. In the assessment of safety issues, the possible occurrence of rapid phase transition phenomena is important. Mechanisms of explosive vaporization discussed in the literature include BLEVE and BLCBE (*Boiling Liquid Collapsed Bubble Explosion*). These phenomena may occur when a vessel containing a pressurized liquid or supercritical fluid is rapidly depressurized, e.g. due to an initial crack or rupture. The sudden depressurization gives a superheated liquid phase that is suddenly vaporized in an explosive manner. This may give a transient overpressure peak inside the vessel, which again may lead to a powerful burst of the whole vessel, with total loss of content, a resulting blast wave and risk of flying fragments. Pettersen and Hakenjos [83] and Pettersen [84] investigated the possible occurrence of BLEVE/BLCBE in CO_2 vessels.

An important reason for considering the possible occurrence of BLEVE with CO_2 is a paper by Kim-E and Reid [85], which pointed to this possibility. The authors applied a thermodynamic model based on the spinodal fluid state, which represents the limit-of-stability for the liquid phase during expansion. In a rapid expansion process, homogeneous nucleation will occur at this state. The predicted shock effects or pressure spikes did not occur in their experiments on CO_2 using a 7-l tank with a 1.5 in. diameter burst disc, however. Reasons for disagreement between theory and experiments may include factors like vapor bubbles on the wall of the vessel and shock waves or disturbances from the mechanism that ruptured the burst disc of the test vessel. The presence of vapor bubbles before depressurization may have given heterogeneous nucleation instead of the homogeneous nucleation required for a BLEVE.

In the general literature on BLEVE, a majority of publications discuss hydrocarbon (LPG, propane) tank explosions. The key safety issues in such incidents are the ignition and combustion of the flammable content when this is vaporized, creating severe damage due to shock waves and burning. Usually, this situation arises due to a fire near the tank or due to an ignition source that starts an explosion of the escaped gas/vapor cloud. The concept of a 'cold' BLEVE is not much focused on, and the few publications that report accidents with CO_2 storage tanks generally do not mention BLEVE effects [86,87].

Pettersen and Hakenjos [83] and Pettersen [84] reported from extensive experiments on a CO_2 test vessel of 1.0 l volume, using burst discs to initiate rapid depressurization. They did not observe significant overpressure spikes in any of their tests at 3.5, 4.5, 6.0 and 10.0 MPa initial pressures with varying liquid fill level and discharge opening, although quite large pressure oscillations in a millisecond-scale occurred in some experiments. The maximum observed pressure amplitude was 0.6 MPa, and the maximum overpressure spike was 0.3 MPa (7% above initial pressure). The authors found that thermal shock effects on the pressure sensors were significant and had to be avoided or corrected for. What initially appeared to be significant overpressure spikes later turned out to be a result of thermal shock caused by the top pressure sensor being contacted by the swelling cold liquid inside the test vessel. It is not clear if similar thermal shock effects have influenced overpressure spikes reported by other authors. Graphs shown by Venart

and Ramier [88] for a 2.4 l R-22 vessel, for instance, have a quite similar shape to graphs from the present tests before the top pressure sensor was insulated. The results have thus not given any reason to expect BLEVE in CO_2 system accumulators or receivers. In real systems the presence of compressor lubricant, particles and contaminants, as well as unstable pressure/temperature, would make homogeneous nucleation even less likely.

Graz and Stenzel [89] outlined a new draft SAE safety standard (J639) for mobile air conditioning and heat pump systems, also including CO_2. Proposed rules for CO_2 (R-744) included:

- Carbon dioxide (CO_2) air-conditioning systems and integrated systems for heating and cooling (heat pumps) shall have a pressure blow-out disk as the overpressure relief device on both the high and low-pressure sides of the system when operating in the heating or cooling modes. The blow-out disc on the high-pressure side shall have a maximum allowable release pressure of 16 MPa, when the system is operating in the cooling mode and a maximum allowable release pressure of 12 MPa when the system is operating in the heating mode. The blow-out disc on the low-pressure side shall have a maximum allowable release pressure of 12 MPa, when the system is operating in the heating or cooling modes.
- Components on the high-pressure side of the system shall have an ultimate burst pressure, when tested at the highest temperature reached by said component under typical operating conditions, which is not less than two times the release pressure of the Pressure Relief Device. In addition, components on the high-pressure side of the system shall have an ultimate burst pressure, when tested at the highest temperature reached by said component under typical operating conditions and after appropriate exposure to the system operating conditions (temperature, pressure, pressure cycling, vibration, corrosion), that is not less than 1.5 times the release pressure of the Pressure Relief Device.
- Components on the low-pressure side of the system shall have an ultimate burst pressure, that is not less than two times the release pressure of the Pressure Relief Device.
- For safety relevant pressurized components of air-conditioning systems and integrated systems a proof of integrity shall be carried out (by calculations, experiments or by a combination of both). Basis is the knowledge about the operational loadings and demanded lifetime of the components as well as of the specific behavior of the used structural material and its process treatment. The proof of integrity shall be carried out against (i) bursting, (ii) failure by fatigue, respectively, creep fatigue due to cycling pressure (pressure cycles between the conditions: system 'in operation'—'out of operation', and (iii) failure by cruising vibrations. Creep fatigue instead of fatigue only has to be considered in case of some structural materials (e.g. aluminum alloys) which point out a time and temperature dependent behavior yielding to a decrease in strength over the time at elevated temperatures.

7. Component design

7.1. Compressors

The vapor pressure of CO_2 is higher than conventional refrigerants and the transcritical CO_2 cycle operates at much higher pressures than the conventional vapor compression systems. Higher pressure gives special requirements regarding the design of suitable components, especially compressors for the CO_2 systems. As the compressor is one of major components of air-conditioning and refrigeration systems and has an important effect on the system performance, compressor technology for the CO_2 transcritical systems has reached an advanced level after years of development. Some examples are recent compressor models shown by Parsch [90], and Bullard [91]. Parsch [90] exploited the potential for a compact design with CO_2 as shown in Fig. 30. Fig. 31 shows a 155 cm^3 R-134a compressor next to a 21 cm^3 CO_2 compressor [91]. The relationship between a compressor's mass and its displacement rate is not an obvious one, and will depend on specific design tradeoffs involving piston diameter and stroke and number, rpm, materials, etc. There is no evidence at the present time to suggest that

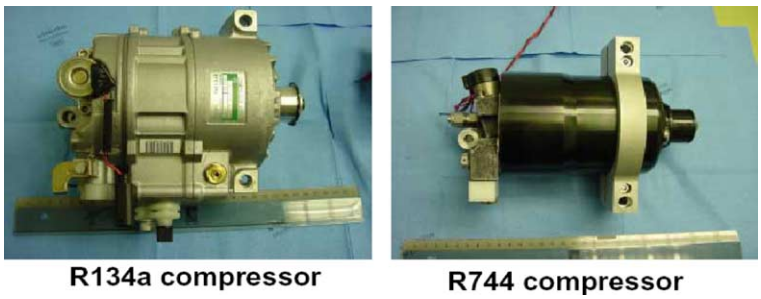

Fig. 30. Mobile air-conditioning compressors with variable displacement. State-of-the-art R-134a design (left) and a recent design for CO_2 (right) [90].

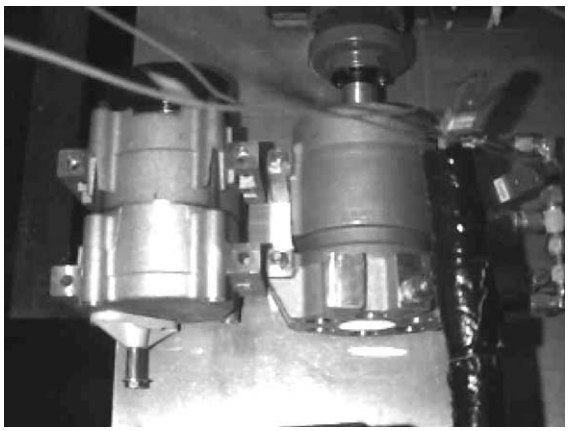

Fig. 31. A 155 cm^3 R-134a compressor (left) next to a 21 cm^3 CO_2 compressor (right) [91].

switching to higher-pressure refrigerants for their capacity advantages would necessarily entail substantial weight penalties in the compressor.

Fagerli [92] evaluated the possibilities for transcritical compression of CO_2 in small hermetic reciprocating compressors, through a theoretical and experimental study. A single-cylinder 2.6 cm^3 hermetic prototype machine with flanged shell was built and instrumented, using some parts from a R-22 machine. Measured isentropic efficiencies for the CO_2 compressor were 9–15% lower than the R-22 machine, while volumetric efficiency was less than 5% lower. These results were considered as promising considering the early stage of development. Theoretical models indicated a potential for higher energy efficiency with CO_2 than with R-22. Lubricant temperatures were acceptable at 15 and 0 °C evaporation, while at −15 °C oil cooling was necessary. Fagerli [92] used mineral oil and had to use a three times higher viscosity grade than for the R-22 machine due to the viscosity reduction caused by dissolved CO_2.

Süss and Kruse [93] reported that high compressor performance could be achieved due to the lower pressure ratio of the transcritical compression process with CO_2. Leakage may have strong influence on the CO_2 compressor performance since the pressure difference is extremely high, but the effect of leakage on the compressor performance can be reduced to a reasonable amount with an appropriate design of the machine. On the other hand, the pressure losses inside a CO_2 compressor have a small influence on the energetic and volumetric efficiency of the compression process.

Süss [94] was quite concerned about internal leakage losses in CO_2 compressors, and did not leave rotary designs (scroll, rotary vane, and rolling piston) much chance for achieving acceptable efficiency. His primary focus was thus reciprocating compressors with piston rings.

Nekså et al. [95] developed a series of semi-hermetic reciprocating CO_2 compressors in the range of 1.7–10.7 m^3/h swept volume. The series comprises single- and two-stage compressors with two cylinders, running at nominal speeds of 1450 and 2900 rpm (50 Hz). This corresponds to cooling capacities in the range of 3–25 kW at −10 °C evaporating temperature. Measurements of compressor efficiencies were presented for a single- and a two-stage compressor in the lower capacity range of the compressor series. The isentropic and volumetric efficiencies were relatively good, taking into consideration that this was a pre-series compressor. At a pressure ratio of 2.6, which was representative for a heat pump water heating application, overall isentropic (including electric motor) and volumetric efficiencies of 0.69 and 0.77 were measured for the single-stage compressor, respectively. There was some leakage in both valves, however, and the stiffness of the discharge reed valves had to be reduced, in order to avoid valve fluttering. Attention should also be given to reduce heat transfer to the suction gas, which may reduce the efficiencies significantly at high pressure ratios.

Measurements on a two-stage version of the compressor [96] showed a potential for 20% COP improvement. This machine was intended for lower-temperature applications, e.g. in commercial refrigeration at freezing temperatures. Two-stage compression may also be of interest in relation to energy saving in air conditioning and heat pump processes, however. Polyolester (POE) lubricant was used in both versions of the compressor.

Suzai et al. [97] and Tadano et al. [98] developed a hermetic two-stage rolling piston compressor (Fig. 32) with a nominal power of 750 W. Compressing in two stages and letting the pressure inside the shell correspond to

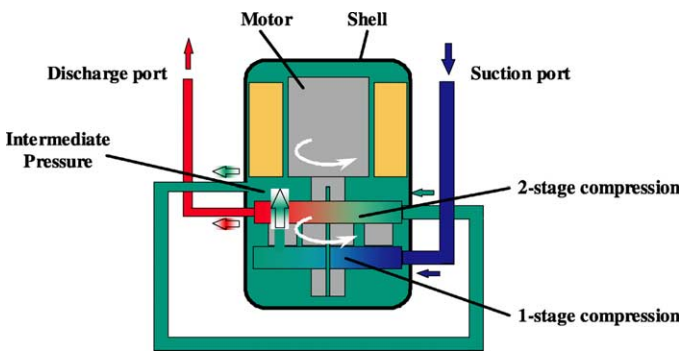

Fig. 32. Schematic of a hermetic two-stage rolling piston CO_2 compressor [98].

Table 2
CO_2 compressor developments in Japan [106]

Companies	Field	System	Compressor	
Denso	Mobile air-conditioning	Direct expansion	Open-type	Swash
Zexel				Swash
MHI				Scroll
Sanyo	Tap water heat pump	Direct expansion	Hermetic	Rotary
TEPCO, Denso and CRIEPI				Scroll
Mayekawa	Commercial	Indirect ice storage	Hermetic	Screw
Matsushita	Residential	Direct expansion	Hermetic	Scroll
Daikin				Swing

the intermediate pressure could reduce internal leakage losses. The machine also became better balanced by having two rolling pistons in 180-degree phase difference. The shell design was comparable to compressors for room air conditioners, and by using high-strength steel the shell could withstand 25 MPa pressure with the same thickness as for R-410A compressors.

Fukuta et al. [99] analyzed the potential for sliding vane machines in CO_2 compression and expansion. Through a mathematical model the influence of various design parameters were analyzed. Leakage flows were the dominant source of losses in the machine, and clearances had to be reduced compared to conventional machines in order to get acceptable efficiency. Vane contact forces and resulting friction losses were high, but could be reduced by pressure equalization on the vane sides. An interesting option was to build a combined compressor/expander unit.

Hiwada and Hokotani [100] and Ohakawa et al. [101] suggested the use of a swing type rotary compressor in what appears to be an air-source heat pump water heater using CO_2 as refrigerant.

Fagerli [102] conducted a theoretical study on scroll compression of CO_2, finding that reduced clearances and axial/radial compliance were needed in order to limit internal leakage flows. Calculations for 134a and CO_2 compressors showed that in order to have equal influence from leakage on energy efficiency the clearances had to be reduced to less than half in the CO_2 machine.

Hasegawa et al. [103] conducted an experimental and theoretical study of a hermetic CO_2 scroll compressor of cooling capacity of 4.3 kW. The compressor displacement was 7.23 cm^3. Relatively low energy efficiency (47%) was measured, while the volumetric efficiency (87%) was quite good. A loss analysis showed that the thrust bearing accounted for approximately 40% of the total loss, and the design of this part had to be modified.

Denso Corporation [104] has developed a single-stage semi-hermetic scroll compressor, but any details on this machine have not been published.

Baumann and Conzett [105] has been developing an oil-free four-cylinder reciprocating compressor prototype with about 500 W power input. Experiments have shown acceptable energy efficiency. A major issue is cost of production due to materials and tolerance requirements.

Süss [106] aims to produce a complete range of machines working with hydrocarbons and CO_2 both for air conditioning and refrigeration. A design study considered a hermetic single-cylinder reciprocating compressor. Süss [106] gave a summary of compressor developments in Japan as shown in Table 2.

The screw compressor by Mayekawa (MYCOM) is a larger machine built for a prototype system of 120 kW cooling capacity. According to Sasaki et al. [107] the compressor is an open-type screw, so the information on a hermetic screw compressor in the table is most likely an error.

The European company Dorin developed the first high-pressure semi-hermetic CO_2 compressor series in the range of 1.7–10.7 m^3/h swept volume [108]. The series comprises single- and two-stage compressors with two cylinders, running at nominal speeds of 1450 and 2900 rpm (50 Hz). This corresponds to cooling capacities in the range of 3–25 kW at $-10\,^{\circ}C$ evaporating temperature. Fig. 33 shows a picture of the compressor, and measured overall isentropic and volumetric efficiency figures for medium sized compressors at the current stage of development [108].

7.2. Heat exchangers

Heat exchangers for mobile and unitary equipment are designed with a finned air-side surface and usually have more than 700 m^2 surface area per m^3 core volume. This ratio is the loosely defined limit for a compact heat exchanger. The heat exchangers may be mechanically expanded flat-fin/round-tube units or brazed aluminum cores, in both cases various enhancements are used on the air and refrigerant side as shown in Fig. 34.

The high working pressure and favorable heat transfer properties of CO_2 enable reduced tube diameters and small refrigerant-side surface areas. Since these reductions may give room for more air-side surface per unit core volume, the compactness can be increased. Depending on the heat

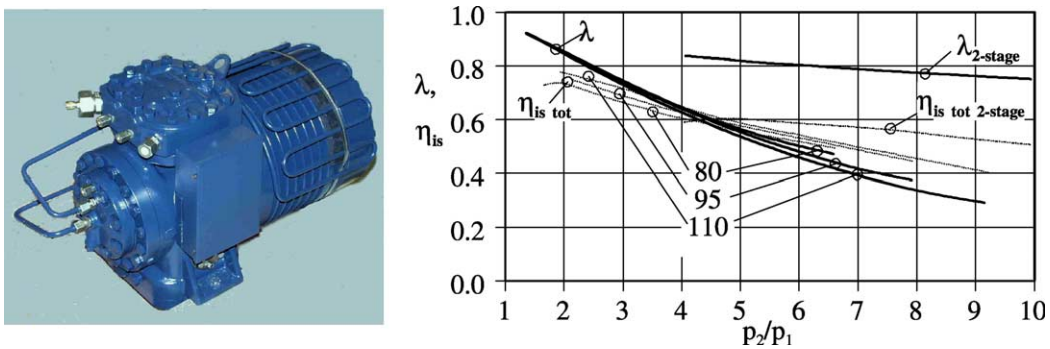

Fig. 33. Compressor design and measured volumetric and isentropic efficiency for a single-stage and a two-stage pre-series CO_2 compressor with a swept volume of 2.7 m^3/h, as function of the pressure ratio, for high-pressures of 80, 95 and 110 bar. A constant suction gas superheat of 10 °C was applied. For the two-stage compressor the intermediate pressure gas was cooled to 20 °C [108].

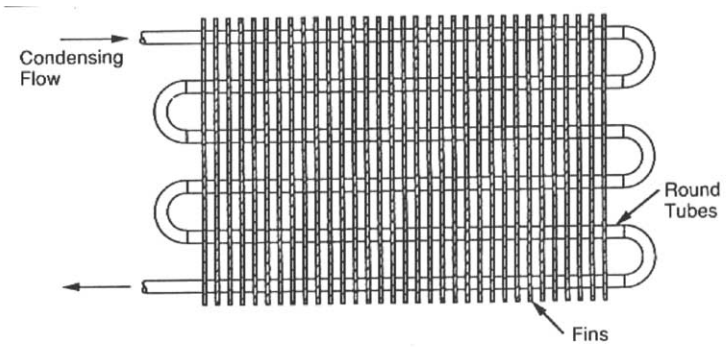

(a)

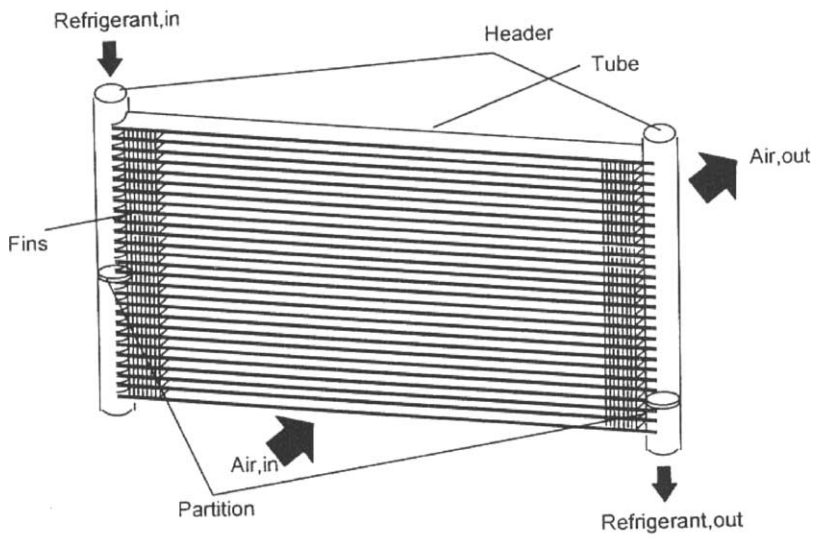

(b)

Fig. 34. Fin-and-tube and brazed aluminum microchannel condensers. (a) Serpentine circuited round-tube condenser, (b) parallel flow brazed aluminum automotive air-cooled condenser.

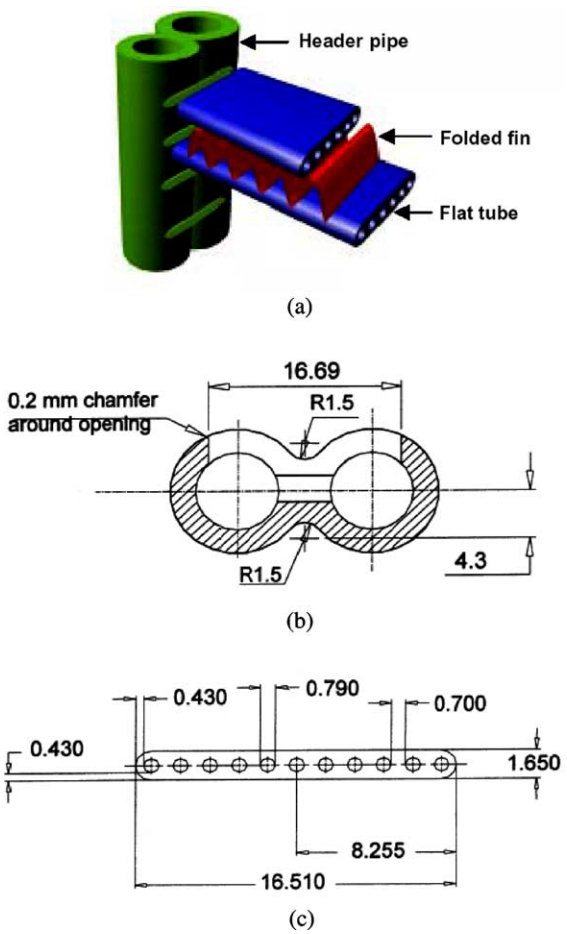

Fig. 35. A prototype microchannel CO_2 gas cooler for a car air-conditioning system [76]. (a) Geometry of heat exchanger, (b) cross-section of header pipe, (c) flat microchannel tube.

exchanger type, the size and mass of high-pressure manifolds or headers may offset some of these advantages. Innovative solutions that benefit from reduced refrigerant-side volume are therefore needed.

Pettersen et al. [76] reported microchannel heat exchangers (gas cooler and evaporator) could be used for CO_2 air-conditioning systems, but several issues remained to be investigated, including frosting formation of outdoor heat exchangers and condensate drainage at low face velocity, for residential systems. Figs. 35 and 36 show gas cooler and evaporator configuration designed by Pettersen et al. [76]. Even though small-diameter round-tube heat exchangers can achieve low weight and compact design for a high-pressure fluid like CO_2, the added performance and compactness of brazed microchannel heat exchangers make these very attractive especially in transport applications.

7.2.1. Gas coolers

To handle the high pressures associated with the CO_2 cycle many CO_2 systems employ heat exchangers with flat multiport (microchannel) tubes as shown in Fig. 35. This technology, with its folded louvered fins, provides additional benefits as a byproduct. Compared to conventional flat-fin/round-tube designs, microchannel heat exchangers increase refrigerant-side area by about a factor of three, and have far less air-side pressure drop due to the streamlined profile presented by the tubes. The flat tubes enable higher face velocities that increase the air-side heat transfer coefficient. Because of high investment costs, microchannel heat exchangers for fluorocarbon refrigerants have appeared first in high-volume applications where compactness is valued.

The flat-fin/round-tube condenser technology for mobile air-conditioning system has now been mostly replaced in automotive applications by flat-tube microchannel condensers as shown in Fig. 34(b). The difference in free flow area

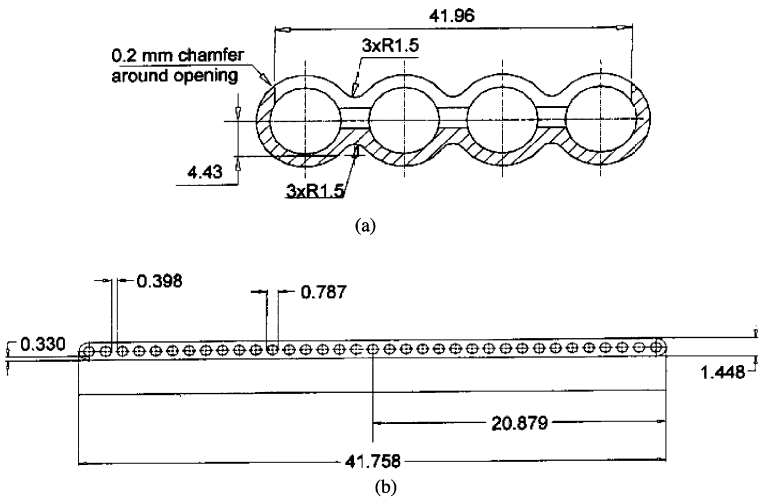

Fig. 36. Cross-section of the header pipe and microchannel tube of a prototype CO_2 evaporator for a car air-conditioning system [76]. (a) Cross-section of header pipe, (b) flat microchannel tube.

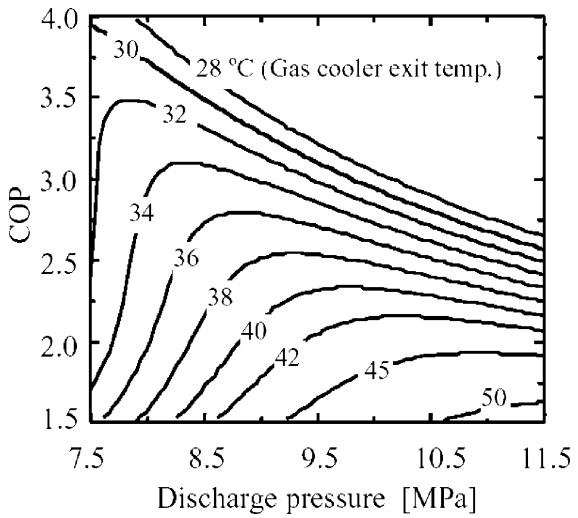

Fig. 37. Effect of gas cooler exit temperature on transcritical cycle COP for realistic high-side pressures.

is obvious, owing to the fact that the flat tubes are usually less than 2-mm thick. What they have in common is their single slab cross-flow configuration that exposes all tubes to the inlet air. Some of the early theoretical analyses of CO_2 system performance assumed that both indoor and outdoor heat exchangers would be of conventional flat-fin/round-tube design [36].

One issue in compact gas cooler design is internal conduction due to large temperature differences across small lengths. As pointed out by Pettersen et al. [76] internal conduction in fins, tubes and manifolds may lead to performance reduction. Solutions to avoid these problems include splitting of fins, use of several heat exchanger sections, and careful design of manifold geometries.

In the transcritical CO_2 cycle, system performance is very sensitive to gas cooler design. A small change in refrigerant exit temperature can produce a large change in gas cooler exit enthalpy (and evaporator inlet enthalpy) because specific heat becomes infinite at the critical point. Fig. 37 shows how COP can be increased 11% and the COP-optimizing discharge pressure reduced 0.5 MPa by a gas cooler in an automotive air-conditioning system ($T_0 = 3.9\,°C$; IHX effectiveness 0.8) that cools the refrigerant exit an additional 2 °C [109]. This indicates that a CO_2 transcritical cycle is so sensitive to the refrigerant exit condition that a counterflow configuration is important for the gas cooler to exploit the large refrigerant-side temperature glide. Moreover, the steep refrigerant temperature glide allows for ideal cycle efficiency to be achieved at finite air flow rate, in contrast to the infinite air flow required to achieve ideal efficiency in the subcritical cycle.

Yin et al. [110] validated a gas cooler simulation model using measured inlet data for a diverse set of 48 operating conditions, predicting refrigerant outlet temperature within $\pm 0.5\,°C$ for most of the experimental data. They proposed a multislab gas cooler design (Fig. 38(b)), and reported the new design offered better performance than the commonly used multipass design (Fig. 38(a)). For the given heat exchanger volume, they reported that a newly designed cross-counter flow gas cooler could be improved system capacity and COP by 3–4 and 5%, respectively, compared to the old design (Fig. 38(a)). Additional details on the selection of heat transfer and pressure drop correlations may be found in [67,111–113]. The model was used to design the next-generation prototype gas cooler shown in Fig. 38(b), where a multislab overall counterflow configuration concentrates the cool air stream on the exiting refrigerant, because the transcritical cycle is so sensitive to this exit condition [31,113,114]. The new gas cooler design achieves approach temperature differences $< 2\,°C$ at most operating conditions because air flowing over the first slab undergoes only a small temperature change, and that ΔT is what places an upper bound on the approach temperature difference [109]. The flat tubes are vertical in this prototype, to facilitate condensate drainage and defrosting in heating mode. Finally, the refrigerant flows in a single pass from the inlet to outlet, with no intermediate headers, to accommodate reversibility and facilitate refrigerant distribution in heating mode. It is clear that flat tubes must be oriented vertically for any air-source heat

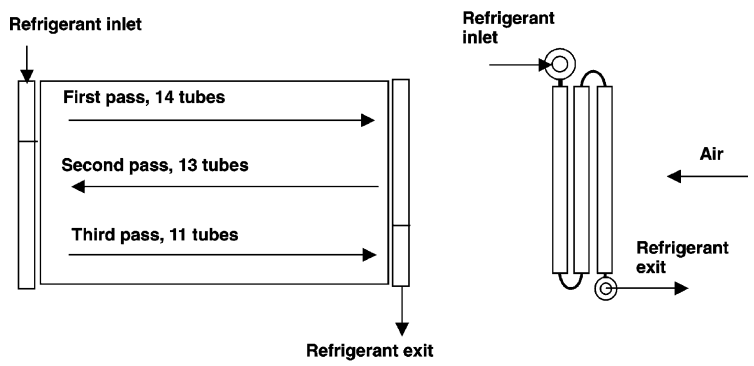

Fig. 38. Gas cooler design for a CO_2 air-conditioning system [110]. (a) One-slab three-pass design, (b) three-slab one-pass design.

pump, for reasons of defrost and condensate drainage, because both indoor and outdoor heat exchangers must function as evaporators as well as gas coolers.

7.2.2. Evaporators

In the auto air-conditioning industry during the 1980s conventional copper tube-aluminum fin evaporators were replaced by lighter, more compact brazed aluminum designs. Refrigerant flows between plates patterned with chevrons or dimples to facilitate refrigerant distribution between the upwind and downwind sides; sets of parallel plates are in cross-flow, usually with several passes between headers, with a variable number of plates per pass to control pressure R-134a pressure drop.

With plate evaporators the auto industry adopted louvered fins, which re-start the boundary every millimeter, increasing air-side heat transfer coefficient by 50–100% over that of plain fins. Condensate retention and blowoff remain a problem, which manufacturers address in a variety of ways to minimize performance degradation and mold growth: e.g. tilting the heat exchanger about 10° off the vertical, optimizing louver angle and spacing; and applying hydrophilic coatings and biocides. Kim et al. [115] reviewed critically the flow structure and its effect on the thermal hydraulic performance of folded louvered fins. They also described air-side heat transfer and pressure drop data and correlations of brazed aluminum heat exchangers under dry and wet conditions.

Microchannel evaporators are currently the subject of research within the automotive air-conditioning industry because of the potential performance improvements obtainable from further increases in refrigerant-side area and higher face velocities. Such prototypes have already been built and tested for CO_2 systems, such as the one shown in Fig. 39, sized for a sport utility vehicle. Next to it is a conventional R-134a evaporator that has less capacity, despite its greater face area, and only slightly shorter depth in the air flow direction. The fins on each heat exchanger are of the louvered folded type. The enhanced performance is attributable to the fact that microchannel tubes are thinner than the brazed plates, allowing the same air volume to pass with greater face velocity through a deeper heat exchanger, without a pressure drop penalty. In both plate evaporators and microchannel evaporators, the challenge is to distribute the two-phase flow uniformly through the parallel circuits. The current strategy for dealing with this problem is to find ways of eliminating it, such as flash gas bypass as described for the residential system prototype in Section 8. Kim and Bullard [116] developed a detailed finite volume model for a multislab microchannel evaporator and validated the model for a two-slab prototype evaporator. Several correlations for air- and refrigerant-side heat transfer and friction loss were compared before selecting appropriate correlations for the model. They reported their model predicted the experimental data with reasonable accuracy, and could be used for the performance analysis and designing of a microchannel evaporator. Currently, all simulation models of microchannel heat exchangers assume perfect distribution on the refrigerant side [116]. Their main focus is on capturing accurately the important air-side phenomena such as the effects of condensate and inclination angle.

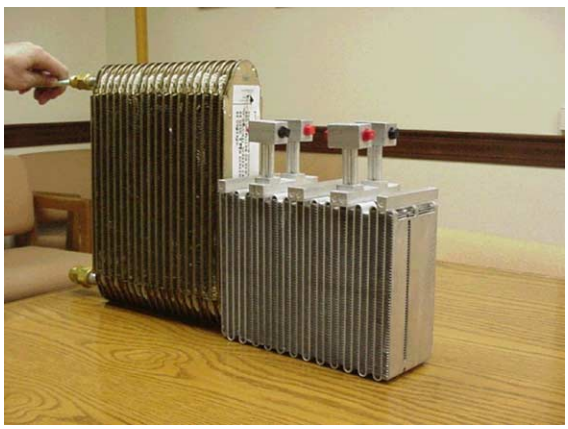

Fig. 39. Conventional (left) and prototype (right) CO_2 evaporator for mobile air-conditioner.

Extremely, high heat transfer coefficients have been reported for flow boiling in microchannel tubes [117], and explored in greater detail by Pettersen [20]. However, only a few experimental studies have been done to measure the effects of condensate retention on the performance of microchannel evaporators. The first study used 30 microchannel heat exchanger samples, and found that the sensible heat transfer coefficient was impaired only slightly by wet surface at low face velocities, but was similar to that for dry a surface at higher face velocities, for fin pitch = 1.4 mm. However, for those with smaller fin pitch, there was clear evidence of performance degradation by condensate bridging across the fins at all operating conditions. Based on these data, j- and f-factor correlations were developed [118]. In another investigation of the effect of inclination angle ($-60 < \theta < 60°$), heat transfer performance for both dry and wet conditions was not influenced significantly, while the pressure drops increased consistently with the inclination angle. The heat transfer coefficients and the pressure drops for the wet conditions revealed the importance of the role of condensate drainage [119].

Also emerging is yet another approach to design of evaporators for automotive applications. That is to use many parallel circuits of small-diameter circular aluminum tubes [76]. The small diameters enable use of higher pressure refrigerants, CO_2 included. Most importantly these heat exchangers use flat fins that can be enhanced with waves or offset strips, which are less susceptible to degradation by condensate retention and are more easily defrosted. In that sense they are taking advantage of all that has been learned through the design of air conditioners and heat pumps for stationary applications. Unlike conventional systems,

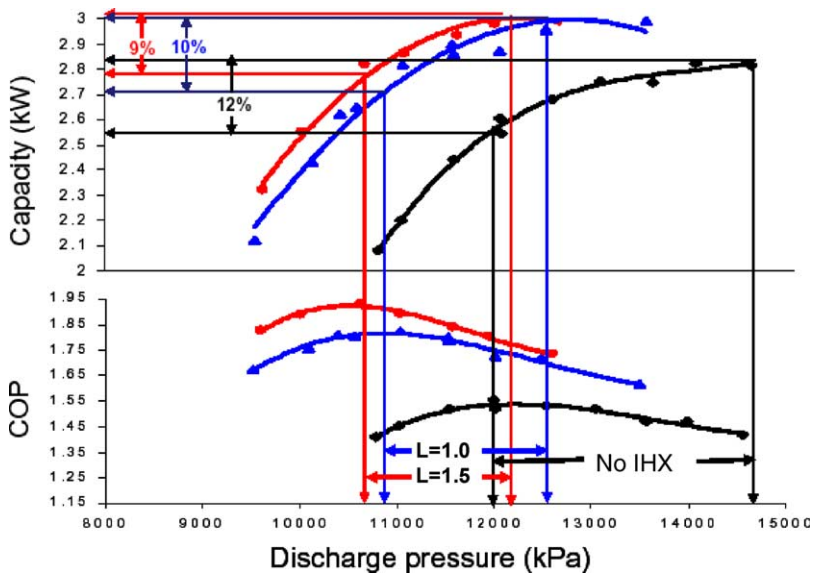

Fig. 40. Effect of internal heat exchanger (IHX) in mobile air-conditioning system at idling speed and 43.3 °C ambient (*L* is the length of IHX in meter).

however, these heat exchangers have much greater primary surface area. At this time there is relatively little published data that would allow detailed comparisons of these heat exchangers with the microchannel type, because their geometry lies outside the range of many correlations developed for stationary applications.

7.2.3. Internal heat exchangers

The benefits of an internal heat exchanger for transcritical automotive air-conditioning systems have been documented through extensive experiments in CO_2 prototype systems, and subsequent analyses using a validated simulation model. It has been demonstrated [120] that internal heat exchange can increase cycle efficiency up to 25%. Fig. 40 shows experimental results for a base case automotive air-conditioning system with no internal heat exchanger, and two others of lengths 1.0 and 1.5 m. The longer internal heat exchanger provides the greatest increase in COP and the greatest decrease in the corresponding optimal discharge pressure. In automotive air-conditioning systems, internal heat exchange provides the greatest capacity enhancement when it is needed most, while idling at high ambient temperatures. Boewe et al. [37] showed how three microchannel tubes could be stacked to provide many parallel ports to control pressure drop in the cold suction gas, while forcing the supercritical fluid through smaller ports to maximize heat transfer coefficients and areas upstream of the expansion device where larger pressure drop can be tolerated. Compared to conventional concentric tube designs, the microchannel configuration shown in Fig. 41 reduced

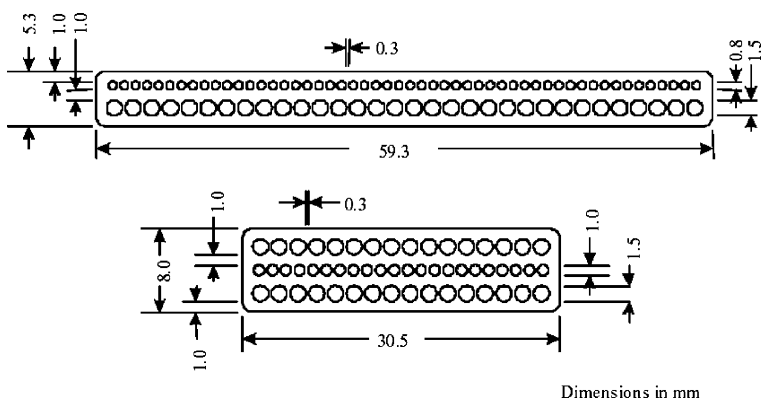

Fig. 41. Illustration of new designs of internal heat exchanger.

material requirements by 50% while eliminating the need for long suction and liquid lines, and increasing effectiveness by 10%.

7.3. Other components

7.3.1. Lubricants

A variety of lubricants can be used for CO_2 applications In certain systems synthetic hydrocarbons such as poly alpha olefins (PAOs) and alkyl benzenes (ABs) can be still used even though they have poor solubility The poor solubility of the synthetic hydrocarbons is compensated for by their excellent low temperature flow properties and can be improved still further by blending with more miscible lubricants (e.g. polyalkylene glycols (PAGs), esters, etc.). A range of individual and blends of synthetic lubricants are therefore being evaluated to find the more cost effective solution for a particular application. Quite often lubricant selection will be based on logistic factors, i.e. a lubricant that can work with a variety of refrigerants [121].

Kawaguchi et al. [122] reported that polyalkylene glycol (PAG) was the primary lubricant candidate since it was partially miscible with CO_2. It had excellent lubricity in boundary condition and supercritical condition, and showed good stability under supercritical condition. Other lubricants tested were polyolester (POE), polycarbonate (PC) and polyvinyl ether (PVE).

Li and Rajewski [123] conducted a screening study on various lubricant candidates for CO_2 systems, including mineral oil, polyalphaolefin (PAO), polyolester (POE), polyalkylene glycol (PAG) and alkyl naphthalene (AN). The experimental results raised concern about the compatibility between POE and CO_2 after significant degradation was found for this lubricant. The authors speculated that carbonic acids formed by dissolution of CO_2 into the moisture in the polyolester (POE) lubricant accelerated the degradation. Dissolved aluminum was found in the polyalkylene glycol (PAG) lubricant, and this was probably caused by a phosphate anti-wear additive which had been converted into aluminium-aggressive alkyl phosphates.

Seeton et al. [124] studied solubility, viscosity, boundary lubrication and miscibility of CO_2 and synthetic lubricants. They concluded that the polyalkylene glycol (PAG) lubricant seemed to give the best lubricity for transcritical applications.

Heide and Fahl [125] studied the miscibility in CO_2 of several candidate lubricants for transcritical systems, including alkyl benzene (AB), alkyl naphthalene (AN), polyalkylene glycol (PAG), polyolester (POE), and polymer ester (PME). The POE lubricants showed good miscibility, while the other candidates had large regions of immiscibility. The results indicated a strong influence of chemical structure of lubricant on phase behavior with CO_2. Investigations on thermal stability of lubricants by Fahl et al. [126] showed that PME and aromatic ester derivates have a good potential for applications with high temperatures.

7.3.2. Elastomers

Some issues are being studied with respect to elastomer materials for seals and hose connections in CO_2 systems Permeation rates are quite high, thus giving potential problems regarding desired leakage rates in automobile air conditioning systems. Explosive decompression may occur when CO_2 systems or components are rapidly depressurized, leading to fractured and ruptured sealing elements [127]. A fluorite elastomer, FKM was regarded as promising due to its wide temperature range of application and the negligible impact of explosive decompression.

7.3.3. Valves and controls

Jain et al. [128] has developed components for CO_2 air-conditioning systems, including electronic expansion valves, accumulators, hoses, o-rings and fittings. The expansion valve is a linear proportional solenoid valve. Several manufacturers are working on expansion valves and controls for CO_2 systems. Saginomiya and Fujikoki in Japan are working on valves (especially expansion valves) and controls for transcritical CO_2 systems, especially heat pump water heaters on the market. In Europe, Danfoss AS is working on various concepts, including mechanical (automatic, thermostatic) and electronic (modulating coil) valves. The German company Otto Egelhof GmbH and Co. is working on a step-motor controlled valve, mainly intended for the mobile air-conditioning market. In addition, Obrist Engineering in Austria is offering valves, controls and other components for prototyping purposes.

8. Application areas

Recent research on transcritical CO_2 systems has investigated a variety of possible applications, mostly with funding from the affected industries. While many government-sponsored R&D programs can afford the luxury of starting with basic research, industry-sponsored efforts generally proceed in two stages. The first task is to prove that the technology will work for a specified application, and then in stage two the state of the art is advanced to enable the technology to compete in the market.

From the standpoint of experimental design, first stage is the horseless carriage stage. Any new technology that challenges an existing one must demonstrate that it is workable, usually on the old technology's terms. The first CO_2 prototype systems were therefore built to mimic the conventional technology in size, weight, air flow rates, etc. In the long run, however, that is an unrealistic and non-sensical demand: like requiring Henry Ford's new invention to compete with a horse-drawn carriage on muddy

roads. Ford's technology was not rejected; instead the system boundary was expanded and roads were paved to capture the benefits of the internal combustion engine.

For most of the application areas discussed below, CO_2 technology is now at the second stage where it must demonstrate competitiveness. It is no longer necessary to mimic the old technology. However, many of the existing publications describe experiments conducted under stage-1 constraints. Current research is aimed at identifying the best way to utilize the unique characteristics of the new technology. In the case of CO_2, these characteristics include certain thermophysical (thermodynamic and transport) properties, which increase heat transfer and boost compressor efficiency. Its high heat rejection temperature, a disadvantage for air conditioning, is a potential advantage for heating by delivering instant high-temperature heat quietly due to the need to move less air than existing heat pump technologies.

During this second stage of prototype development the main question is how closely the ideal cycle can be approached at reasonable cost—a question that goes beyond simple thermodynamic cycle comparisons. The air flow rates and heat exchanger circuiting for an optimized CO_2 system will differ greatly from conventional systems. While questions related to cost are being explored on a proprietary basis, papers in the open literature are suggesting ways of approaching ideal cycle efficiency by exploiting the unique characteristics of CO_2, such as the slope of its vapor-pressure curve, boiling behavior near the critical point, high capacity at low temperatures, and its supercritical temperature glide. Other papers suggest ways of altering the transcritical cycle to increase the ideal efficiency, for example, through use of expanders, internal heat exchangers and multistage compression. In all cases, however, the path of technology development is defined by market needs for lightweight and ultra-compact systems (e.g. mobile air-conditioning, and portable air-conditioning units for the military), or the need for high-temperature heat (space and water heating; dryers), and needs for high refrigerating capacity at moderate to low temperatures. Examples are described in the following sections.

8.1. Automotive air conditioning

For several reasons, mobile air conditioning applications were among the first to be considered for application of the transcritical CO_2 cycle The most obvious was the high leakage rate of R-12 (and later R-134a, both greenhouse gases) through the flexible nylon or butyl rubber hoses needed for vibration protection, and through the compressor shaft seal needed to avoid the additional weight and conversion losses associated with the hermetic electric compressors used in other applications. In automobiles, the chief thermodynamic disadvantage of CO_2—its high temperature of heat rejection—makes it possible to design an ultra-compact gas cooler, which increases energy efficiency indirectly by enabling more aerodynamically streamlined vehicle design.

The earliest analyses of R-134a and CO_2 for automotive air conditioning began with ideal cycle comparisons [129,130], and rested on assumptions that failed to account properly for the unique thermodynamic and transport properties of CO_2, even though experimental data for a prototype CO_2 system had already shown competitive performance to a state-of-the-art R-12 system [3]. Not surprisingly the theoretical studies concluded that the total global warming impact of CO_2 systems would exceed that of R-134a, considering both direct (leakage) and indirect (fuel combustion) emissions of greenhouse gases. The first experimentally based assessment of TEWI [131] showed that in practice the energy consumption of the systems was comparable, thus giving considerably reduced warming impact due to elimination of the direct effect. Through improvements in system operation and control [28], compressor performance, and heat exchanger performance [76], the CO_2 technology was able to compete even with the improved R-134a systems that were introduced in the mid-1990s.

The European RACE project from 1994 to 1997 [132] focused on development and testing of car-installed prototype systems, with results confirming the potential for CO_2-based mobile air conditioning. Members in the RACE project included five European car manufacturers, two system suppliers, and one compressor manufacturer.

Based on these initially promising results, a rigorous side-by-side test program was undertaken, and conducted in specially designed well-instrumented facilities, using microchannel heat exchangers built to match closely the weight, heat exchanger dimensions, face velocities and air-side pressure drops of a commercially available clutch-cycling R-134a system for a Ford Escort. Separate environmental chambers were constructed to simulate a very wide range of indoor and outdoor climate conditions. To produce data on both systems and components, each chamber contained a wind tunnel, and had parallel sets of refrigerant piping to facilitate comparisons of CO_2 and other refrigerants. The heavily insulated walls with heat transmission measurement, plus accurate metering of refrigerant and air mass flow rates made it possible to obtain three energy balances for both the indoor and outdoor heat exchangers: air-side, refrigerant-side and room calorimetry. Detailed descriptions of the mobile and residential air conditioning facilities may be found in Refs. [133,134].

Heat exchangers for the CO_2 system were made of flat aluminum extruded multiport tubes to deal with the high-pressure refrigerant, making it possible to maximize air-side heat transfer area within the overall weight constraint. Photographs of the evaporators (top) and condenser/gas cooler (bottom) are shown in Fig. 42. The 21.0 cm^3 compressor shown in Fig. 31 was of swash-plate design, and the high-side pressure could be controlled by either a needle valve or a backpressure valve.

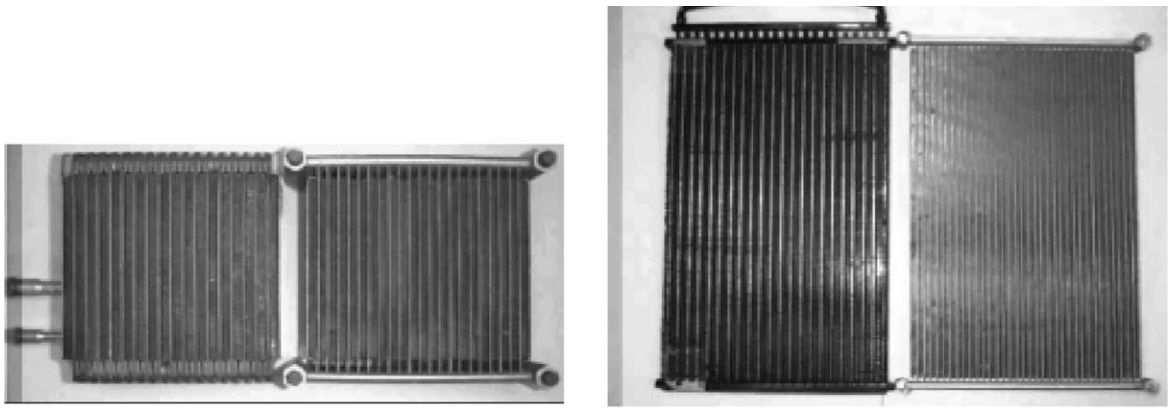

Fig. 42. Heat exchangers of CO_2 mobile air-conditioning system prototype (right) compared to R-134a baseline (left). (a) Evaporator, (b) condenser or gas cooler.

Test matrices were defined for the purpose of developing and validating component and system simulation models, as well as supporting data-to-data comparisons of CO_2 and R-134a at normal, seasonal and extreme operating conditions.

The results demonstrated that comparable cooling COPs could be obtained at most operating conditions (Fig. 43). The CO_2 system was sized to provide approximately equal capacity at the extreme high-temperature (54.4 °C) idling condition, as shown in Fig. 44. However, its COP fell 10% short of the baseline system at that point. At outdoor ambient temperatures below 40 °C where most air-conditioning operation occurs, the CO_2 system COP exceeded that of the baseline R-134a system up to 40%. The lines in Fig. 44 connect points having equal outdoor air flow rates, V_c, while the indoor air temperatures and air flow rates are shown in boxes. The 22 data points represent only a subset of the conditions investigated. Several factors were found to be responsible for these results: (1) higher real compressor efficiency due to lower compression ratio; (2) higher evaporating temperature due to superior thermophysical properties and greater tolerance of pressure drop due to the slope of the vapor pressure curve; (3) closer approach temperature differences at the gas cooler outlet. More detailed data can be found in Refs. [133,135–137].

Experiments were conducted on both systems in both steady state and cycling modes. Cycling behavior is very sensitive to the type of expansion device used. A fixed orifice is simplest, but is unable to maintain the high-side pressure at its COP-optimizing level during the on-cycle as reflected by the large differences between refrigerant flow rates shown in Fig. 45 [137]. It is also clear that the backpressure valve

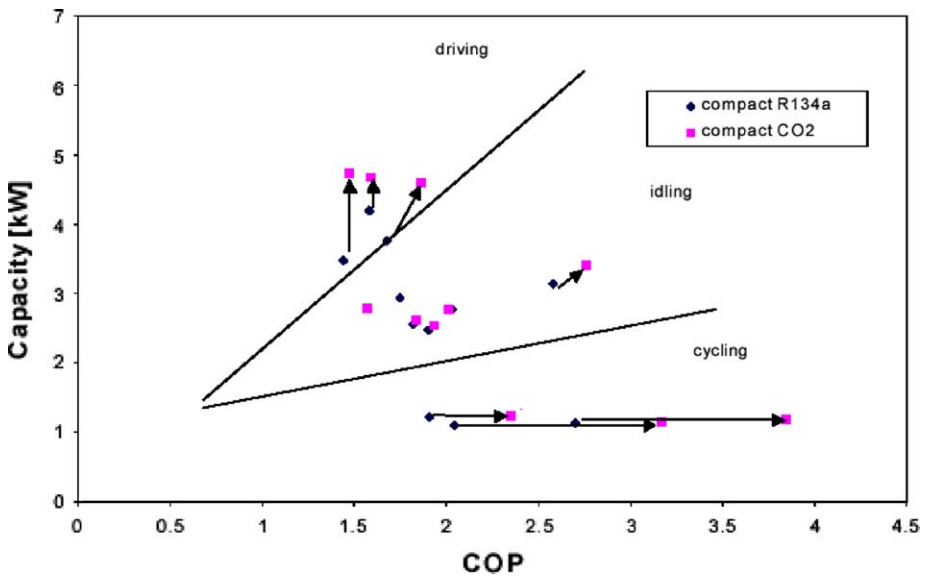

Fig. 43. Measured performance of automotive air-conditioning systems.

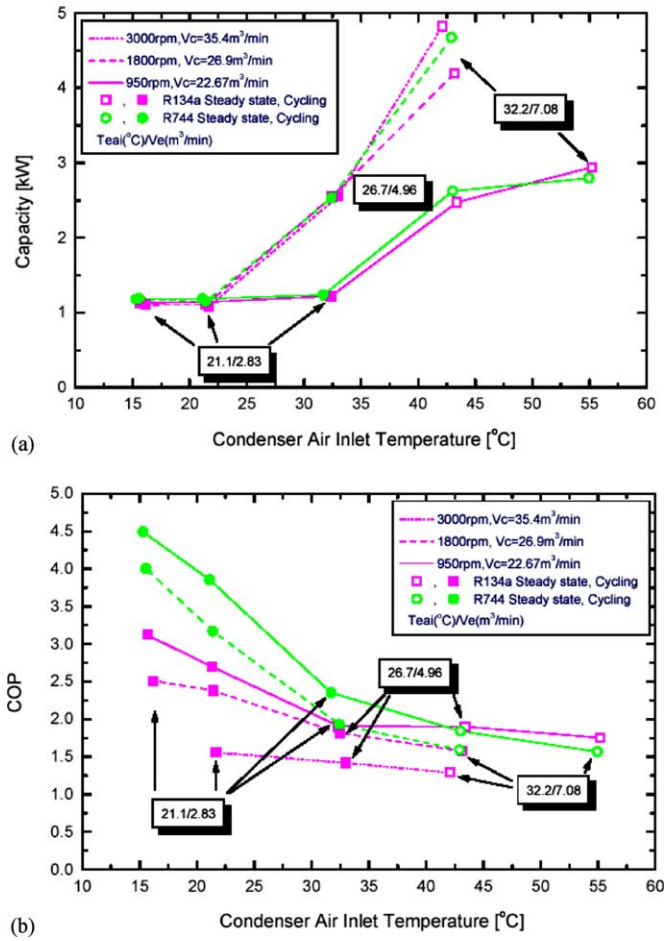

Fig. 44. Comparison of CO_2 mobile air-conditioning system prototype performance to R-134a baseline. (a) Capacity, (b) coefficient of performance.

maintains a steadier compressor torque, F_c, than the fixed orifice (needle valve in fixed position). Control options are discussed in Refs. [138,139]. Additional experimental results and a more detailed investigation of the time averaged COP-maximizing high side pressure strategy is presented in Ref. [140], which found a linear relationship between gas cooler exit temperature and COP maximums over a wide range of operating conditions.

Based on the results of an analysis of a large number of experiments and some new concepts, next-generation prototype systems have been designed and are serving as the focus for current research. Most are equipped with variable-displacement compressors, and heat exchangers configured to exploit the unique transport and thermodynamic properties of CO_2. Some of these design features and model validation results are discussed in Section 7.

Research and development of transcritical CO_2 technology marked a significant departure from mobile air conditioning industry's traditional product development programs, which are dominated by internally funded proprietary efforts. The involvement of academic research at such an early stage is unprecedented, and illustrates two distinct types of value delivered by the academy to the industry. The first is not new: peer-reviewed research elucidates the fundamental physical processes, and provides a physical basis for discontinuous technological change,

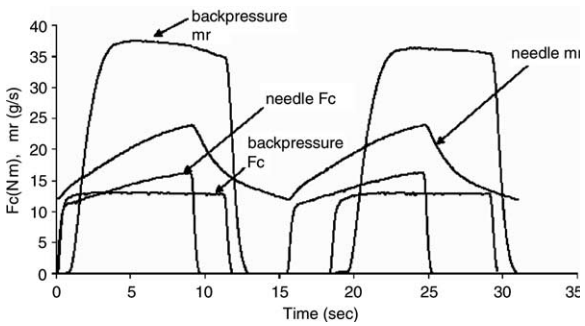

Fig. 45. Characteristic behavior in cycling.

which is less risky than extrapolating empirical data. The second type of value stems from the uncertain timetable for dealing with global warming, which is quite aggressive in some parts of the world and creates a need for detailed, credible peer-reviewed results of carefully designed experiments. In both cases the world auto industry—OEM's and component suppliers—have decided to pool resources and share the cost of producing such information. The results of the European RACE consortium's efforts were produced by member companies and shared internally, and later placed in the public domain [132]. To enhance acceptance, a broader-based cooperative research program is now being undertaken by SAE and conducted at the University of Illinois. That 18-month effort involves a rigorous experimental evaluation of several competing systems, with extensive instrumentation under identical operating conditions [141]. The systems are: baseline production R-134a; advanced R-134a; transcritical CO_2; and propane (R-290) with a secondary loop containing a non-flammable coolant.

Laboratory experiments—carefully designed and documented—are one important step along the path to commercializing any new technology. Designing and retooling to accommodate the high pressures in CO_2 refrigeration systems, and dealing with safety concerns are generic issues to be faced by any companies involved in a transition to CO_2 systems. The auto industry is positioned to benefit from existence of captive vehicle fleets, which can provide test-beds for confirming the conclusions drawn from laboratory experiments. On the other hand the industry is beset with a variety of logistical concerns related to the worldwide service infrastructure: the need for technicians to handle not only the new technology but also its overlap with conventional systems. Maintenance problems are more prominent in vehicles than in stationary applications because of the need for more extensive spatial, mechanical and electrical integration of the air-conditioning unit with other subsystems (severe packaging constraints; compressor mechanical drive; and the need for reheating dehumidified air for defogging). Moreover, the auto industry is accustomed to producing cars capable of operating in almost any climate. Therefore, investigations of advanced cooling applications are being accompanied by experiments in heating mode, because many of today's efficient cars reject too little waste heat to the engine coolant to keep cars comfortable in severe winter conditions.

8.2. Automotive heating

Modern cars with efficient fuel-injection engines often have insufficient waste heat for heating of the passenger compartment in the winter season. The long heating-up period and slow defroster action is unacceptable both in terms of safety and comfort. Supplementary heating is therefore necessary, and one attractive solution may be to operate the air conditioning system as a heat pump. CO_2 systems have special benefits in heat pump mode, since high capacity and COP can be achieved also at low ambient temperature and with high air supply temperature to the passenger compartment.

The first results of CO_2 heat pump experiments were obtained by running an auto air-conditioning prototype system in reverse [142–144]. Although the cross-counterflow interior heat exchangers were far from ideal, the data shown in Fig. 46 show the essential features of an automotive heat pump: capacity is highest at startup when it is needed most; the capacity is at least three times higher than what could be obtained from an electric resistance or friction heater due to the high heat pumping efficiency; and capacity and efficiency (heating performance factor, HPF) decline slowly due to reduced volumetric and isentropic compressor efficiencies at higher temperature lift, as the car warms up and heat becomes available from the engine coolant. These initial results have proven quite valuable in guiding the design and development of improved components for next-generation systems. Next-generation prototypes will need to address such operational issues as defogging.

One reason heat pumps are not currently employed in automobiles is that R-134a has disadvantages as a heat pump fluid (e.g. large compressor displacement; air in-leakage in compressor shaft seal at subatmospheric suction pressures). Regardless of the fluid, however, air-to-air heat pumps present substantial technological challenges that have not yet been addressed: the outdoor heat exchanger will accumulate frost, and perhaps ice as water is splashed on it from the road. Very little is known about frosting and condensate drainage from ultra-compact microchannel heat exchangers, and what is known suggests that the difficulties may be substantial [143–146]. Residential heat pumps defrost by switching into air conditioning

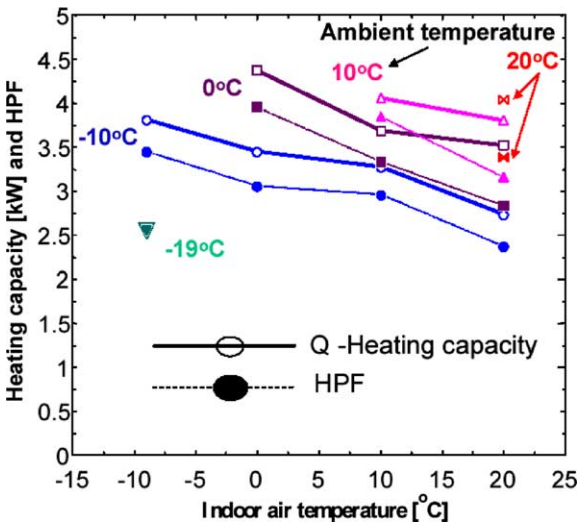

Fig. 46. Automotive heat pump performances at different indoor and outdoor conditions.

mode, but that is not a feasible option for automobiles because the small volume of air in the passenger compartment would cool immediately. Connecting to another heat source for defrosting may also be problematic, especially after a series of short trips during which the engine never reaches normal operating temperature. On the other hand, during normal operation, the heat pump needs only to provide supplemental capacity for a short period after startup, while the engine is warming up. After that, sufficient heat should be available for defrosting; the only problem is how to transfer it. Other options for avoiding frosting, such as obtaining heat from the engine coolant, have their own unique difficulties: for example, causing the engine to operate at suboptimal temperatures and exceed air pollutant emission standards. These difficulties might be avoided through careful design in the future, by integrating and improving thermal management within the engine.

Hammer and Wertenbach [147] showed test data for an Audi A4 car with 1.6 l gasoline engine, comparing a standard heater and a CO_2 heat pump system based on engine coolant as heat source. Fig. 47 shows measured air temperatures at foot outlet nozzles and passenger compartment temperatures using standard heater core ('production'), and a heat pump system (without heater core). The more rapid heating up with heat pump is clear, with almost 50% reduction in the heating-up time from −20 to +20 °C. Since the heat pump used engine coolant as heat source, the possible risk of extended heating-up time for the engine was of some concern. Measurements showed that owing to the added load on the engine by the heat pump compressor, the heating-up time was in fact slightly reduced even when heat was absorbed from the coolant circuit.

Despite the technical challenges, the ability of a heat pump to provide 'instant heat,' and the capability of a CO_2 heat pump to deliver that heat at higher temperatures while moving less air, create value that may warrant development of more complex automotive climate control systems. This feature, combined with the long-term need for increasing vehicle efficiency, is driving ongoing research in both universities and industry. Moreover, the emergence of electric and hybrid vehicles is causing the scope of the investigations to be expanded to reconsider electrically driven hermetically sealed heat pumps.

8.3. Residential cooling

The first assessment of transcritical CO_2 systems for residential air conditioning was done by simulating operation of an Asian-style ductless minisplit system, comparing CO_2 to a baseline R-22 system [148].

Evaporator temperatures were higher in the CO_2 system, and very small approach temperatures were estimated for the CO_2 gas cooler. The mechanically expanded round-tube heat exchangers were designed within the same core dimensions and air-side pressure drop in both systems. The effects of pressure drop, particularly in the evaporator and suction line of the R-22 system and the superheat characteristics of the expansion valve, gave cooling COPs (summer operation) that were similar in both systems, even at high ambient temperatures.

An extensive set of experiments was conducted on a prototype North American-style ducted split air conditioning system. The baseline R-410A system selected was the most efficient commercially available, and the CO_2

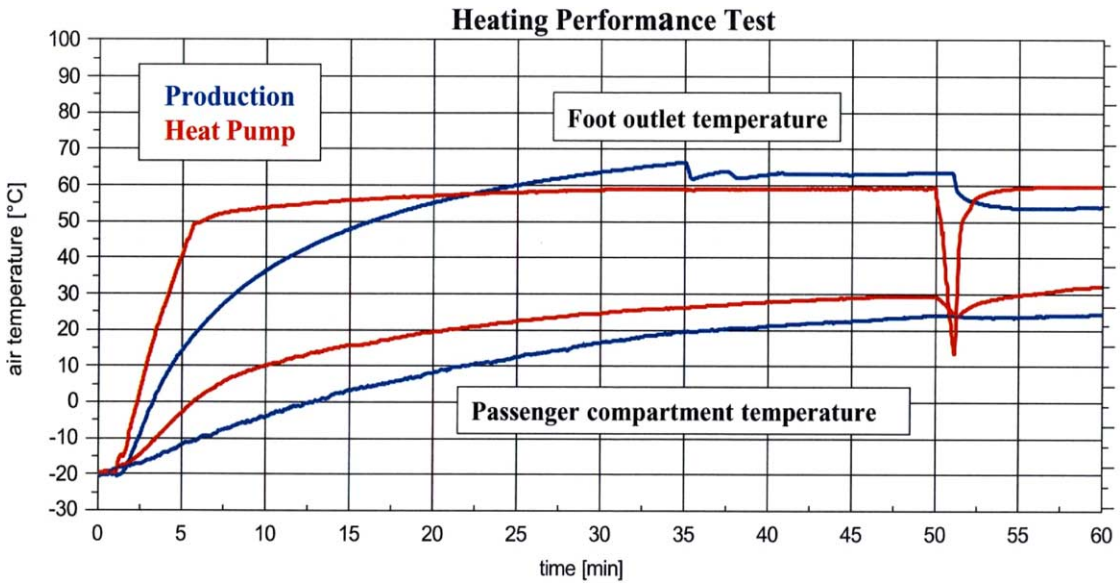

Fig. 47. Measured air temperatures in during start-up of an Audi A4 test vehicle (production) and same car with CO_2 heat pump ('heat pump') [147].

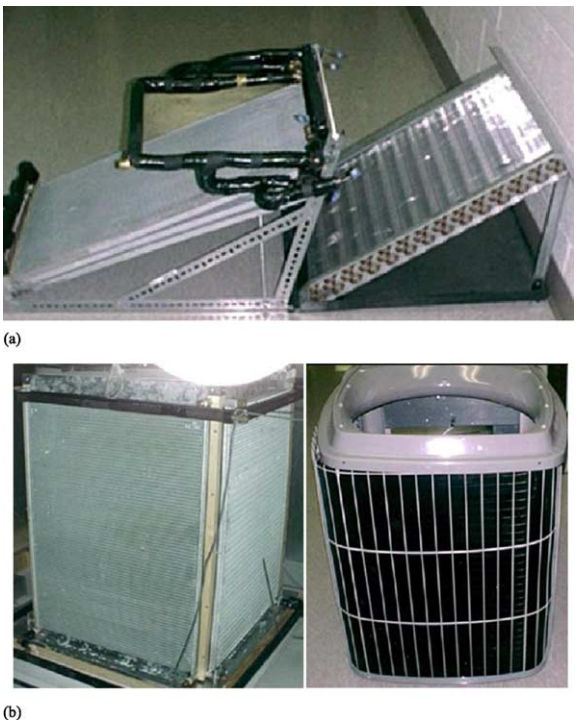

Fig. 48. Heat exchangers of CO_2 residential air-conditioning system prototype (left) compared to R-410A baseline (right) [134]. (a) Indoor heat exchangers, (b) outdoor heat exchangers.

prototype heat exchangers were designed to match as closely as possible its overall package dimensions, as shown in Fig. 48. Detailed experiments were conducted on each system at three standard ARI test conditions, and the prototype CO_2 system achieved approximately the same cycle COP (omitting fan and blower powers) as the baseline R-410A system at ARI test conditions B and C (26.7/27.8 °C) [149]. The raw data in Fig. 49 should be adjusted downward about 10% for comparison with the hermetic R-410A compressor, because the CO_2 prototype compressor was an open automotive prototype where power input could only be measured on the shaft. As expected, the CO_2 exhibited a substantially lower COP at the higher ambient temperature condition A (26.7/35 °C). Results shown in Fig. 49 demonstrated how the lower air-side pressure drop of microchannel heat exchangers enabled the CO_2 system to benefit from greater air flow rate with no penalty in fan or blower power. The test matrix was designed to guide next-generation component designs, for example: as alternatives to increasing air flow rate, direct fan power savings could be realized, or air-side heat transfer area could be increased until pressure drop matched that of the baseline.

The model validation effort was based on these initial experiments, and a large discrepancy was noted between simulation and data for the evaporator. A thermocouple grid

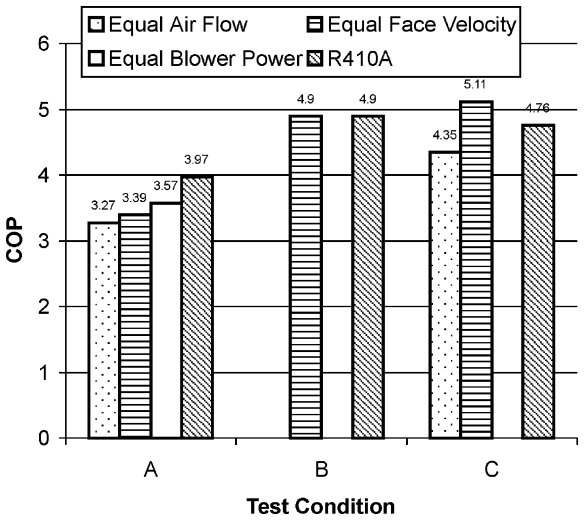

Fig. 49. CO_2 residential air-conditioning system data compared to R-410A baseline.

was then installed downwind of evaporator, and provided evidence of significant refrigerant maldistribution among the parallel microchannel tubes (Fig. 50). As shown in Fig. 50(b), even symmetrical feeding of the header results in the middle tubes receiving excess liquid while the outer ones receive excess vapor. Fig. 50(c) shows how this problem was eliminated through use of controlled flash gas bypass—a new concept to improve distribution and increase heat transfer coefficients while reducing pressure drop in evaporator—increasing heat exchanger effectiveness by 17% and increasing the evaporating temperature by 3.8 °C as described in Ref. [150]. Since compact high-performance heat exchangers such as these are likely to be needed for efficient heat pumps in the future, solving the two-phase refrigerant distribution problem has become a high priority for systems using any kind of refrigerants. Accordingly, a substantial amount of research is now being initiated to understand the behavior of developing two-phase flow in headers, and on schemes for bypassing vapor to minimize degradation of evaporator performance.

8.4. Residential heating

Today's residential heat pumps deliver large amounts of air at temperatures very near that of human skin, causing discomfort via evaporative cooling. On the other hand the transcritical cycle can deliver air at 60 °C, achieving the same level of comfort as a gas forced air furnace while quietly moving substantially less air than conventional heat pumps. Similarly, CO_2 can provide heat via a hydronic secondary loop without the energy penalty that would be incurred in a heat pump operating on a subcritical cycle. Several analytical studies of the global warming implications of alternative heat pumping systems have

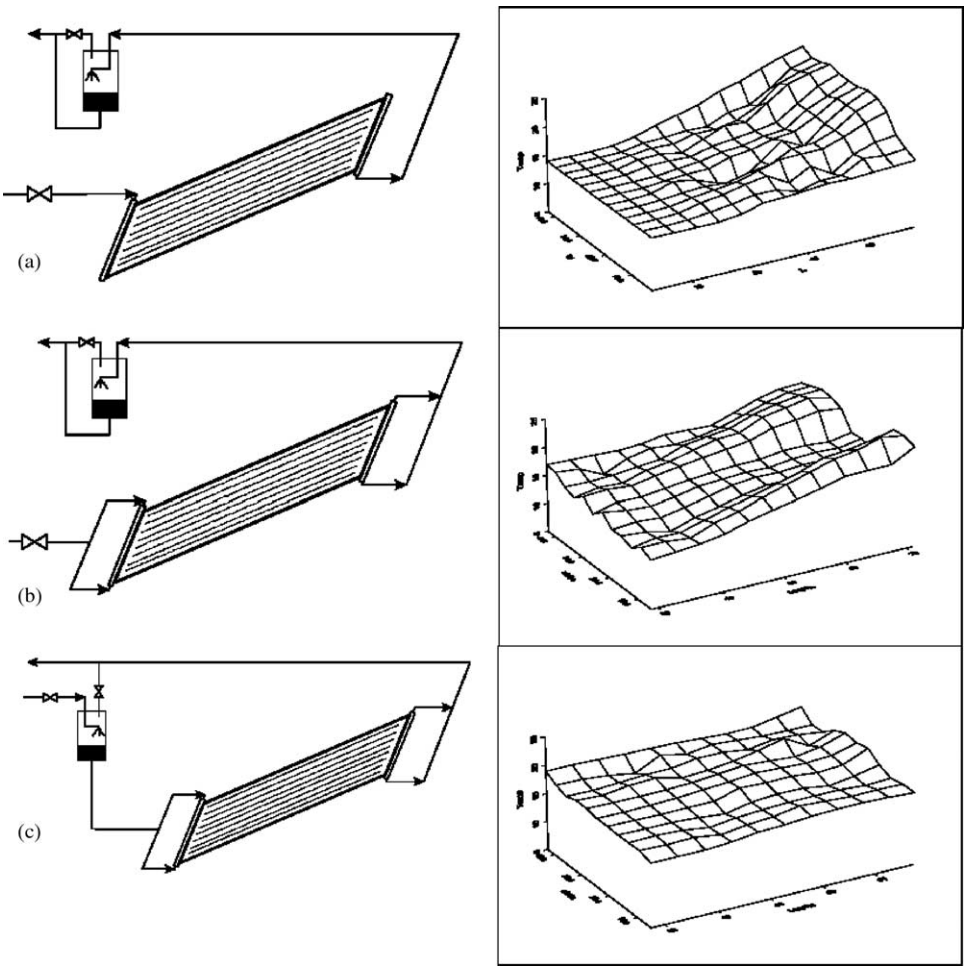

Fig. 50. Effects of flash gas bypass expressed through air exit temperature profiles shown on the right. On the left (a) regular HX configuration with single side inlet, (b) same as (a) just with two inlets and (c) flash gas bypass. All three operations are completed with same evaporator capacity. In both (a) and (b) cases evaporation temperature was 7 °C while in (c) it was 10.8 °C that consequently increased COP by 17%.

concluded that the direct effect of refrigerant emissions is relatively small, compared to the indirect effects associated with differences in energy efficiency [151]. Accordingly, for almost all applications except automotive air-conditioning and supermarket refrigeration, the highest R&D priority is to maximize the efficiency of CO_2 systems.

8.4.1. Direct air heating

Differences in heating capacity characteristics between CO_2 and R-22 are important for the seasonal heating performance (winter operation), since differences in the need for supplementary heating affect the total system energy efficiency. In their model-based study, Pettersen et al. [148] found that the CO_2 system was able to maintain a higher heating capacity than the R-22 system at low ambient temperatures, thereby saving supplementary heat. Even though the heating COPs of the two heat pump circuits were similar, the overall result was a 20% increase in system energy efficiency (HSPF) for the CO_2 system, due to a lower need for supplementary heat of any kind.

Experimental investigations of transcritical CO_2 systems for residential space heating were conducted on a prototype residential split system, originally designed for cooling only, by simply reversing its operation to study heating performance [152]. Since the original baseline system was obtained before the first R-410A heat pump system became available, the package dimensions for the heating comparisons were no longer equal: the baseline subcritical R-410A system had larger heat exchangers. Nevertheless, system performance was compared for two configurations: first when the CO_2 prototype semi-hermetic compressor speed was set to match heating capacity at 8.2 °C outdoors and 21.1 °C indoors; and second when the air conditioning capacity was matched at 35 °C outdoors and 26.5 °C indoors. The CO_2 system had similar cycle COP in heating mode, but its higher capacity at lower outdoor temperatures increased its heating performance factor (HPF) by reducing

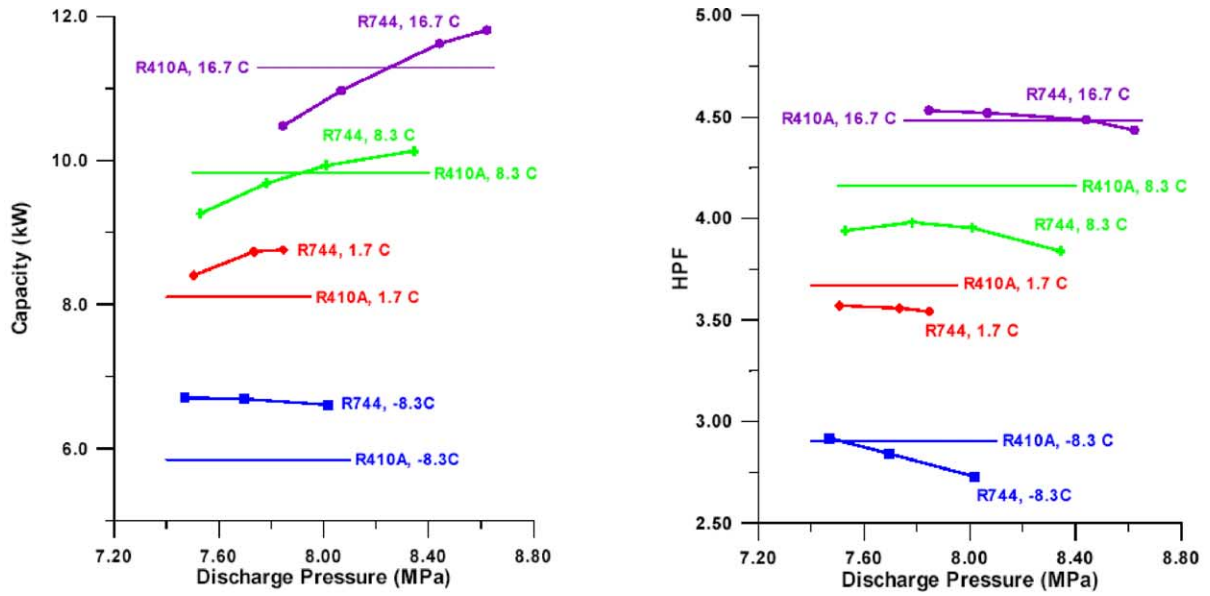

(a)

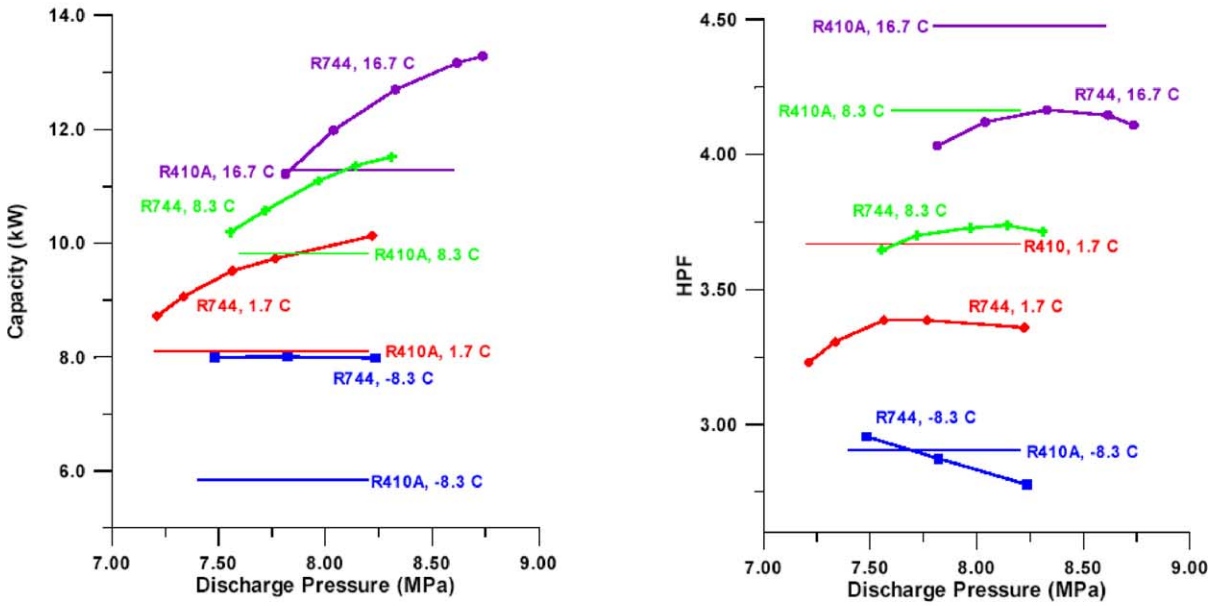

(b)

Fig. 51. Residential CO_2 system controls of capacity and efficiency. (a) Heat pump, (b) air-conditioning.

the need for supplemental heat (Fig. 51), which illustrates the CO_2 system's ability to select a compressor discharge pressure that gives it extra capacity or efficiency when needed. These results helped establish priorities for subsequent analyses of the effects of CO_2's transport properties on heat exchanger temperature differences, and ways to optimize the geometry of the next generation of reversible heat exchangers for transcritical CO_2 heat pump systems.

To complement the experimental comparisons of competing systems, a parallel analytical effort was undertaken to develop a relatively simple simulation model that could analyze many of the essential differences between transcritical and subcritical systems [153].

To ensure that the comparison was geometry-independent, the air-side heat transfer and pressure drop characteristics were assumed to be identical, and the 'ideal' assumption of infinite heat exchanger areas was retained. The analysis began with a simple comparison of ideal thermodynamic cycles, which, as expected, showed R-410A to be more efficient in both heating and cooling modes. Then as constraints and non-ideal considerations (e.g. finite air flow rates required to achieve comfort and limit fan power) were introduced simultaneously for both systems, the efficiency gap narrowed. The results suggest that CO_2 heat pumps could be more efficient than R-410A in cold climates, due to their higher capacity at cold temperatures and correspondingly less need for electric resistance backup heat. In climates dominated by cooling loads, such as the southern US, subcritical R-410A systems have a clear advantage in annual average efficiency, as shown in Fig. 52. The abscissa spans a wide range of climates, indicating the outdoor temperature at which the magnitude of the heating load on an average-insulated house equals the cooling load (normalized to 1 kW) at the 45 °C design condition for which the system was sized. Imposition of finite-area constraints on the heat exchangers would benefit CO_2 preferentially, but probably not enough to reverse the result for warm climates.

Despite its simplicity, the analysis helped quantify the individual differences between the two systems and cycles. The pressure ratio of the CO_2 cycle is lower, real compressor efficiencies are higher. The superior thermophysical properties of CO_2, together with the small slope of the vapor pressure curve, allow for substantially increased heat transfer coefficients with negligible thermodynamic penalties from the associated pressure drop, enabling CO_2 systems to meet a given dehumidification constraint at a slightly higher evaporating temperature than R-410A. At supply air temperatures greater than 40 °C, the ideal CO_2 cycle is slightly more efficient than R-410A and provides substantially higher capacity at colder outdoor temperatures. This advantage appears not only for air-to-air heat pumps, but also for hydronic heating systems where higher quality heat is required. In hydronic systems water chilling may be a preferred option for the cooling season; it has been investigated experimentally and analytically, and found to have efficiency similar to that of R-22 [154–156].

Rieberer and Halozan [157] and Rieberer et al. [158] made detailed theoretical studies of controlled ventilation air heating systems with an integrated CO_2 heat pump. The results look very promising. The overall system seasonal performance factor for a Graz, Austria climate was calculated to be in the range 6.15–6.5. This corresponds to a seasonal performance factor of the heat pump of above 4 (author's remark).

8.4.2. Hydronic heating

Schiefloe and Nekså [159] investigated a system design as shown in Fig. 53. In order to achieve a lowest possible return temperature from the heating system, the radiator and air heating are connected in series. Tap water is pre-heated in parallel with the space heating and heat exchange against hot discharge gas is used to achieve the required hot water

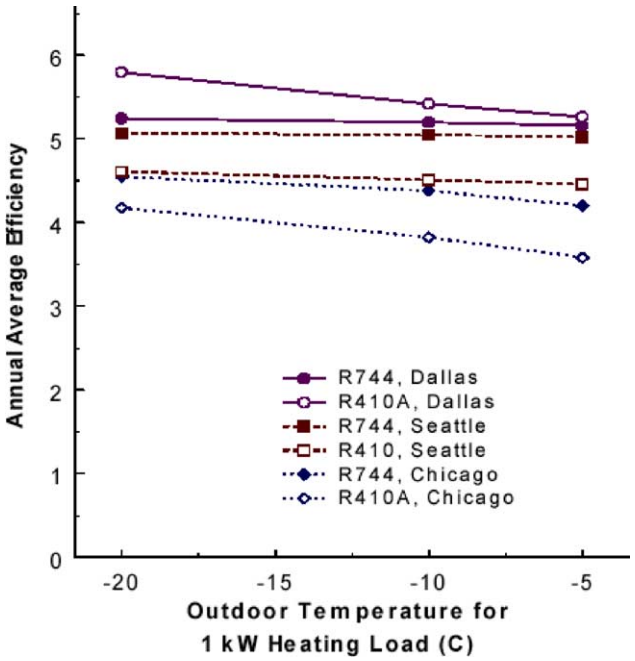

Fig. 52. Annual average efficiency for R-410A and CO_2 systems as function of heating load requirement for 60 °C supply air in heating-model predictions.

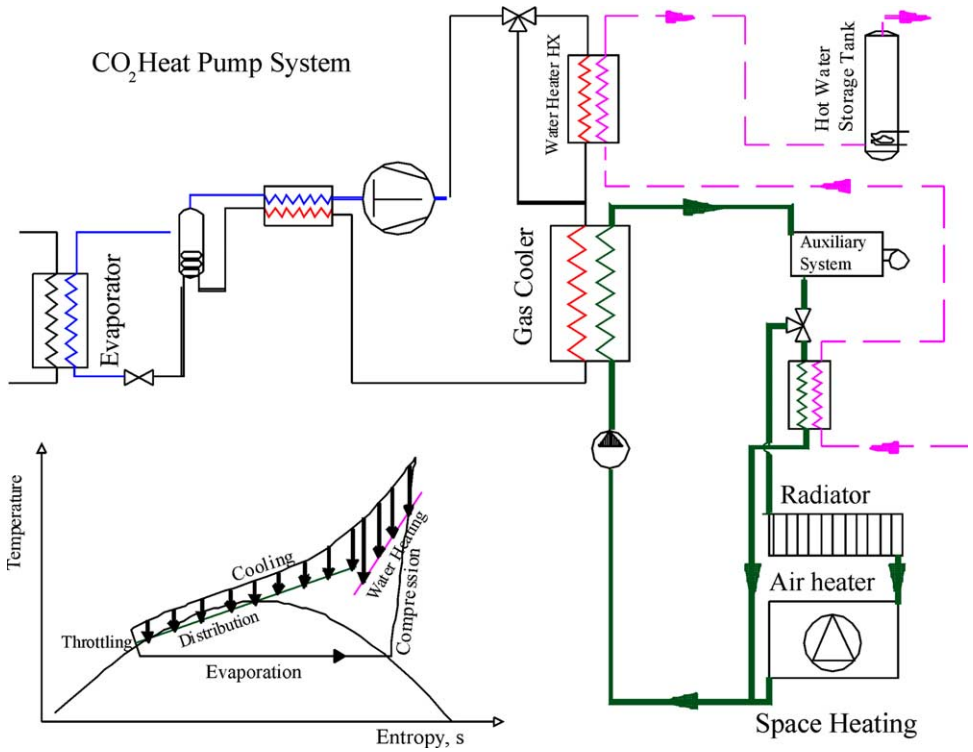

Fig. 53. System design for a combined space and water heating system. The process is also illustrated in the $T-s$ diagram.

temperature. In order to simplify the system design, the tap water heating part could also be implemented as a separate system or covered when space heating is not required.

Compared to a system using R-134a as working fluid the proposed CO_2 system showed favorable seasonal performance when more than 30% of the power demand for space heating was covered by the air heating system. The rest was then covered by the radiator system. A 70/50 °C radiator system and heat recovery efficiency of the balanced ventilation system of 60% was assumed. In larger buildings in Norway typically more than 50% of the heating demand is air heating and this percentage is increasing due to better insulation and increased air quality requirements. This indicates that CO_2 may be a promising candidate for this application.

Enkemann et al. [160] made a theoretical study on CO_2 heat pumps for retrofit in typical hydronic heating systems in Western Europe. A system originally designed for temperatures 70/50 °C was modified by reducing the mass flow rate of water to obtain a 93/40 °C system, which should give a corresponding heat output using the existing radiator system. The seasonal performance was then increased from 2.8 to 3.2. In addition, this system will be able to supply hot tap water without any loss in energetic efficiency. Experimental results from two prototype systems for this application are reported in Ref. [161]. Efficiency figures in the same range as the calculated were reported.

Professor Gustav Lorentzen published several papers describing the possibilities of using CO_2 as working fluid in heat pumps and refrigeration systems. Lorentzen [32,162] outlined possible system design of large heat pumps for district heating. This is a high-capacity application where turbo expanders may be possible to realize in a cost efficient manner. Also described is the possibility to combine refrigeration/freezing and tap water heating, which will give very high overall system efficiency.

8.5. Water heating

The first application of CO_2 systems on the market is heat pump water heaters, where the thermodynamic properties are very favorable Fig. 54 shows, in a temperature–entropy diagram, how the temperature characteristics of the transcritical cycle matches the temperature profiles of the heat source and heat sink, giving small heat transfer losses and high efficiency. A pre-condition for high efficiency is a low water inlet temperature, giving a low refrigerant inlet temperature to the throttling device. Thus, the design of the hot water accumulating system for temperature stratification is essential in order to achieve high heating COP.

Studies on CO_2 heat pump water heaters were initiated at SINTEF/NTNU from the late 1980s, and a full-scale prototype system of 50 kW heating capacity was completed in 1996 as shown in Fig. 55 [108]. Results from extensive measurements on this prototype showed that a COP above 4

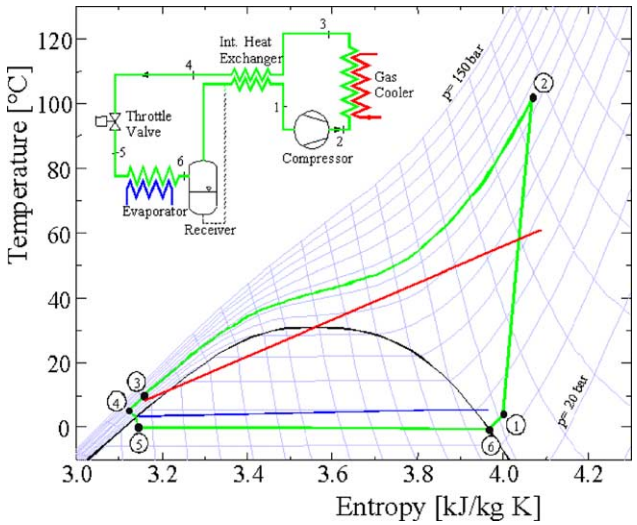

Fig. 54. $T-s$ diagram showing the transcritical CO_2 cycle used for water heating.

was achievable even for a hot water temperature of 60 °C as shown in Fig. 56 [163]. The high process efficiency is partly due to good adaptation of the process to the application, but also due to efficient compression and the good heat transfer characteristics for CO_2. A CO_2 heat pump water heater may produce hot water with temperatures up to 90 °C without operational problems and with only a small loss in efficiency. Increasing the required hot water temperature from 60 to 80 °C reduces the heating COP only slightly (from 4.3 to 3.6 at an evaporating temperature of 0 °C), and one of the big advantages of this technology is the ability to supply water at high temperature with good COP. Important application areas for commercial-size systems are in hotels, apartment houses, hospitals, and food industries.

The above heat pump water heater system was included in the European Union (EU) cooperative project 'COHEPS' from 1996 to 1998, where research groups in Austria (Graz University of Technology), Norway (SINTEF/NTNU), Germany (University of Hanover, Essen University) and Belgium (Catholic University of Leuven) together with their industrial partners studied various aspects of heat pumping applications for CO_2, including commercial-scale heat pumps, residential heat pumps, systems for hydronic heating circuits, and drying heat pumps. Hwang and Radermacher [164] published data on water heater, and used model to show 10% COP improvement over R-22.

Fig. 55. Fifty kilowatt prototype heat pump water heater in SINTEF/NTNU laboratory [108].

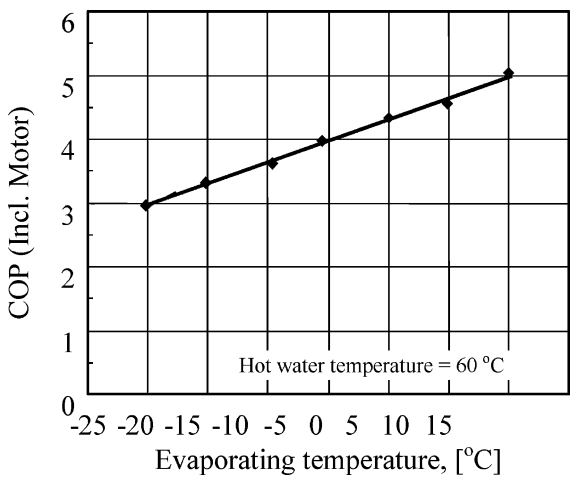

Fig. 56. Measured heating COP of laboratory prototype system, at water inlet temperature 10 °C.

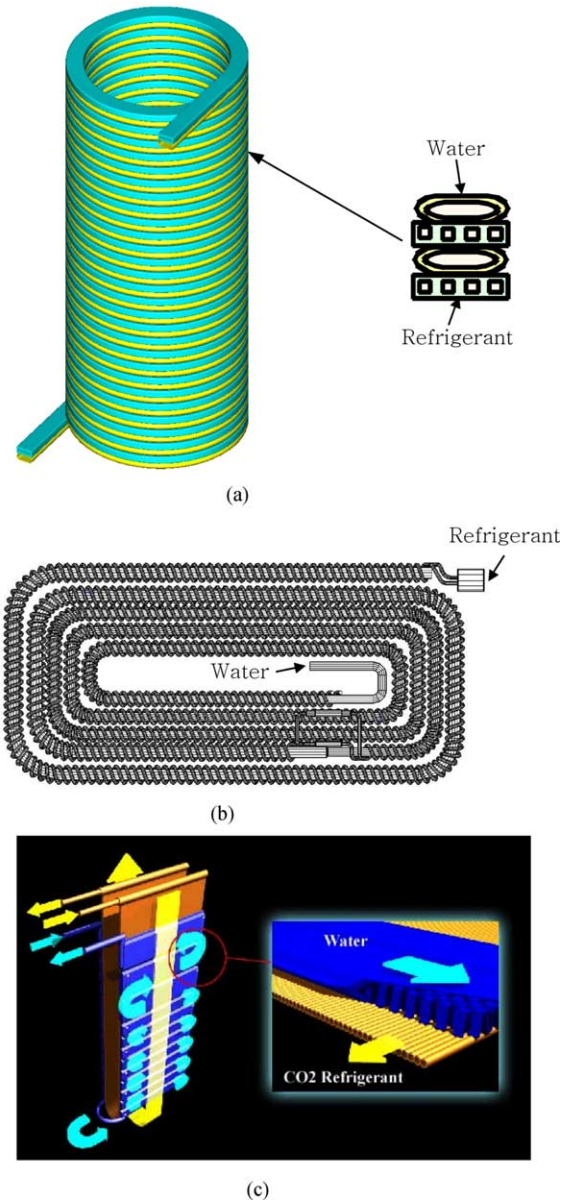

Fig. 57. Gas coolers for CO_2 heat pump water heaters [168].

A 25 kW pilot plant was installed in a food-processing factory in Larvik, Norway in 1999, using waste heat from an industrial NH_3 refrigerating system as a heat source. Performance has exceeded the initial expectations, and the system has proven to be a very profitable investment for the company. A new pilot plant is now under erection in Oslo, Norway.

Several Japanese manufacturers put CO_2 heat pump water heaters on the market in 2001/2002 [165]. The typical rated heating capacity and COP are 4.5 kW and over 3.0, respectively, based on the JRA Standard 4050 [166] which provides test standards and terminologies of small CO_2 heat pump water heaters (capacity, $Q < 11.8$ kW). These water heater systems produce hot water using cheap late-night electric power, and stores hot water in a tank for daytime use [167]. These CO_2 heat pump water heaters used several different types of gas coolers for the cost effective compact systems as shown in Fig. 57 [168].

8.6. Environmental control units

Military needs for space conditioning systems for temporary shelters, command modules, and vehicles have traditionally been met by procurement rather than R&D, using custom-built units based on the same basic technology used for commercial applications. The conventional Mil-Std (Military-Standard) ECU (Environmental Control Unit) consists of a reciprocating compressor, copper tube and aluminum fin coils, scroll cage fan assemblies, and a housing that has been hardened to meet the military unique requirements as shown in Fig. 58 [73]. However, two recent developments have motivated the US military to sponsor research on CO_2 systems to meet its operational requirements for (1) lightweight ultra-compact units for rapid deployment via air transport, and (2) a refrigerant that is globally available and free of the diverse and extensive regulatory requirements and logistical challenges associated with greenhouse gases. That body of research has spanned a relatively wide spectrum, from the first demonstration of space heating operation [152] to investigations of ways to make evaporators more compact: bypassing flash gas [150]; and fundamental investigations of boiling behavior near the critical point [20]. One of the earliest theoretical analyses of

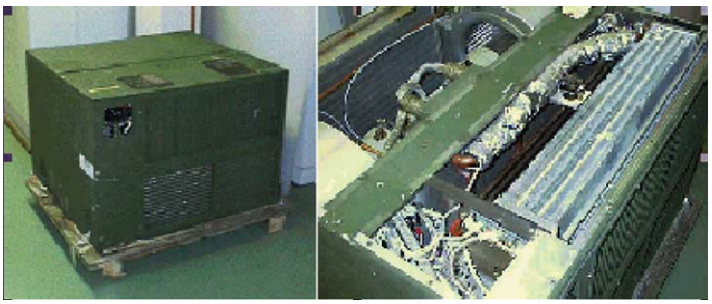

Fig. 58. Military environmental control unit [73].

Table 3
Summary of capacity and COP for the different configurations [169]

		R-22 Mil-Std	CO_2 Basic	CO_2 Plus
Average[a]	Capacity (kW)	9.91	7.62	8.20
	COP	1.46	0.96	1.03
Peak[b]	Capacity (kW)	12.9	11.62	11.47
	COP	2.10	1.34	1.54
Design condition[c]	Capacity (kW)	9.60	6.75	8.47
	COP	1.40	0.97	1.03

[a] Average values across all sixteen test conditions (indoor: 32 °C/50 and 90% RH, and 26.7 °C/50 and 90% RH, outdoor: 52, 49, 43, and 38 °C).
[b] The one test condition out of sixteen where the value was greatest (R-22 Mil-Std: at 26.7 °C/50% RH indoor and 38 °C outdoor, CO_2 Basic: at 32 °C/50% RH indoor and 38 °C outdoor, CO_2 Plus: at 32 °C/90% RH and 38 °C outdoor).
[c] It reflects the current military rating point of 32 °C/50% RH indoor and 49 °C outdoor. Future Mil-Std design conditions will be raised to 32 °C/50% RH indoor and 52 °C outdoor.

this type of system compared performance of CO_2 and R-22 and found them roughly equivalent under some conditions, even if the CO_2 unit used conventional fin-and-tube heat exchangers [36].

The first data from a microchannel-based CO_2 prototype ECU were presented in 2002 as shown in Table 3 [169]. The 'CO_2 Basic' unit consists of an automotive reciprocating compressor, microchannel heat exchangers, an accumulator, and an expansion devise which was a hand-adjusted metering valve. The system was designed with a safety factor of four times the expected working pressure, which is common for current military systems. The design burst pressure was 62.0 MPa since the high-side system pressure was limited to 15.5 MPa. The CO_2 Basic ECU did not perform as well as the R-22 Mil-Std ECU in terms of capacity and COP. The addition of internal heat exchanger ('CO_2 Plus' unit) improved the capacity and COP but still fell short of the R-22 baseline. They speculated that the system capacity and COP could be further improved by using an appropriate compressor, and a change in fan type. These government-sponsored research efforts have augmented the already substantial industry-funded efforts to identify opportunities for improving system efficiency by developing advanced component technologies for the next generation of prototype residential space conditioning systems.

8.7. Transport refrigeration

Research interest in CO_2 has also been renewed in the area of transport refrigeration for two reasons The first relates to the relatively high density and capacity of CO_2 at low temperatures, compared to alternatives such as hydrocarbons or ammonia; the advent of lightweight compact microchannel heat exchangers presents new opportunities for system optimization. Second, the world-wide availability of CO_2 and freedom from HFC-related regulatory uncertainties fits well with the global nature of the transport refrigeration industry. Shipping containers must comply with regulations at all ports, and mass-produced trucks must be capable of operating at the farthest reaches of the 'cold chain' in rural developing countries where fluorocarbon refrigerants and trained recovery technicians may not be available.

Preliminary test results on a prototype CO_2 system for truck refrigeration gave COP data that matched equally sized systems using R-502 and R-507 [170]. A Danish study predicted the performance of refrigerating systems for transport containers, concluding with COP values that were 15–20% below those of R-134a systems, not including the effects of differences in compressor efficiency and refrigerant-side pressure drops [171]. Jakobsen and Nekså [172] conducted more detailed simulations including the effects of capacity control and varying compressor efficiency at varying compression ratio. The results showed very similar COP values in freezing mode for CO_2 and R-134a over the full range of ambient temperature. In cooling mode, the excess capacity was much greater with R-134a than with CO_2 due to differences in refrigerant properties. When the influence on COP by suction throttling or cylinder unloading was included, the estimated COP in freezing mode became slightly (3–10%) higher for the CO_2 system than for the R-134a system. One problem with CO_2 may be very high compressor discharge temperature for freezing operation at high ambient temperature.

8.8. Commercial refrigeration

Commercial refrigeration systems for shops, supermarkets, larger kitchens, etc. have large refrigerant emissions, and the energy use is in many cases high. Thus, there is a need for efficient, safe and environmentally friendly refrigeration systems. New concepts based on CO_2 have been demonstrated for centralized systems using CO_2 as a secondary heat transfer fluid or in a low-temperature cascade stage, and recently decentralized concepts with heat recovery have been shown. Some of these developments are outlined in the following text.

Eggen and Aflekt [173] reviewed the possibilities for CO_2: (i) as secondary refrigerant, (ii) as a primary refrigerant in a low temperature stage in a cascade system, and (iii) in all-CO_2 centralized systems. They also presented a prototype CO_2/NH_3 cascade system built in Norway. A large number of secondary fluid systems are already operating in the Nordic countries using CO_2 as a volatile secondary refrigerant. The safety aspects and good thermo-physical properties of CO_2, leading to small pipe dimensions and good heat transfer, make it a preferable

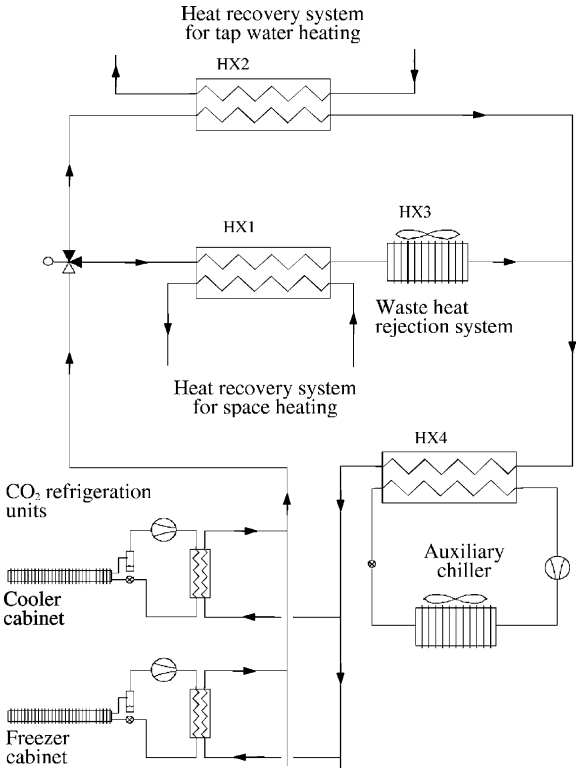

Fig. 59. Distributed CO_2 supermarket refrigeration system with central heat recovery.

fluid in indirect systems. Further advantages of cascade systems include the greatly reduced low-temperature compressor sizes, the absence of a liquid pump, and fewer stages of heat transfer. With heat recovery, centralized all-CO_2 systems may also have an interesting potential.

The decentralized supermarket system described by Nekså et al. [174] uses CO_2 as the only refrigerant in a system with heat recovery. Self-contained display cabinets each with CO_2 refrigeration units are connected to a hydronic heat recovery circuit that heats service water and buildings (Fig. 59).

By utilizing the transcritical CO_2 process, it is possible to have a large temperature glide in the hydronic circuit, typically 50–60 K, and a correspondingly low volume flow rate and small pipe dimensions. Waste heat with high temperature (70–75 °C) is available for tap water and/or space heating. Excess heat is rejected to the ambient air by direct heat exchange. The system offers a very easy installation and gives the owner of the store a great flexibility in arranging and rearranging the cabinets.

System simulations for a medium size supermarket have been carried out. Optimum hydronic supply and return temperatures to the cooling and freezing cabinets were identified. A comparison between the CO_2 system and a conventional R-22 system with respect to the overall energy consumption of the supermarket for one year of operation in a southern European climate was carried out. The CO_2 system was found to reduce the total energy consumption for refrigeration and heating by 32% compared to the R-22 system. Each CO_2 unit can also be equipped with a condensing unit in order to reject heat directly to the shopping area when space heating is required. In the warm season with a heat surplus, the waste heat recovery circuit removes the heat. This concept reduces the power demand for the refrigeration units to the same level as for the baseline R-22 system, and the resulting overall energy consumption of the supermarket will then be further reduced.

8.9. Dryers

Another interesting application of CO_2 vapor compression cycle is heat pump dryer One example is the prototype of a commercial size dryer as shown in Fig. 60, which shows the schemes of the heat pump and the hot air circuit [175]. The auxiliary heat exchanger is located

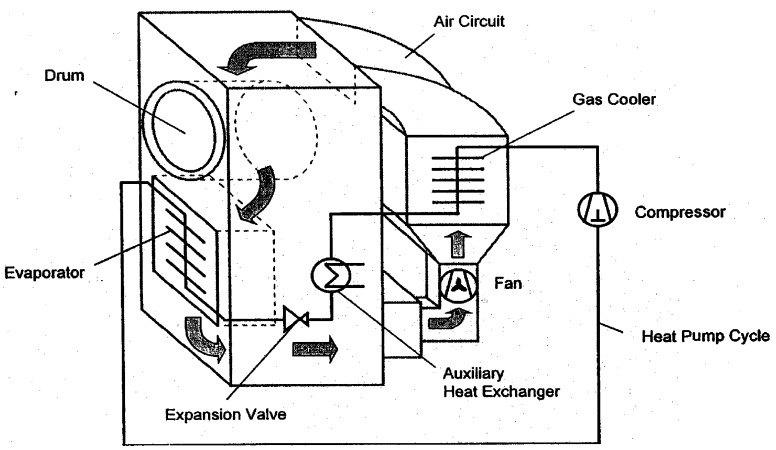

Fig. 60. CO_2 heat pump dryer [175].

between a gas cooler and an expansion valve, thus contributing to additional cooling of the supercritical CO_2. Based on theoretical considerations, Steimle [176] reported that energy saving is possible due to better temperature adaptation in the heat exchangers, compared to subcritical processes. It is also possible to achieve higher air temperatures without loss in efficiency, thus increasing the moisture extraction rate. Schmidt et al. [175,177] compared the thermodynamic behavior of two dehumidification heat pump cycles: the subcritical R-134a process and the transcritical CO_2 process. Experimental results from Schmidt et al. [175] report heat pump COPs in the range 5.5 and 55% reduction in the energy consumption, including fan power, compared to traditional electrically heated clothes dryer. The results were achieved after a first optimization of the prototype system and it was claimed that further improvements still could be realized.

9. Concluding remarks

The state of the art for the transcritical CO_2 cycle technology in various refrigeration, air-conditioning and heat pump applications was critically reviewed. The article covered the history and re-emergence of the natural refrigerant CO_2, its thermodynamic and transport properties, basic CO_2 transcritical cycles and some options of cycle modifications (advanced cycles), heat transfer and pressure drop characteristics in CO_2 systems, and issues and design characteristics related to high operating pressure. It also explored component design issues and possible applications for the earliest markets, and those barriers to be overcome before commercialization.

The prospects for CO_2 and its transcritical cycle are still uncertain, mainly because of the many simultaneous component and system innovations required, e.g. to handle the high pressures, and to develop microchannel evaporators that tolerate frost and condensate while distributing refrigerant uniformly. The greatest obstacle it faces is its high temperature of heat rejection, which explains why its first commercial opportunities are occurring in water heating, and in space heating applications where high delivery temperatures are required. Its inherent advantage—negligible global warming impact—has focused most of the early research on automotive air conditioning applications where direct refrigerant leakage has been a significant contributor to global warming.

The re-emergence of the 'old refrigerant' CO_2 provides a historical context for making several important observations about the path of technological innovation in air conditioning and refrigeration systems and components. A century ago, the earliest engineering development efforts focused on the compressor because it was the most costly component, and efficiency improvements accompanied cost reduction. With the advent of CFCs that could operate at low pressures with reasonable thermodynamic cycle efficiencies and avoid the toxicity or flammability risks of ammonia and hydrocarbons, system costs dropped to the point where mass production became feasible. Declining real energy prices over most of the twentieth century expanded the market for air conditioning, so the industry realized the economies of mass production by (1) focusing on the simple 'standard' vapor-compression cycle to minimize the number of components, and (2) optimizing the components to make the actual cycle approach the refrigerant's ideal thermodynamic efficiency, for example, by taking full advantage of the particular refrigerant's transport properties.

Over the last decade the situation began to change dramatically as chlorofluorocarbon refrigerants were phased out, and the prospect of global warming signaled higher energy costs and controls on fluorocarbon refrigerants. In parts of the world where energy prices are already high, the simple vapor-compression cycle efficiency has been increased by adding sensors, actuators and controls to allow modulating refrigerant flow rate, thereby minimizing temperature differences across the heat exchangers at all operating conditions. Unfortunately, the maximum efficiency attainable through this approach is refrigerant-specific: the COP of that particular refrigerant on the standard cycle. Today's research is focusing on ways to modify the standard vapor-compression cycle, for example, through use of multistage compression, intercooling, internal heat exchangers and expanders as is now done routinely in industrial-scale systems where energy costs dominate.

As the cycle is modified by addition of such components and controls, the system COP depends less on the thermodynamic properties of the refrigerant and more on the cost of manufacturing the more complex systems. Therefore, refrigerants will be chosen in the future for their environmental safety and compatibility with various cycle-improving component designs, rather than their simple-cycle ideal efficiency. If the cost of sensors, actuators and microprocessor controls continue to decrease, along with the cost of embedding them in mass produced items, the cost advantage now enjoyed by refrigerants having favorable thermodynamic properties may diminish. Modern manufacturing technologies (e.g. for making small diameter tubes) have already reduced the weight and volume penalties once associated with high-pressure refrigerants like CO_2, and various methods for refrigerant-side area enhancement have further decreased the importance of refrigerant transport properties.

Strictly speaking, the Carnot cycle is not always the ideal because heat sources and sinks are finite in all heat pumping applications. This is especially true in heating mode where substantial increases in air or water temperatures are required; the temperature glide of the transcritical CO_2 cycle provides a distinct advantage in such cases. While such loads are generally met today by direct fossil fuel combustion at COPs less than one, in the future they are

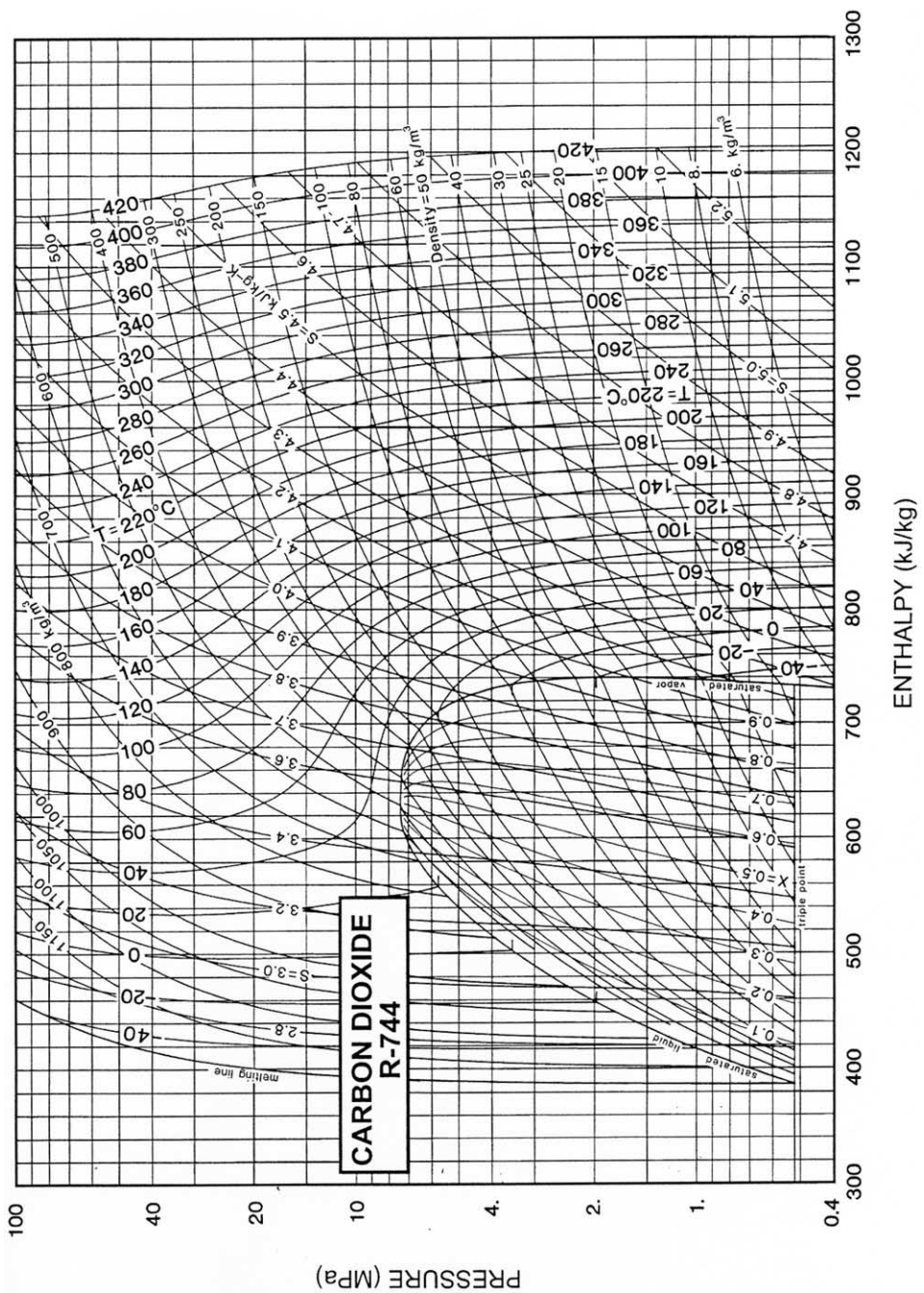

Fig. A1. Pressure–enthalpy diagram of CO_2 [19].

Table A1
Refrigerant CO_2 properties of saturated liquid and vapor [19]

Temperature[a], °C	Pressure, MPa	Density (liquid), kg/m^3	Volume (Vapour), m^3/kg	Enthalpy, kJ/kg		Entropy, kJ/(kg K)		Specific heat, c_p, kJ/(kg K)		c_p/c_v	Velocity of sound, m/s		Viscosity, μPa s		Thermal conductivity, mW/(m K)		Surface tension, mN/m	Temp., °C
				Liquid	Vapour	Liquid	Vapour	Liquid	Vapour	Vapour	Liquid	Vapour	Liquid	Vapour	Liquid	Vapour		
−56.56a	0.51796	1178.5	0.07267	80.04	430.42	0.5213	2.1390	1.953	0.909	1.444	976.0	222.8	256.7	10.95	180.6	11.01	17.16	−56.56
−50.00	0.68234	1154.6	0.05579	92.94	432.69	0.5794	2.1018	1.971	0.952	1.468	928.0	223.4	229.3	11.31	172.1	11.58	15.53	−50.00
−48.00	0.73949	1147.1	0.05162	96.90	433.29	0.5968	2.0909	1.978	0.967	1.477	914.0	223.5	221.6	11.42	169.5	11.76	15.04	−48.00
−46.00	0.80015	1139.6	0.04782	100.88	433.86	0.6142	2.0801	1.985	0.982	1.486	900.0	223.6	214.3	11.53	166.9	11.95	14.56	−46.00
−44.00	0.86445	1132.0	0.04435	104.87	434.39	0.6314	2.0694	1.993	0.998	1.496	885.0	223.6	207.2	11.64	164.4	12.14	14.07	−44.00
−42.00	0.93252	1124.2	0.04118	108.88	434.88	0.6486	2.0589	2.002	1.015	1.507	871.0	223.6	200.3	11.75	161.8	12.34	13.60	−42.00
−40.00	1.0045	1116.4	0.03828	112.90	435.32	0.6656	2.0485	2.012	1.033	1.518	856.0	223.5	193.8	11.87	159.3	12.54	13.12	−40.00
−38.00	1.0805	1108.5	0.03562	116.95	432.72	0.6826	2.0382	2.022	1.052	1.530	842.0	223.4	187.4	11.98	156.8	12.75	12.65	−38.00
−36.00	1.1607	1100.5	0.03318	121.01	436.07	0.6995	2.0281	2.033	1.072	1.544	827.0	223.2	181.3	12.10	154.3	12.97	12.18	−36.00
−34.00	1.2452	1092.4	0.03093	125.10	436.37	0.7163	2.0180	2.045	1.094	1.558	813.0	223.1	175.4	12.22	151.8	13.20	11.72	−34.00
−32.00	1.3342	1084.1	0.02886	129.20	436.62	0.7331	2.0079	2.059	1.116	1.573	798.0	222.8	169.7	12.34	149.3	13.43	11.26	−32.00
−30.00	1.4278	1075.7	0.02696	133.34	436.82	0.7498	1.9980	2.073	1.141	1.590	783.0	222.5	164.2	12.46	146.9	13.68	10.80	−30.00
−28.00	1.5261	1067.2	0.02519	137.50	436.96	0.7665	1.9880	2.089	1.166	1.608	768.0	222.2	158.9	12.59	144.4	13.94	10.35	−28.00
−26.00	1.6293	1058.6	0.02356	141.69	437.04	0.7831	1.9781	2.105	1.194	1.627	753.0	221.8	153.8	12.72	141.9	14.20	9.90	−26.00
−24.00	1.7375	1049.8	0.02205	145.91	437.06	0.7997	1.9683	2.124	1.223	1.648	738.0	221.4	148.8	12.85	139.5	14.49	9.46	−24.00
−22.00	1.8509	1040.8	0.02065	150.16	437.01	0.8163	1.9584	2.144	1.255	1.671	723.0	220.9	144.0	12.98	137.1	14.78	9.02	−22.00
−20.00	1.9696	1031.7	0.01934	154.45	436.89	0.8328	1.9485	2.165	1.289	1.696	708.0	220.4	139.3	13.12	134.6	15.09	8.59	−20.00
−19.00	2.0310	1027.0	0.01873	156.61	436.81	0.8411	1.9436	2.177	1.307	1.709	700.0	220.1	137.1	13.18	133.4	15.25	8.37	−19.00
−18.00	2.0938	1022.3	0.01813	158.77	436.70	0.8494	1.9386	2.189	1.326	1.723	692.0	219.8	134.8	13.26	132.2	15.42	8.16	−18.00
−17.00	2.1581	1017.6	0.01756	160.95	436.58	0.8576	1.9337	2.201	1.346	1.738	684.0	219.5	132.6	13.33	131.0	15.59	7.95	−17.00
−16.00	2.2237	1012.8	0.01700	163.14	436.44	0.8659	1.9287	2.215	1.366	1.753	676.0	219.2	130.4	13.40	129.8	15.77	7.74	−16.00
−15.00	2.2908	1008.0	0.01647	165.34	436.27	0.8742	1.9237	2.228	1.388	1.768	668.0	218.8	128.3	13.47	128.6	15.95	7.53	−15.00
−14.00	2.3593	1003.1	0.01595	167.55	436.09	0.8825	1.9187	2.243	1.410	1.785	660.0	218.5	126.2	13.55	127.4	16.14	7.32	−14.00
−13.00	2.4294	998.1	0.01545	169.78	435.89	0.8908	1.9137	2.258	1.433	1.802	651.0	218.1	124.1	13.63	126.2	16.34	7.11	−13.00
−12.00	2.5010	993.1	0.01497	172.01	435.66	0.8991	1.9086	2.273	1.457	1.821	643.0	217.7	122.0	13.70	125.0	16.54	6.90	−12.00
−11.00	2.5740	988.1	0.01450	174.26	435.41	0.9074	1.9036	2.290	1.483	1.840	635.0	217.4	120.0	13.78	123.8	16.74	6.70	−11.00
−10.00	2.6487	982.9	0.01405	176.52	435.14	0.9157	1.8985	2.307	1.509	1.860	626.0	216.9	118.0	13.86	122.5	16.96	6.50	−10.00
−9.00	2.7249	977.7	0.01361	178.80	434.84	0.9240	1.8934	2.325	1.537	1.881	617.0	216.5	116.1	13.95	121.3	17.18	6.29	−9.00
−8.00	2.8027	972.5	0.01319	181.09	434.51	0.9324	1.8882	2.345	1.566	1.904	609.0	216.1	114.1	14.03	120.1	17.42	6.09	−8.00
−7.00	2.8821	967.1	0.01278	183.39	434.17	0.9408	1.8830	2.365	1.597	1.927	600.0	215.6	112.2	14.12	118.9	17.66	5.89	−7.00
−6.00	2.9632	961.7	0.01238	185.71	433.79	0.9491	1.8778	2.386	1.629	1.952	591.0	215.2	110.3	14.20	117.7	17.91	5.70	−6.00
−5.00	3.0459	956.2	0.01200	188.05	433.38	0.9576	1.8725	2.408	1.663	1.979	582.0	214.7	108.4	14.30	116.5	18.17	5.50	−5.00
−4.00	3.1303	950.6	0.01162	190.40	432.95	0.9660	1.8672	2.432	1.699	2.007	573.0	214.2	106.6	14.39	115.3	18.44	5.30	−4.00
−3.00	3.2164	945.0	0.01126	192.77	432.48	0.9744	1.8618	2.457	1.737	2.037	564.0	213.7	104.8	14.48	114.1	18.73	5.11	−3.00
−2.00	3.3042	939.2	0.01091	195.16	431.99	0.9829	1.8563	2.484	1.777	2.068	555.0	213.1	102.9	14.58	112.9	19.03	4.92	−2.00
−1.00	3.3938	933.4	0.01057	197.57	431.46	0.9914	1.8509	2.512	1.819	2.102	546.0	212.6	101.2	14.68	111.6	19.34	4.73	−1.00

(*continued on next page*)

Table A1 (*continued*)

Temperature[a], °C	Pressure, MPa	Density (liquid), kg/m^3	Volume (Vapour), m^3/kg	Enthalpy, kJ/kg		Entropy, kJ/(kg K)		Specific heat, c_p, kJ/(kg K)		c_p/c_v	Velocity of sound, m/s		Viscosity, μPa s		Thermal conductivity, mW/(m K)		Surface tension, mN/m	Temp., °C
				Liquid	Vapour	Liquid	Vapour	Liquid	Vapour	Vapour	Liquid	Vapour	Liquid	Vapour	Liquid	Vapour		
0.00	3.4851	927.4	0.01024	200.00	430.89	1.0000	1.8453	2.542	1.865	2.138	536.0	212.0	99.4	14.79	110.4	19.67	4.54	0.00
1.00	3.5783	921.4	0.00992	202.45	430.29	1.0086	1.8397	2.574	1.913	2.176	527.0	211.5	97.6	14.89	109.2	20.02	4.35	1.00
2.00	3.6733	915.2	0.00961	204.93	429.65	1.0172	1.8340	2.609	1.965	2.218	518.0	210.9	95.9	15.00	108.0	20.38	4.17	2.00
3.00	3.7701	909.0	0.00931	207.43	428.97	1.0259	1.8282	2.645	2.020	2.262	508.0	210.3	94.2	15.12	106.8	20.76	3.99	3.00
4.00	3.8688	902.6	0.00901	209.95	428.25	1.0346	1.8223	2.685	2.080	2.309	499.0	209.6	92.5	15.24	105.5	21.17	3.80	4.00
5.00	3.9695	896.0	0.00872	212.50	427.48	1.0434	1.8163	2.727	2.144	2.360	489.0	209.0	90.8	15.36	104.3	21.60	3.62	5.00
6.00	4.0720	889.4	0.00845	215.08	426.67	1.0523	1.8102	2.772	2.213	2.416	480.0	208.3	89.1	15.49	103.1	22.06	3.45	6.00
7.00	4.1765	882.6	0.00817	217.69	425.81	1.0612	1.8041	2.822	2.289	2.476	470.0	207.6	87.5	15.62	101.8	22.54	3.27	7.00
8.00	4.2831	875.6	0.00791	220.34	424.89	1.0702	1.7977	2.875	2.370	2.541	460.0	206.9	85.8	15.76	100.6	23.06	3.10	8.00
9.00	4.3916	868.4	0.00765	223.01	423.92	1.0792	1.7913	2.934	2.460	2.612	451.0	206.2	84.2	15.91	99.4	23.61	2.93	9.00
10.00	4.5022	861.1	0.00740	225.73	422.88	1.0884	1.7847	2.998	2.558	2.690	441.0	205.4	82.6	16.06	98.1	24.21	2.76	10.00
11.00	4.6149	853.6	0.00715	228.49	421.79	1.0976	1.7779	3.068	2.666	2.776	431.0	204.6	80.9	16.22	96.9	24.84	2.59	11.00
12.00	4.7297	845.9	0.00691	231.29	420.62	1.1070	1.7710	3.145	2.786	2.871	421.0	203.8	79.3	16.39	95.6	25.53	2.42	12.00
13.00	4.8466	837.9	0.00668	234.13	419.37	1.1165	1.7638	3.232	2.919	2.977	411.0	203.0	77.7	16.56	94.4	26.27	2.26	13.00
14.00	4.9658	829.7	0.00645	237.03	418.05	1.1261	1.7565	3.328	3.068	3.095	401.0	202.1	76.1	16.75	93.1	27.08	2.10	14.00
15.00	5.0871	821.2	0.00622	239.99	416.64	1.1359	1.7489	3.436	3.237	3.228	391.0	201.2	74.4	16.95	91.9	27.96	1.95	15.00
16.00	5.2108	812.4	0.00600	243.01	415.12	1.1458	1.7411	3.558	3.429	3.378	381.0	200.3	72.8	17.16	90.6	28.93	1.79	16.00
17.00	5.3368	803.3	0.00578	246.10	413.50	1.1559	1.7329	3.698	3.649	3.550	370.0	199.3	71.2	17.39	89.4	29.99	1.64	17.00
18.00	5.4651	793.8	0.00557	249.26	411.76	1.1663	1.7244	3.858	3.905	3.748	360.0	198.3	69.5	17.64	88.1	31.16	1.49	18.00
19.00	5.5958	783.8	0.00536	252.52	409.89	1.1769	1.7155	4.044	4.204	3.979	349.0	197.2	67.8	17.90	86.9	32.47	1.35	19.00
20.00	5.7291	773.4	0.00515	255.87	407.87	1.1877	1.7062	4.264	4.560	4.252	338.0	196.1	66.1	18.19	85.7	33.94	1.20	20.00
21.00	5.8648	762.4	0.00494	259.33	405.67	1.1989	1.6964	4.526	4.990	4.578	326.0	194.9	64.4	18.50	84.5	35.61	1.06	21.00
22.00	6.0031	750.8	0.00474	262.93	403.26	1.2105	1.6860	4.846	5.519	4.976	314.0	193.6	62.7	18.85	83.4	37.52	0.93	22.00
23.00	6.1440	738.4	0.00453	266.68	400.63	1.2225	1.6749	5.248	6.185	5.472	302.0	192.3	60.9	19.23	82.4	39.74	0.80	23.00
24.00	6.2877	725.0	0.00433	270.61	397.70	1.2352	1.6629	5.767	7.049	6.107	288.0	190.8	59.0	19.66	81.5	42.35	0.67	24.00
25.00	6.4342	710.5	0.00412	274.78	394.43	1.2485	1.6498	6.467	8.212	6.949	274.0	189.1	57.0	20.16	80.8	45.51	0.55	25.00
26.00	6.5837	694.5	0.00391	279.26	391.71	1.2627	1.6353	7.460	9.862	8.121	259.0	187.2	55.0	20.73	80.5	49.44	0.44	26.00
27.00	6.7361	676.4	0.00369	284.14	386.39	1.2783	1.6189	8.97	12.38	9.87	243.0	185.0	52.8	21.42	80.7	54.56	0.33	27.00
28.00	6.8918	655.3	0.00346	289.62	381.20	1.2958	1.5999	11.55	16.69	12.78	225.0	182.1	50.3	22.27	81.9	61.73	0.23	28.00
29.00	7.0509	629.4	0.00320	296.07	374.61	1.3163	1.5763	16.95	25.74	18.63	205.0	178.2	47.5	23.41	85.2	73.19	0.13	29.00
30.00	7.2137	593.3	0.00290	304.55	365.13	1.3435	1.5433	35.34	55.82	36.66	177.0	171.3	43.8	25.17	95.4	98.02	0.02	30.00
30.98c	7.3773	467.6	0.00214	332.25	332.25	1.4336	1.4336	∞	∞	∞	0.0	0.0	–	–	∞	∞	0.00	30.98

[a] Temperatures are on the ITS-90 scale. a, triple point; c, critical point.

likely to be met by heat pumps at COP $\gg 1$ as regulation of greenhouse gas emissions requires that fossil fuels be used more efficiently. The early introduction of transcritical CO_2 systems into the Asian domestic water heating market is providing the first test of this hypothesis, since earlier attempts to introduce subcritical systems have failed.

Research on alternative refrigerants is continuing on many parallel paths, including explorations of the use of hydrocarbons or ammonia by minimizing charge or using secondary refrigerant loops. Each of these paths efforts is yielding surprising results, as illustrated by this review for the case of CO_2. What these efforts have in common is that they are bring fundamental research to bear on a technology whose development has been driven for decades by reliability concerns, and therefore characterized by incremental improvements built on a massive empirical database. After the Montreal and Kyoto Protocols rendered much of this data useless, the industry entered an era of discontinuous technological change that required development of new technology within the industry, as well as importing technology from outside.

Acknowledgements

This work was partly supported by the Brain Korea 21 Program, by Shecco Technology, and by the member companies of the Air Conditioning and Refrigeration Center at the University of Illinois at Urbana-Champaign.

Appendix A. Pressure–enthalpy diagram and saturation properties for CO_2

See Fig. A1 and Table A1.

References

[1] The Kyoto Protocol to the United Nations Framework Convention on Climate Change, 1997.
[2] Billiard F. Refrigeration and air conditioning: what's new at regulatory level. The Ninth European Conference on Technological Innovations in Refrigeration, Air Conditioning and in the Food Industry, Politecnico di Milano; 2001.
[3] Lorentzen G, Pettersen J. New possibilities for non-CFC refrigeration. In: Pettersen J, editor. IIR International Symposium on Refrigeration, Energy and Environment, Trondheim, Norway. 1992. p. 147–63.
[4] Bodinus WS. The rise and fall of carbon dioxide systems. In: Will HM, editor. The first century of air conditioning. Atlanta, GA: ASHRAE; 1999. p. 29–34.
[5] Thevenot R. A history of refrigeration throughout the world. Paris: IIR; 1979. [Fidler JC, Trans.].
[6] Donaldson B, Nagengast B. Heat and cold: mastering the great indoors. Atlanta, GA: ASHRAE; 1994.
[7] Kohlendioxid. Besonderheiten und Einsatzchancen als Kältemittel. Statusbericht des Deutschen Kälte- und Klimatechnischen Vereins. Nr 20. DKV, Stuttgart; 1998.
[8] Stera A. Ammonia refrigerating plant on reefer ships. Introduction to ammonia as a marine refrigerant. Lloyd's Register Technical Seminar, London; 1992.
[9] Plank R. Amerikanische Kältetechnik. Berlin: VDI-Verlag; 1929.
[10] Voorhees G. Improvements relating to systems of fluid compression and to compressors thereof. British Patent 4448; 1905.
[11] Lorentzen G. Trans-critical vapour compression cycle device. International Patent Publication WO 90/07683; 1990.
[12] Morley J, Bivens D. Trends in environmental issues and implications for automotive air conditioning. Vehicle Thermal Management Systems Conference, London; 1995. p. 405–12.
[13] Bhatti M. A critical look at R-744 and R-134a mobile air conditioning systems. SAE Paper No. 970527; 1997.
[14] Rieberer R. CO_2 as working fluid for heat pump. PhD Thesis. Institute of Thermal Engineering, Graz University, Austria; 1998.
[15] Lorentzen G. The use of natural refrigerants: a complete solution to the CFC/HCFC predicament. Int J Refrig 1995; 18(3):190–7.
[16] Vesovic V, Wakeham WA, Olchowy GA, Sengers JV, Watson JTR, Millat J. The transport properties of carbon dioxide. J Phys Chem Ref Data 1990;19:763–808.
[17] Fenghour A, Wakeham W, Vesovic V. The viscosity of carbon dioxide. J Phys Chem Ref Data 1998;27(1):31–44.
[18] VDI, VDI Wärmeatlas: Berechnungsblätter für den Wärmeübergang. Düsseldorf, Germany: VDI Verlag; 1994.
[19] ASHRAE, ASHRAE handbook: fundamentals. Atlanta, GA: American Society of Heating, Refrigerating and Air-Conditioning Engineers; 2001.
[20] Pettersen J. Flow vaporization of CO_2 in microchannel tubes. PhD Thesis, Norwegian University of Science and Technology, Norway; 2002.
[21] Liley P, Desai P. Thermophysical properties of refrigerants, SI ed. ASHRAE; 1993. p. 259–67.
[22] Klein S, Alvarado F. Engineering equation solver, version 6.242. F-Chart Software; 2001.
[23] Span R, Wagner W. A new equation of state for carbon dioxide covering the fluid region from the triple-point temperature to 1100 K at pressure up to 800 MPa. J Phys Chem Ref Data 1996;26:1509–96.
[24] Bredesen A, Hafner A, Pettersen J, Aflekt K. Heat transfer and pressure drop for in-tube evaporation of CO_2. International Conference on Heat Transfer Issues in Natural Refrigerants, College Park, MD; 1997. p. 1–15.
[25] Rathjen W, Straub J. Temperature dependence of surface tension, coexistence curve, and vapor pressure of CO_2, $CClF_3$, $CBrF_3$, and SF_6. Heat transfer in boiling, New York: Academic Press; 1977 [chapter 18].
[26] Estrada-Alexanders AF, Trusler JPM. Speed of sound in carbon dioxide at temperatures between (220 and 450) K and pressures up to 14 MPa. J Chem Thermodyn 1998;30(12): 1589–601.
[27] Liao S, Zhao T. Measurements of heat transfer coefficients from supercritical carbon dioxide flowing in horizontal mini/meso channels. J Heat Transfer 2002;124:413–20.

[28] Pettersen J, Skaugen G. Operation of trans-critical CO_2 vapour compression systems in vehicle air conditioning. IIR International Conference on New Applications of Natural Working Fluids in Refrigeration and Air Conditioning, Hanover, Germany; 1994. p. 495–505.
[29] Inokuty H. Graphical method of finding compression pressure of CO_2 refrigerating machine for maximum coefficient of performance. The Fifth International Congress of Refrigeration, Rome; 1928. p. 185–92.
[30] Pettersen J. Process with high-pressure control. Kohlendioxid: Besonderheiten und Einsatzchancen als Kältemittel, Statusbericht des DKV, No. 20, German Association of Refrigeration and Air Conditioning; 1998. p. 64–74.
[31] Pettersen J. Experimental results of carbon dioxide in compression systems. ASHRAE/NIST Conference Refrigerants for the 21st Century, Gaithersburg, MD; 1997. p. 27–37.
[32] Lorentzen G. Revival of carbon dioxide as a refrigerant. Int J Refrig 1993;17(5):292–301.
[33] Domanski P, Didion D, Doyle J. Evaluation of suction-line/liquid-line heat exchange in the refrigeration cycle. Int J Refrig 1994;17(7):487–93.
[34] Kim M-H. Performance evaluation of R-22 alternative mixtures in a heat pump with pure cross-flow condenser and counter-flow evaporator. Energy 2002;27(2):167–81.
[35] Vakil H. Thermodynamics of heat exchange in refrigeration cycles with non-azeotropic mixtures. Part II. Suction line heat exchange and evaporative cooling of capillary. Proceedings of the International Congress of Refrigeration, Paris, France: IIR; 1983. p. 533–8.
[36] Robinson D, Groll E. Efficiencies of transcritical CO_2 cycles with and without an expansion turbine. Int J Refrig 1998; 21(7):577–89.
[37] Boewe D, Yin J, Park Y, Bullard C, Hrnjak P. The role of suction line heat exchanger in transcritical R744 mobile A/C systems. SAE Paper No. 1999-01-0583; 1999.
[38] Negishi M. Refrigeration air conditioner. Japan No. JP11094379; 1997.
[39] Plank R. Arbeitsverfahren an Kompressionskältemaschinen, insbesondere für Kälteträger mit tiefer kritischer Temperatur. German Patent No. DE278095; 1912.
[40] Ikoma M, Hasegawa H, Shintaku H. Refrigeration cycle device and its control method. Japan Patent No. JP2002022298; 2000.
[41] Maurer T, Zinn T. Untersuchung von Entspannungsmaschinen mit mechanischer Leistungsauskopplung für die transkritische CO_2-Kältemaschine. DKV-Tagungsbericht 26, Berlin; 1999. p. 264–77.
[42] Heyl P, Quack H. Transcritical CO_2 cycle with expander–compressor. In: Groll EA, Robinson DM, editors. The Fourth IIR-Gustav Lorentzen Conference on Natural Working Fluids, West Lafayette, IN. 2000. p. 471–80.
[43] Stosic N, Smith I, Kovacevic A. A twin screw combined compressor and expander for CO_2 refrigeration systems. In: Soedel W, editor. Proceedings of the International Compressor Engineering Conference at Purdue, West Lafayette, IN. Paper No. C21-2; 2002. p. 703–10.
[44] Huff H-J, Lindsay D, Radermacher R. Positive displacement compressor and expander simulation. In: Soedel W, editor. Proceedings of the International Compressor Engineering Conference at Purdue, West Lafayette, IN. Paper No. C9-2; 2002. p. 209–16.
[45] Baek J, Groll E, Lawless P. Development of a piston-cylinder expansion device for the transcritical carbon dioxide cycle. In: Groll EA, editor. Proceedings of the International Refrigeration and Air Conditioning Conference at Purdue, West Lafayette, IN, Paper No. R11-8. 2002.
[46] Heyl P, Quack H. Free piston expander–compressor for CO_2: design, applications and results. The 20th International Congress of Refrigeration, Sydney, Australia; 1999.
[47] Nickl J, Will G, Kraus W, Quack H. Design considerations for a second generation CO_2-expander. In: Xu Z, Fan J, Huang W, editors. The Fifth IIR-Gustav Lorentzen Conference on Natural Working Fluids. Guangzhou, China. 2002. p. 189–96.
[48] Hess U, Tiedemann T. Klimaanlage für Kraftfahrzeuge und Verfahren zum Betreiben einer Klimaanlage für Kraftfahrzeuge. German Patent No. DE19959439, 1999.
[49] Adachi Y, Kazuo K, Masahiro I. Vapor compression type refrigerator. Japan Patent No. JP2000241033; 1999.
[50] Heidelck R, Kruse H. Expansion machines for carbon dioxide based on modified reciprocating machines. In: Groll EA, Robinson DM, editors. The Fourth IIR-Gustav Lorentzen Conference on Natural Working Fluids, West Lafayette, IN. 2000. p. 455–62.
[51] Hesse U. Klimaanlage, insbesondere für Kraftfahrzeuge und Verfahren zum Betreiben einer Klimaanlage, insbesondere für Kraftfahrzeuge. German Patent No. DE10013191; 2000.
[52] Plank R. Ueber den Ideal-Prozess von Kältemaschinen bei Verbund-Kompression. Zeitschrift für die gesamte Kälte-Industrie 1928;35:17–24.
[53] Thiessen H. Verfahren zum Betrieb einer Kompressionskälteanlage. German Patent No. DE19522884; 1995.
[54] Ozaki Y, Sakajo Y, Sakakibara H, Uchida, K. Vapor compression type refrigerating system. European Patent No. EP0837291; 1997.
[55] Shunichi F, Hiroshi K. Refrigerating cycle. European Patent No. EP0976991; 1999.
[56] Okaza N, Nishiwaki F, Fukunara S, Matsuo M, Yoshida Y. Refrigeration cycle. Japan Patent No. JP2001133058; 1999.
[57] Pettersen J. Cycle options for CO_2. Workshop on Vapor Compression with the Critical Point in Mind, College Park, MD; 2000.
[58] Huff H-J, Hwang Y, Radermacher R. Options for a two-stage transcritical carbon dioxide cycle. In: Xu Z, Fan J, Huang W, editors. The Fifth IIR-Gustav Lorentzen Conference on Natural Working Fluids, Guangzhou, China. 2002. p. 143–9.
[59] Inagaki M, Sasaya H, Ozakli Y. Pointing to the future: two-stage CO_2 compression. Heat transfer issues in natural refrigerants, International Institute of Refrigeration; 1997. p. 131–40.
[60] Olson D. Heat transfer of supercritical carbon dioxide flowing in a cooled horizontal tube. In: Groll EA, Robinson DM, editors. The Fourth IIR-Gustav Lorentzen Conference on Natural Working Fluids, West Lafayette, IN. 2000. p. 251–8.
[61] Gnielinski V. New equations for heat and mass transfer in turbulent pipe and channel flow. Int Chem Engng 1976;16(2): 359–68.
[62] Krasnoshchekov E, Protopopov V. A generalized relationship for calculation of heat transfer to carbon dioxide at

supercritical pressure. Telofizika Vysokikh Temperatur 1972;9(6):1314.
[63] Pitla S, Robinson D, Zingerli A, Groll E, Ramadhyani S. Heat transfer and pressure drop characteristics during in-tube gas cooling of supercritical carbon dioxide. ASHRAE 913-RP, report HL 2000-10 No. 3613-1, Herrick Laboratories, Purdue University; 2000.
[64] Pitla S, Robinson D, Groll E, Ramadhyani S. Heat transfer from supercritical carbon dioxide in tube flow: a critical review. Int J HVAC&R Res 1998;4(3):281–301.
[65] Pitla S, Groll E, Ramadhyani S. Convective heat transfer from in-tube flow of turbulent supercritical carbon dioxide. Part 1. Numerical analysis. Int J HVAC&R Res 2001;7(4): 345–66.
[66] Pitla S, Groll E, Ramadhyani S. Convective heat transfer from in-tube cooling of turbulent supercritical carbon dioxide. Part 2. Experimental data and numerical predictions. Int J HVAC&R Res 2001;7(4):367–82.
[67] Pettersen J, Rieberer R, Leister A. Heat transfer and pressure drop characteristics of supercritical carbon dioxide in microchannel tubes under cooling. In: Groll EA, Robinson DM, editors. The Fourth IIR-Gustav Lorentzen Conference on Natural Working Fluids, West Lafayette, IN. 2000. p. 99–106.
[68] Sun Z, Groll E. CO_2 flow boiling in horizontal tubes. Internal report No. HL-2001-8, Ray W. Herrick Laboratories, Purdue University; 2000.
[69] Hihara E, Tanaka S. Boiling heat transfer of carbon dioxide in horizontal tubes. In: Groll EA, Robinson DM, editors. The Fourth IIR-Gustav Lorentzen Conference on Natural Working Fluids, West Lafayette, IN. 2000. p. 279–84.
[70] Lombardi C, Carsana C. A dimensionless pressure drop correlation for two-phase mixtures flowing upflow in vertical ducts covering wide parameter range. Heat Technol 1992; 10(1-2):125–41.
[71] Kattan N, Thome J, Favrat D. Flow boiling in horizontal tubes. Part 1. Development of a diabatic two-phase flow pattern map. J Heat Transfer 1998;120:140–7.
[72] Weisman J, Duncan D, Gibson J, Crawford T. Effect of fluid properties and pipe diameter on two-phase flow pattern in horizontal lines. Int J Multiphase Flow 1979;5:437–62.
[73] Groll E, Cohen R. Review of recent research on the use of CO_2 for air conditioning and refrigeration. CLIMA 2000, The Seventh Rehva World Congress, Naples, Italy; 2000.
[74] Süss J, Kruse H. Einfluss von Leckage auf die Effizienz von Verdichtern für Kohlendioxid. Ki Luft- und Kältetechnik 1997;173–6.
[75] Fagerli B. CO_2 compressor development. IEA/IIR Workshop on CO_2 Technologies in Refrigeration, Heat Pump and Air Conditioning Systems, Trondheim, Norway 1997;13–14.
[76] Pettersen J, Hafner A, Skaugen G, Rekstad H. Development of compact heat exchangers for CO_2 air-conditioning systems. Int J Refrig 1998;21(3):180–93.
[77] Pettersen J, Brånås M, Hafner A. Some safety aspects of CO_2 vapor compression systems. IEA Annex 27 Workshop Proceedings: Selected Issues on CO_2 as Working Fluid in Compression Systems, Trondheim, Norway 2000; p. 61–75.
[78] NIOSH. US National Institute for Occupational Safety and Health; 1996, http://www.cdc.gov/niosh/idlh/124389.html.
[79] Berghmans J, Duprez H. Safety aspects of CO_2 heat pumps. IEA/IZWe.V./IIR Workshop on CO_2 Technology in Refrigeration, Heat Pump and Air Conditioning Systems, Mainz, Germany; 1999.
[80] Amin J, Dienhart B, Wertenbach J. Safety aspects of an A/C system with carbon dioxide as refrigerant. The SAE Automotive Alternate Refrigerants Systems Symposium, Scottsdale, AZ; 1999.
[81] Pettersen J. Comparison of explosion energies in residential air-conditioning systems based on HCFC-22 and CO_2. Proceedings of the 20th International Congress of Refrigeration (IIR), Sydney, Australia; 1999.
[82] Pettersen J. Refrigerant R-744 fundamentals. VDA Alternate Refrigerant Winter Meeting, Saalfelden, Austria; 2002.
[83] Pettersen J, Hakenjos J. Boiling liquid expanding vapor explosions (BLEVE) in CO_2 vessels: initial experiments. In: Groll EA, Robinson DM, editors. The Fourth IIR-Gustav Lorentzen Conference on Natural Working Fluids, West Lafayette, IN. 2000. p. 216–24.
[84] Pettersen J. Experimental study on boiling liquid expansion in a CO_2 vessel. In: Xu Z, Fan J, Huang W, editors. The Fifth IIR-Gustav Lorentzen Conference on Natural Working Fluids. Guangzhou, China. 2002. p. 92–9.
[85] Kim-E M, Reid R. The rapid depressurization of hot, high pressure liquids or supercritical fluids. Chemical engineering at supercritical fluid conditions, Michigan: Ann Arbor Science; 1983.
[86] Clayton W, Griffin M. Catastrophic failure of a liquid carbon dioxide storage vessel. Process Safety Prog 1994;13(4): 202–9.
[87] Vörös M, Honti G. Explosion of a liquid CO_2 storage vessel in a carbon dioxide plant. The First International Loss Prevention Symposium, The Hague/Delft, the Netherlands; 1974. p. 337–46.
[88] Venart J, Ramier S. Boiling liquid expanding vapor explosions (BLEVE): the influence of dynamic re-pressurization and two-phase discharge. PVP-vol. 377-2, Computational technologies for fluid/thermal/structural/chemical systems with industrial application, vol. II.; 1998. p. 249–54.
[89] Graz M, Stenzel A. Overview of the proposed J639 working draft about safety and containment of refrigerant for mechanical vapor compression systems used for mobile air conditioning systems. VDA Alternate Refrigerant Winter Meeting, Saalfelden, Austria; 2002.
[90] Parsch W. Status of compressor development for R-744 systems. VDA Alternative Refrigerant Winter Meeting, Saalfelden, Austria; 2002.
[91] Bullard C, Hrnjak P. Advanced technologies for auto a/c components. The Seventh IEA Conference on Heat Pumping Technologies, Beijing, China; 2002. p. 112–24.
[92] Fagerli B. On the feasibility of compressing CO_2 as working fluid in hermetic reciprocating compressors. Dr Ing Thesis. Department of Refrigeration and Air Conditioning, Norwegian University of Science and Technology, Norway; 1997.
[93] Süss J, Kruse H. Efficiency of the indicated process of CO_2 compressors. Int J Refrig 1998;21(3):194–205.
[94] Fagerli B. On the feasibility of compressing CO_2 as working fluid in hermetic reciprocating compressors. Dr Ing Thesis. Department of Refrigeration and Air Conditioning, Norwegian University of Science and Technology, Norway; 1997.
[95] Nekså P, Rekstad H, Zakeri G, Schiefloe P, Svensson M. Commercial heat pumps for water heating and heat recovery. IEA/IZWe.V./IIR Workshop on CO_2 Technology in

Refrigeration, Heat Pump and Air Conditioning Systems, Mainz, Germany; 1999.
[96] Nekså P, Dorin F, Rekstad M, Bredesen A. Development of two-stage semi-hermetic CO_2-compressors. In: Groll EA, Robinson DM, editors. The Fourth IIR-Gustav Lorentzen Conference on Natural Working Fluids, West Lafayette, IN. 2000. p. 355–62.
[97] Suzai T, Sato A, Tadano M, Komatsubara T, Ebara T, Oda A. Development of a carbon dioxide compressor for refrigerators and air conditioners. Conference of the Japan Society of Refrigerating and Air Conditioning Engineers, Tokyo; 1999.
[98] Tadano M, Ebara T, Oda A, Susai T, Kikuo T, Izaki H, Komatsubara T. Development of the CO_2 hermetic compressor. In: Groll EA, Robinson DM, editors. The Fourth IIR-Gustav Lorentzen Conference on Natural Working Fluids, West Lafayette, IN. 2000. p. 323–30.
[99] Fukuta M, Radermacher R, Lindsay D, Yanagisawa T. Performance of vane compressor for CO_2 cycle. In: Groll EA, Robinson DM, editors. The Fourth IIR-Gustav Lorentzen Conference on Natural Working Fluids, West Lafayette, IN. 2000. p. 339–46.
[100] Hiwada T, Hokotani K. Carbon dioxide refrigerating machine. Japan Patent No. JP2001065888; 1999.
[101] Ohakawa T, Kumakura E, Saitani K, Higuchi M, Taniwa H, Ozawa H. Development of hermetic swing compressors for CO_2 refrigerant. In: Soedel W, editor. Proceedings of the International compressor engineering conference at Purdue, West Lafayette, IN, Paper No. C25-1. 2002. p. 841–52.
[102] Fagerli B. Theoretical analysis of compressing CO_2 in scroll compressors. Proceedings of the Third IIR-Gustav Lorentzen Conference on Natural Working Fluids, Oslo, Norway; 1998. p. 249–59.
[103] Hasegawa H, Ikoma M, Nishawaki F, Shintaku H, Yakumaru Y. Experimental and theoretical study of hermetic CO_2 scroll compressor. In: Groll EA, Robinson DM, editors. The Fourth IIR-Gustav Lorentzen Conference on Natural Working Fluids, West Lafayette, IN. 2000. p. 347–53.
[104] Hihara E. R&D on heat pumps with natural working fluids in Japan. The Seventh International Energy Agency Conference on Heat Pump Technologies, Beijing, China; 2002. p. 272–9.
[105] Baumann H, Conzett M. Small oil free piston type compressor for CO_2. In: Soedel W, editor. Proceedings of International Compressor Engineering Conference at Purdue, West Lafayette, IN, Paper No. C25-3. 2002. p. 861–8.
[106] Süss J. Kompressoren und Expansionsorgane für das Kältemittel CO_2. Seminar Stand und Anwendung natürlicher Kältemittel, Mainz, Germany; 2002.
[107] Sasaki M, Koyatsu M, Yoshikawa C, Fujima K, Mizuno T, Kawai S, Hashizume T. The effectiveness of a refrigeration system using CO_2 as a working fluid in the trans-critical region. ASHRAE Trans 2002;108(1):413–8.
[108] Pettersen J, Nekså P. CO_2 refrigeration, air conditioning and heat pump technology development in Europe. Mag Soc Air-Conditioning Refrig Engrs Korea 2002;31(7):53–64.
[109] Bullard C, Yin M, Hrnjak P. Compact counterflow gas cooler for R-744. ASHRAE Trans 2002;108(1):487–91.
[110] Yin J, Bullard C, Hrnjak P. R-7.4.4. gas cooler model development and validation. Int J Refrig 2001;24:652–9.
[111] Fang X, Bullard C, Hrnjak P. Heat transfer and pressure drop of gas coolers. ASHRAE Trans 2001;107(1):255–66.
[112] Fang X, Bullard C, Hrnjak P. Modeling and analysis of gas coolers. ASHRAE Trans 2001;107(1):4–13.
[113] Yin J, Bullard C, Hrnjak P. Single-phase pressure drop measurements in a microchannel heat exchanger. Heat Transfer Engng 2002;23(4):3–12.
[114] Yin J, Bullard C, Hrnjak P. Design strategies for R744 gas coolers. Proceedings of the International Refrigeration Conference at Purdue, West Lafayette, IN; 2002. p. 315–22.
[115] Kim M-H, Lee S, Mehendale S, Webb R. Microchannel heat exchanger design for evaporator and condenser applications. Adv Heat Transfer 2003;37:297–429.
[116] Kim M-H, Bullard C. Development of a microchannel evaporator model for a carbon dioxide air conditioning system. Energy 2001;26(10):931–48.
[117] Zhao Y, Molki M, Ohadi M, Dessiatoun S. Flow boiling of CO_2 in microchannels. ASHRAE Trans 2000;106(1): 437–45.
[118] Kim M-H, Youn B, Bullard C. Effect of inclination on air side performance of a brazed aluminum heat exchanger under dry and wet conditions. Int J Heat Mass Transfer 2001;44: 4613–23.
[119] Kim M-H, Bullard C. Air-side thermal hydraulic performance of multi-louvered aluminum heat exchangers. Int J Refrig 2002;25(3):390–400.
[120] Boewe D, Bullard C, Yin J, Hrnjak P. Contribution of internal heat exchanger to transcritical R744 cycle performance. Int J HVAC&R Res 2001;7(2):155–68.
[121] Randles S, Pasquin S, Gibb P. A critical assessment of synthetic lubricant technologies for alternative refrigerants. The 10th European Conference on Technological Innovations in Air-Conditioning and Refrigeration Industry, Milan; 2003.
[122] Kawaguchi Y, Takesue M, Kaneko M, Tazaki T. Performance study of refrigerating oils with CO_2. The SAE Automotive Alternate Refrigerants Systems Symposium, Scottsdale, AZ; 2000.
[123] Li H, Rajewski T. Experimental study of lubricant candidates for the CO_2 refrigeration system. In: Groll EA, Robinson DM, editors. The Fourth IIR-Gustav Lorentzen Conference on Natural Working Fluids, West Lafayette, IN. 2000. p. 409–16.
[124] Seeton C, Fahl J, Henderson D. Solubility, viscosity, boundary lubrication and miscibility of CO_2 and synthetic lubricants. In: Groll EA, Robinson DM, editors. The Fourth IIR-Gustav Lorentzen Conference on Natural Working Fluids, West Lafayette, IN. 2000. p. 417–24.
[125] Heide R, Fahl J. Mischbarkeit von Schmierölen mit Kohlendioxid. KI Luft- und Kältetechnik 2001;No. 10: 456–70.
[126] Fahl J, Bruns B, Langenberg E, Pötke W. Thermoanalyse synthetischer Schmieröle mit DSC und TGA. KI Luft- und Kältetechnik 2001;No. 7:309–13.
[127] Leisenheimer B, Fritz T. Interaction between CO_2 and elastomers with respect to permeation and explosive decompression. In: Groll EA, Robinson DM, editors. The Fourth IIR-Gustav Lorentzen Conference on Natural Working Fluids, West Lafayette, IN. 2000. p. 201–8.
[128] Jain V, Haramoto C, Shilad I, Pfister J. Components for CO_2 A/C systems. The SAE Automotive Alternate Refrigerants Systems Symposium, Scottsdale, AZ; 2000.

[129] Bhatti M. A critical look at R-744 and R-134a mobile air conditioning systems. SAE Paper No. 970527; 1997.
[130] Fischer S, Sand J. Total Environmental Impact (TEWI) calculations for alternative automotive air-conditioning systems. SAE Paper No. 970526; 1997.
[131] Pettersen J, Hafner A. Energetischer Wirkungsgrad und TEWI von CO_2-Fahrzeug-Klimaanlagen. Seminar: Fahrzeugklimatisierung mit Naturlichen Kaetlemitteln, Karlsruhe, C.F. Mueller Verlag; March 8, 1997.
[132] Gentner H. Passenger car air conditioning using carbon dioxide as refrigerant. Proceedings of the Third IIR-Gustav Lorentzen Conference on Natural Working Fluids, Oslo, Norway; 1998. p. 303–13.
[133] Boewe D, McEnaney R, Park Y, Yin J, Bullard C, Hrnjak P. Comparative experimental study of subcritical R134a and transcritical R744 refrigeration systems for mobile applications. ACRC report CR-17. University of Illinois at Urbana-Champaign, Illinois; 1999.
[134] Beaver A, Yin J, Bullard C. An experimental investigation of transcritical carbon dioxide systems for residential air conditioning. ACRC report CR-18. University of Illinois at Urbana-Champaign, Illinois; 1999.
[135] Yin J, Park Y, Boewe D, McEnaney R, Beaver A, Bullard C, Hrnjak P. Experimental and model comparison of transcritical CO_2 versus R134a and R410 system performance. Proceedings of the Third IIR-Gustav Lorentzen Conference on Natural Working Fluids, Oslo, Norway; 1998. p. 331–40.
[136] McEnaney R, Boewe D, Yin J, Park Y, Bullard C, Hrnjak P. Experimental comparison of mobile A/C systems when operated with transcritical CO_2 versus conventional R134a. Proceedings of the Third IIR-Gustav Lorentzen Conference on Natural Working Fluids, Oslo, Norway; 1998. p. 145–50.
[137] McEnaney R, Park Y, Yin J, Bullard C, Hrnjak P. Performance of the prototype of a transcritical R744 mobile A/C system. SAE Paper No. 99PC-6-7; 1999.
[138] McEnaney R, Hrnjak P. Control strategies for transcritical R744 systems. SAE Paper No. 2000-01-1272; 2000.
[139] McEnaney R, Yin J, Bullard C, Hrnjak P. An investigation of control-related issues in transcritical R744 and subcritical R134a mobile air conditioning systems. ACRC report CR-19. University of Illinois at Urbana-Champaign, Illinois; 1999.
[140] Park Y, Yin J, Bullard C, Hrnjak P. Experimental and model analysis of control and operating parameters of transcritical CO_2 mobile A/C system. Proceedings of VTMS-4 Conference, London, England; 1999. p. 163–70.
[141] Hrnjak P. Some lessons learned from SAE AR CRP. The SAE Automotive Alternative Refrigerant Systems Symposium, Scottsdale, AZ; 2002.
[142] Giannavola M, Murphy R, Yin J, Kim M-H, Bullard C, Hrnjak P. Experimental investigations of an automotive heat pump prototype for military, SUV and compact cars. In: Groll EA, Robinson DM, editors. The Fourth IIR-Gustav Lorentzen Conference on Natural Working Fluids, West Lafayette, IN. 2000. p. 115–22.
[143] Hafner A. Experimental study on heat pump operation of prototype CO_2 mobile air conditioning system. In: Groll EA, Robinson DM, editors. The Fourth IIR-Gustav Lorentzen Conference on Natural Working Fluids, West Lafayette, IN. 2000. p. 183–90.
[144] Giannavola M. Experimental study of system performance improvements in transcritical R744 systems for mobile air-conditioning and heat pumping. MS Thesis. University of Illinois at Urbana-Champaign, Illinois; 2002.
[145] Itoh M, Kogure H, Yoshinaga S, Hoshino R, Wakabayashi N, Kudoh M, Kusumoto H. Study on parallel-flow-type heat exchangers for residential heat pump systems. Proceedings of the JAR Annual Conference; 1996. p. 73–6.
[146] Song S, Bullard C, Hrnjak P. Frost deposition and refrigerant distribution in microchannel heat exchangers. ASHRAE Trans 2002;108(2):944–53.
[147] Hammer H, Wertenbach J. Carbon dioxide (R-744) as supplementary heating device. The SAE Automotive Alternate Refrigerants Systems Symposium, Scottsdale, AZ; 2000.
[148] Pettersen J, Aarlien R, Nekså P, Skaugen G, Aflekt K. A comparative evaluation of CO_2 and HCFC-22 residential air-conditioning systems in a Japanese climate. IEA/IIR Workshop on CO_2 Technologies in Refrigeration, Heat Pump and Air Conditioning Systems, Trondheim, Norway; 1997.
[149] ARI, Standard 210/240, Standard for air-conditioning and air-source heat pump. Arlington, VA: Air-conditioning and Refrigeration Institute; 1994.
[150] Beaver A, Hrnjak P, Yin J, Bullard C. Effects of distribution in headers of microchannel evaporators on transcritical CO_2 heat pump performance. In: Garimella S, Von Spakovsky M, Somasundaram S, editors. The ASME advanced energy systems division, AES-vol. 40. New York: ASME; 2000. p. 55–64.
[151] Sand J, Fischer S, Baxter V. Comparison of TEWI for fluorocarbon alternative refrigerants and technologies in residential heat pumps and air-conditionings. ASHRAE Trans 1999;105(1):1209–18.
[152] Richter M, Song S, Yin J, Kim M-H, Bullard C, Hrnjak P. Experimental results of transcritical CO_2 heat pump for residential application. Energy 2003;28:1005–19.
[153] Richter M, Bullard C, Hrnjak P. Effect of comfort constraints on cycle efficiencies. In: Hernandez-Guerrero A, editor. The ASME advanced energy systems division, AES-vol. 41. New York: ASME; 2001. p. 275–86.
[154] Nekså P, Zakeri G, Aarlien R, Jakobsen A. Carbon dioxide as working fluid in air conditioning and heat pump systems. The Earth Technologies Forum, Washington, DC; 1998.
[155] Hwang Y, Radermacher R. Theoretical evaluation of carbon dioxide refrigeration cycle. Int J HVAC&R Res 1998;4(3): 245–63.
[156] Hwang Y, Radermacher R. Experimental investigation of the CO_2 refrigeration cycle. ASHRAE Trans 1999;105(1): 1219–27.
[157] Rieberer R, Halozan H. CO_2 heat pumps in controlled ventilation systems. Proceedings of the Third IIR-Gustav Lorentzen Conference on Natural Working Fluids, Oslo, Norway; 1998. p. 212–22.
[158] Rieberer R, Kasper G, Halozan H. CO_2: a chance for once-through heat pump heaters. CO_2 technology in refrigeration, heat pumps and air conditioning systems, Trondheim, Norway; 1997.
[159] Schiefloe P, Nekså P. CO_2 varmepumpe for bygningsoppvarming. forprosjekt (Project report, in Norwegian). Trondheim, Norway: SINTEF Energy Research; 1999.
[160] Enkemann T, Kruse H, Oostendorp P. CO_2 as a heat pump working fluid for retrofitting hydronic heating systems in

western Europe. IEA/IIR Workshop on CO_2 Technologies in Refrigeration, Heat Pump and Air Conditioning Systems, Trondheim, Norway; 1997.

[161] Brandes H. Energy efficient and environmentally friendly heat pumping systems using CO_2 as working fluid. IEA/IZWe.V./IIR Workshop on CO_2 Technology in Refrigeration, Heat Pump and Air Conditioning Systems, Mainz, Germany; 1999.

[162] Lorentzen G. Large heat pumps using CO_2 refrigerant. Energy efficiency in refrigeration and global warming impact, Gent, Belgium: IIR; 1993.

[163] Nekså P, Rekstad H, Zakeri G, Schiefloe P. CO_2-heat pump water heater: characteristics, system design and experimental results. Int J Refrig 1998;21:172–9.

[164] Hwang Y, Radermacher R. Experimental evaluation of CO_2 water heater. Proceedings of the Third IIR-Gustav Lorentzen Conference on Natural Working Fluids, Oslo, Norway; 1998. p. 368–75.

[165] Kim M-H. Research and development trends of CO_2 heat pump water heaters in Japan. Mag Soc Air-Conditioning Refrig Engrs Korea 2002;31(7):65–70.

[166] JRAIA, JRA Standard 4050: heat pump water heaters using carbon dioxide refrigerant. The Japan Refrigeration and Air Conditioning Industry Association; 2001.

[167] Hihara E. R&D on heat pumps with natural working fluids in Japan. The Seventh International Energy Agency Conference on Heat Pump Technologies, Beijing, China; 2002. p. 272–9.

[168] Kim M-H. Unpublished technical report. Samsung Electronics, Co., Ltd; 2002.

[169] Manzione J, Calkins F. Evaluation of transcritical CO_2 using an automotive compressor in a packaged-unitary military ECU. ASHRAE Trans 2002;108(2):937–43.

[170] Sonnekalb M, Köhler J. Transport refrigeration with a transcritical refrigeration cycle using carbon dioxide as refrigerant. Proceedings of the International Conference on Ozone Protection Technologies, Washington DC; 1997. p. 124–33.

[171] Kauffeld M, Christensen K. REEFER: a new energy-efficient reefer container concept using carbon dioxide as refrigerant. Proceedings of the Third IIR: Gustav Lorentzen Conference on Natural Working Fluids, Oslo, Norway; 1998. p. 399–410.

[172] Jakobsen A, Nekså P. Carbon dioxide in marine refrigeration applications. Earth Technologies Forum Conference, Washington, DC; 1998. p. 153–62.

[173] Eggen G, Aflekt K. Commercial refirgeration with ammonia and CO_2 as working fluids. Proceedings of the Third IIR: Gustav Lorentzen Conference on Natural Working Fluids, Oslo, Norway; 1998. p. 281–92.

[174] Nekså P, Girotto S, Schiefloe P. Commercial refrigeration using CO_2 as refrigerant: system design and experimental results. Proceedings of the Third IIR: Gustav Lorentzen Conference on Natural Working Fluids, Oslo, Norway; 1998. p. 270–80.

[175] Schmidt E, Klöcker K, Flacke N. Heat pumps for dehumidification and drying processes in residential and commercial applications. IEA/IZWe.V./IIR Workshop on CO_2 Technology in Refrigeration, Heat Pump and Air Conditioning Systems, Mainz, Germany; 1999.

[176] Steimle F. CO_2-drying heat pumps. CO_2 Technology in Refrigeration, Heat Pump and Air Conditioning Systems, Trondheim, Norway; 1997.

[177] Schmidt E, Klöcker K, Flacke N, Steimle F. Applying the transcritical CO_2 process to a drying heat pump. Int J Refrig 1998;21(3):202–11.